Characterization of Alcohol Dehydrogenases from *Hyperthermus butylicus*

by

Ching Tse

A thesis
presented to the University of Waterloo
in fulfilment of the
thesis requirement for the degree of
Master of science
in
Biology

Waterloo, Ontario, Canada, 2016

© Ching Tse 2016

Author’s Declaration

I hereby declare that I am the sole author of this thesis. This is a true copy of the thesis, including any required final revisions, as accepted by my examiners.

I understand that my thesis may be made electronically available to the public

Abstract

Hyperthermophiles grow optimally at 80 ^{o}C and above, and many of them use carbohydrates and peptides for their growth. *Hyperthermus butylicus* is a peptide-fermenting hyperthermophilic archaeon producing 1-butanol as an end-product. Alcohol dehydrogenase (ADH) is a key enzyme responsible for alcohol production, catalyzing the interconversion of alcohols and corresponding ketones or aldehydes. ADHs from hyperthermophiles are of great interests due to their thermostability, high activity and enantioselectivity. The pathway for 1-butanol production in *H. butylicus* is unknown. The aims of the study are to examine the metabolite end-products of *H. butylicus* and identify the ADH responsible for 1-butanol production.

Metabolic end-products from *H. butylicus* culture were measured using High Performance Liquid Chromatography. It showed that in addition to 1-butanol there were other previously unreported end-products including acetone, 2-propanol, and butyrate, which are similar to those of *Clostridium* species. The production of 1-butanol suggests ADH is present in *H. butylicus*, however, the gene encoding the enzyme is unknown. From the *H. butylicus* genome sequence, the gene Hbut_0414 is the only gene annotated as zinc-containing ADH, but it was unclear if it would be the enzyme catalyzing the production of 1-butanol. The gene was cloned and overexpressed in *Escherichia coli*. The recombinant enzyme (ADH1) encoded by Hbut_0414 showed ADH activity with a wide range of substrates, and it was NAD(H)-specific and lost 50% of its activity when incubated at 60 ^{o}C for 3 hours. The ADH activity in the cell-free extract of *H. butylicus* was 1.4 U/mg and could use both NAD(H) and NADP(H) as a cofactor. This suggests there is another ADH (ADH2) present in *H. butylicus* but its gene is not annotated. The ADH2 was purified from the cell-free extract of *H. butylicus* and its protein sequence was identified using mass spectrometry. It was found to be encoded by a gene annotated as a hypothetical protein, which shared low sequence identities with other hyperthermophilic ADHs. The purified ADH2 was thermostable with a time of 25 hours for losing 50% of its activity at 95 ^{o}C. It had an apparent K_m value of 0.59 mM and specificity constant k_{cat}/K_m of 13,559 $s^{-1}M^{-1}$ with butyraldehyde, which was the substrate with the highest catalytic activity examined. Its substrate specificity, enzyme kinetics, and thermostability suggest it is the ADH responsible for 1-butanol production in *H. butylicus*. The putative conserved motifs sites for $NAD(P)^{+}$ and iron binding were identified using sequence alignment of ADHs from *Crenarchaeota*, suggesting ADH2 to be an iron-containing ADH.

Acknowledgments

Most importantly, I express my deepest gratitude to my supervisor, **Dr. Kesen Ma** for giving me this opportunity for working on this project. I am very grateful for his patient guidance and time. His endless passion for science and working attitude is truly a role model for those who wish to embark a career in research. I would also like to thank my committee members, **Dr. Andrew Doxey** and **Dr. Todd Holyoak** for their time and helpful comments for my project.

I greatly appreciate all the help from my labmates, Tina Suen, Emma Chen, Sarah Kim and Dr. Nasser El-din lbrahim. It is not just for their generous help, but also for giving me this enjoyable experience to work with them.

I express my most sincere thanks to my family for their support and care and my friends for their advices and encouragement.

Table of Contents

List of Figures

List of Tables

List of Abbreviations

ADH	Alcohol dehydrogenase
*Ap*ADH	*Archaeoglobus profundus* alcohol dehydrogenase
Atm	Atmosphere
CAPS	3-(Cyclohexylamino)-1-propanesulfonic acid
CoA	Coenzyme A
*Df*ADH	*Desulfurococcus fermentans* alcohol dehydrogenase
*Dm*ADH	*Desulfurococcus mucosus* alcohol dehydrogenase
DTT	Dithiothreitol
EDTA	Ethylenediaminetetraacetic acid
EPPS	N-(2-hydroxyethyl)-piperazine-N'-(3-propanedulfonic acid)
Fe	Iron
FPLC	Fast Protein Liquid Chromatography
*Hb*ADH	*Hyperthermus butylicus* alcohol dehydrogenase
HEPES	4-(2-Hydroxyethyl)-1-piperazineethanesulfonic acid
HPLC	High Performance Liquid Chromatography
MS	Mass spectrometry
NAD(H)	Nicotinamide adenine dinucleotide (reduced)
NADP(H)	Nicotinamide adenine dinucleotide phosphate (reduced)
PCR	Polymerase chain reaction
*Pf*ADH	*Pyrolobus fumarii* alcohol dehydrogenase
*Pi*ADH	*Pyrobaculum islandium* alcohol dehydrogenase
PIPES	1,4-Piperazine-bis-(ethanesulfonic acid)
SDS-PAGE	Sodium dodecyl sulfate-polyacrylamide gel electrophoresis
SDT	Sodium dithionite
*Ss*ADH	*Sulfolobus solfataricus* P2 alcohol dehydrogenase
*Ta*ADH	*Thermosphaera aggregans* alcohol dehydrogenase
*Tc*ADH	*Thermogladius cellulolyticus* alcohol dehydrogenase
*Tg*ADH	*Thermococcus guaymasensis* alcohol dehydrogeanse
Tris	2-Amino-2-hydroxymethyl-1,3-propanediol
*Vs*ADH	*Vibrio* sp. EJY3 alcohol dehydrogenase
Zn	Zinc

Chapter 1 Introduction

1.1 Hyperthermophiles

Hyperthermophiles are organisms with optimal growth temperatures of 80 ^{o}C and above or capable of growing at 90 ^{o}C (Kelly and Adams 1994, Stetter 1996). A great diversity of hyperthermophilic archaea have been isolated from hydrothermal, geothermal and anthropogenic high-temperature ecosystems having diverse biochemical, physiological and phylogeny properties (Stetter 1998, Huber, Huber et al. 2000, Stetter 2005). Hyperthermophiles are suggested to be the primitive forms of life present as they occupy the deepest and shortest branches in the phylogenetic tree of life based on the 16S rDNA sequences (Atomi 2005). Hyperthermophiles are capable of growing on a broad range of substrates and due to their metabolic flexibility, they play an important role in biogeochemical processes (Huber, Huber et al. 2000). Their great resistance to heat also makes them interesting objects for basic research both in term of understanding the mechanisms for thermostability and thermostable enzymes for biotechnology applications. One of the most interesting thermostable enzymes is alcohol dehydrogenase (ADHs, EC 1.1.1.1). ADHs from hyperthermophiles for commercial use include the production of biofuels and synthesis of chiral pharmaceutical agents (Lamed and Zeikus 1981, Simon, Bader et al. 1985, Atomi, Sato et al. 2011).

1.2 Alcohol production by mesophiles and thermophiles

1.2.1. Alcohol production by mesophiles and key enzymes involved

Ethanol and butanol are alcohols produced by many mesophilic microorganisms that also have great industrial applications (Antoni, Zverlov et al. 2007). Ethanol produced from *S. cerevisiae* has been widely used for wine and beer production and is currently being investigated to be used as a renewable energy source to replace petroleum (Balat, Balat et al. 2008). Ethanol is a major fermentation product in various mesophilic yeasts and bacteria (Zeikus 1980). Mesophilic yeasts that produce high concentrations of ethanol include different strains of *S. cerevisiae*, which produces ethanol concentrations as high as 18% of the fermentation broth (Dombek and Ingram 1987). Other mesophilic yeasts such as *Kluyveromyces fragilis*, *Kluyveromyces marxianus*, *Candida utilis*, and *Pachysolen tannophilus,* are also known to be producers of ethanol (Jeffries 1981, Schneider, Wang et al. 1981, Margaritis and Bajpai 1982, Ballesteros, Oliva et al. 2004). Mesophilic bacteria that produce significant amounts of ethanol (more than 24 g per l liter of fermented broth) include *Zymomonas mobilis*, *Escherichia coli LY01* and *Klebsiella aerogenes* (Rogers, Lee et al. 1982, Tolan and Finn 1987, Zaldivar, Martinez et al. 1999). Biomaterials such as hemi/cellulose and starch can be hydrolyzed into simple sugars by microbial enzymes such as cellulase, xylanase and amylase (Cardona and Sánchez 2007, Balat, Balat et al. 2008). Simple sugars, including xylose and glucose, are converted into pyruvate by different metabolic pathways including the Embden-Meyerhof-Parnas pathway, the Entner-Doudoroff (ED) pathway and the Pentose Phosphate pathway (Aristidou and Penttilä 2000, Doran Peterson, Cook et al. 2008). Unlike other ethanol producing mesophiles, *Z. mobilis* exclusively uses the ED pathway, anaerobically, for sugar metabolism (Rogers, Jeon et al. 2007). As a consequence of the low ATP yield in the ED pathway, *Z. mobilis* maintains a high glucose flux through the ED pathway and enzymes involved in the ethanol fermentation are highly expressed (Conway 1992). Key enzymes in the ethanol

fermentation pathway include pyruvate decarboxylase, which converts pyruvate into acetaldehyde with the release of CO_2, and ADH that subsequently catalyzes the reduction of acetaldehyde into ethanol (Ingram, Aldrich et al. 1999, Zamora 2009).

Butanol is produced by different strains of *clostridia* (Lee, Park et al. 2008). In comparison to ethanol producing mesophiles, *Clostridium* species are able to utilize a wide range of substrates for butanol production, including hemicellulose-derived pentose, cellobiose, lactose, raffinose, mannose, and arabinose (Qureshi and Maddox 1995, Ezeji, Qureshi et al. 2007). *Clostridium acetobutylicum* is a well-characterized and second most widely used microorganism for fermentation (Papoutsakis 2008). Other known *Clostridium* species capable of producing butanol as a major fermentation product include *Clostridium aurantibutylicum*, *Clostridium beijerinckii*, *Clostridium tetanomorphum*, *Clostridium saccharobutylicum* and *Clostridium saccharoperbutylacetonicum* (George and Chen 1983, Gottwald, Hippe et al. 1984, Mitchell 1997). The production of butanol in *Clostridium* species involves several key enzymes, which are CoA-dependent aldehyde dehydrogenase and ADH, for the conversion of butyryl-CoA into butanol, and pyruvate ferredoxin-oxidoreductase for the continual supply of reducing power for the generation of the cofactor NAD(P)H (Menon and Ragsdale 1997, Zhang, Rodriguez et al. 2011). *Butyribacterium methylotrophicum* produces 2.7 g of butanol per liter of fermented broth from carbon monoxide (Grethlein, Worden et al. 1991). The pathway for butanol production in *B. methylotrophicum* is similar to that in *Clostridium* species due to similarity in the anaerobic production of acetate and butyrate. Moreover, both produce butanol and ethanol at lower pH values (Grethlein, Worden et al. 1991). The ability to produce butanol from carbon monoxide is also observed in *Clostridium carboxidivorans* strain PT7 (Bruant, Lévesque et al. 2010). This validates the idea of producing butanol from an alternative economic source such as CO.

1.2.2 Alcohol production by thermophiles and key enzymes involved

The majority of ethanol producing mesophiles utilize six-carbon sugars for fermentation, and the high cost of converting biomass into sugars impedes the establishment of a cellulosic biofuels industry. Use of thermophilic bacteria is one approach to lower this cost as they have enzymes for hydrolyzing celluloses and hemicelluloses. Thermophiles for ethanol production at higher temperatures also facilitate process design and downstream product recovery of volatile alcohols. Cellulolytic thermophiles, such as *Clostridium thermocellum* and *Clostridium thermohydrosulfuricum,* and hemicellulolytic thermophiles, including *Thermoanaerobacter ethanolicus*, *Thermoanaerobacter mathranii* and *Geobacillus kaustophilus,* are studied for bioethanol production (Lamed and Zeikus 1980, Ng, Ben-Bassat et al. 1981, Wiegel, Carreira et al. 1983, Lovitt, Longin et al. 1984, Peng, Wu et al. 2008, Brown, Guss et al. 2011) . Similar to mesophiles, the key enzymes for ethanol production include CoA-dependent acetaldehyde dehydrogenase and ADH (Lamed and Zeikus 1980). There are, however, other unwanted side products such as lactate, acetate, formate, which are resulted from the high activity of lactate dehydrogenase, acetate kinase and pyruvate-formate lyase in thermophiles (Shaw, Podkaminer et al. 2008).

With the same advantage for lignocelluloses utilization, thermophiles have also been studied for biobutanol production. There is no reported thermophilic *Clostridium* species that can produce butanol (Taylor, Eley et al. 2009). *Thermoanaerobacterium thermosaccharolyticum* (formerly known as *Clostridium thermosaccharolyticum*) produces butanol from cellulosic biomass (Bhandiwad, Guseva et al. 2013). The butanol production pathway in this species has not been characterized but in the genome there are similar genes involved for butanol production as in mesophilic *clostridia* (Bhandiwad, Guseva et al. 2013). It is also suggested that the butyryl CoA dehydrogenase in *T. thermosaccharolyticum* is coupled to ferredoxin reduction, as there is no activity detectable without the addition of ferredoxin in the assay mixture (Bhandiwad, Guseva et al. 2013).

Moreover, genes encoding butyryl CoA dehydrogenase show high homology to *C. kluyveri* butyryl CoA dehydrogenase, which is coupled to ferredoxin reduction (Li, Hinderberger et al. 2008). This exergonic reduction of crotonyl CoA into butyryl CoA is coupled to the endergonic reduction of ferredoxin and requires an additional NADH as an electron donor (Wang, Huang et al. 2010). There are two ways to supply additional NAD(P)H: one way is through the production of acetate, and the second way is to directly transfer electrons from reduced ferredoxin to NAD^+ catalyze by ferredoxin: nicotinamide oxidoreductase (Girbal, Croux et al. 1995, Shaw, Jenney et al. 2008). The production of butanol has shown to be dependent on the production of acetate in *Thermoanaerobacterium saccharolyticum*, which is used as a heterologous host for the synthesis of butanol using enzymes from *T. thermosaccharolyticum* and *C. acetobuytlicum* (Bhandiwad, Shaw et al. 2014).

In hyperthermophiles, several species including *Pyrococcus furiosus*, *Thermococcus* strain ES-1, *Thermococcus guaymasensis* and *Thermotoga hypogea* have been reported to produce small amounts of ethanol (1-2 mM) but *H. butylicus* is the only hyperthermophile reported to produce 1-butanol (Fiala and Stetter 1986, Pledger and Baross 1989, Zillig, Holz et al. 1990, Godfroy, Lesongeur et al. 1997, Canganella, Jones et al. 1998). *Thermococcus* strain ES-1 is another hyperthermophile that may produce butanol, but it is not confirmed due to the limitation to differentiate ethanol and butanol using gas chromatography at that time (Ma, Loessner et al. 1995). Although there is few study on the metabolic pathway for alcohol production in hyperthermophiles, it is certain that ADH is an essential enzyme.

1.2.3 Butanol production pathway

1.2.3.1 Acetone-butanol-ethanol fermentation in *Clostridium*

To date, there are two well-studied pathways for 1-butanol production. In *Clostridium* species, the pathway is known as acetone-butanol-ethanol fermentation (Gheshlaghi, Scharer et al. 2009). The pathway for butanol-production is identified from *C. acetobutylicum* (Antoni, Zverlov et al. 2007). The fermentation is biphasic, the first phase is an acidogenic phase and the second phase is a solventogenic phase (Johnson, Peterson et al. 1931). Organic acids such as butyric acid and acetic acid are accumulated in the first phase and butanol is produced in the second phase (Johnson, Peterson et al. 1931). In *C. acetobutylicum*, the butanol production pathway begins with the condensation of two acetyl-CoA molecules into one acetoacetyl-CoA, which is then converted into butyryl-CoA through a step-wise conversion (Park, Geng et al. 1993). The genes encoding the enzymes catalyzing the step-wise conversion are clustered together in the polycistronic butyryl-CoA synthesis operon (Boynton, Bennet et al. 1996). *C. acetobutylicum* has two distinct butanol dehydrogenase isozymes for butanol production and the specificity for reduction is higher than oxidation (Walter, Bennett et al. 1992).

There are nine enzymes required in this pathway for converting pyruvate into butanol, which are pyruvate: ferredoxin oxidoreductase (POR), thiolase, β-hydroxybutyryl-CoA dehydrogenase, crotonase, butyryl-CoA dehydrogenase, acetoacetyl-CoA: acetate:CoA transferase, acetoacetyl-CoA: butyrate:CoA transferase, butyraldehyde dehydrogenase and butanol dehydrogenase **(Fig 1)**.

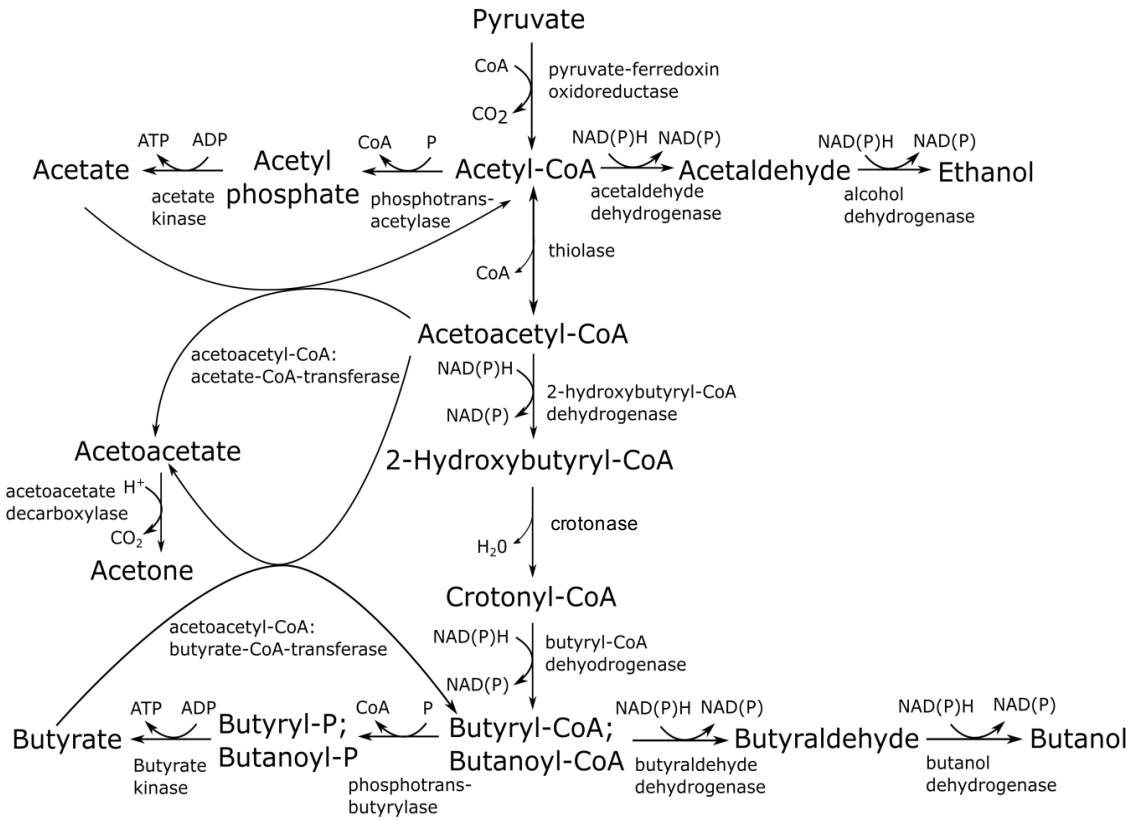

Figure 1. Schematic diagram showing the fermentation pathway leading to butanol production in *Clostridium* species. In the early exponential growth phase, cells produce carboxylic acids rapidly, mostly acetate and butyrate; they are excreted externally and lower the pH. These acids are suggested to act as inducers for the biosynthesis of the solventogenic enzymes during the second fermentative phase. The acids would re-enter the cells and act as co-substrates for the production of neutral solvents. This together with the cease in the production of acid due to the decrease of cell growth increases pH gradually. It is also suggested that the switch to solvent production is an adaptive response of the cells (Gheshlaghi, Scharer et al. 2009)

1.2.3.2 Butanol production pathway in *S. cerevisiae* and synthetic n-butanol production in *E. coli*

Another pathway for butanol production utilizes intermediates from the catabolism of amino acids. Amino acids (ie. threonine, glycine) can be converted into 2-ketovalerate, which is then decarboxylated into the corresponding aldehydes. *S. cerevisiae* has a natural pathway to produce 1-butanol from glycine (Branduardi, Longo et al. 2013) **(Fig 2B)**. The discovery of this pathway is based on the Ehrlich pathway, by which microorganisms decarboxylate α-ketoacids from the deamination of branched-chain amino acids into the respective aldehydes and subsequently alcohols (Kondo, Tezuka et al. 2012). Interest in this pathway is initiated by Atsumi et al, who successfully produce long-chained alcohols, including 1-butanol, using engineered *E. coli* strains (Atsumi, Hanai et al. 2008). In both pathways, the respective amino acid is converted into 3-ethylmalate, and the NADH produced in the conversion of 3-ethylmalate into 2-ketovalerate is consumed in the next step for the production of alcohols (Atsumi, Hanai et al. 2008, Branduardi, Longo et al. 2013) **(Fig 2A and B)**. In both engineered strains of *E. coli* and *S. cerevisiae*, 1-butanol yield is higher with the engineered butanol pathway utilizing peptides than the natural fermentation pathway using carbohydrates as substrate **(Table 1)**.

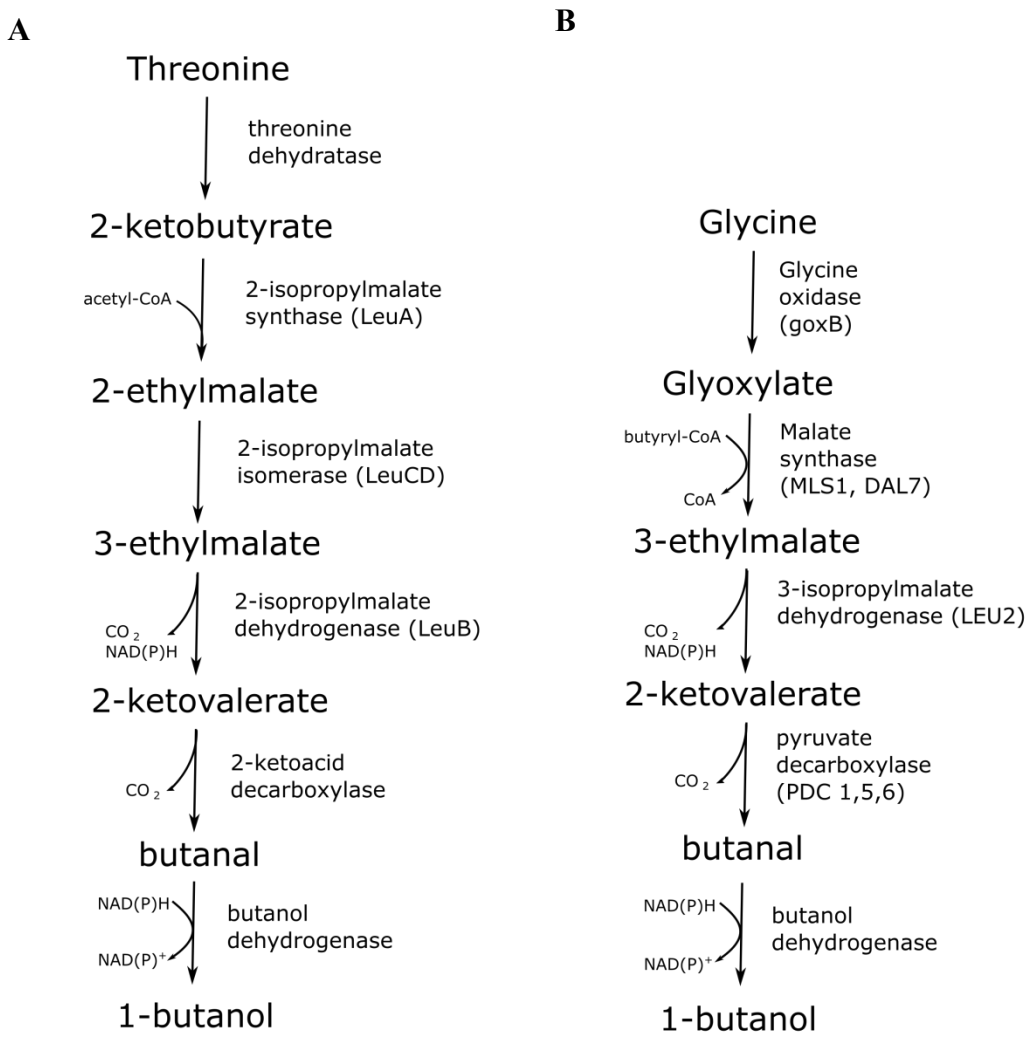

Figure 2. Schematic diagram showing the metabolic pathway of butanol production from (A) *E. coli* BW25113 and (B) *S. cerevisiae* 288c. Synthetic pathway in engineered *E.coli* using amino acid intermediates from the threonine pathway with enzymes LeuA from *Salmonella typhimurium* and 2-ketoisovalerate decarboxylase gene from *Lactococcus lactis* and a natural pathway in *S. cerevisiae* is deduced by mutagenesis on key enzymes naturally present in *S. cerevisiae* except goxB from *Bacillus subtilis* XF-1

Table 1. Maximum amount of butanol production in genetic engineered heterologous bacteria host with different substrates

Microorganisms/Host	Butanol		Reference
	Carbohydrate	Peptides	
C. acetobutylicum ATCC 824	18.9 g/L	N/A	(Jang, Lee et al. 2012)
E. coli BW25113	552 mg/L	800 mg/L	(Atsumi, Cann et al. 2008, Atsumi, Hanai et al. 2008, Inui, Suda et al. 2008, Shen and Liao 2008)
S. cerevisiae BY4742	2.5 mg/L	92 mg/L	(Steen, Chan et al. 2008, Branduardi, Longo et al. 2013)
P. putida PS1.0	122 mg/L	N/A	(Nielsen, Leonard et al. 2009)
B. *subtilis* BK1.0	24 mg/L	N/A	(Nielsen, Leonard et al. 2009)
L. brevis ATCC 327	300 mg/L	N/A	(Berezina, Zakharova et al. 2010)

N/A-Not available because no study has been done

1.2.3.3 Industrial applications of butanol fermentation and comparison of butanol producing microorganisms

With the world's rapid development, demand for energy is increasing and biofuel production from fermentation that once lost its competitiveness has regained interest (Weber, Farwick et al. 2010). Two commercially available biofuels are bioethanol and biodiesel, which are used in Brazil and the United Stated (Ragauskas, Williams et al. 2006). Another biofuel, biobutanol, is only in the pilot plant stage but has several distinct advantages compared to these other biofuels (Nielsen, Leonard et al. 2009). Biobutanol has great similarity to gasoline, in terms of thermodynamic and physical properties, which make it an ideal candidate as a direct fuel replacement or as a blending agent with gasoline in conventional vehicles (Antoni, Zverlov et al. 2007). In addition, compared to ethanol, it has higher energy content, lower volatility and higher hydrophobicity that makes it possible to distribute in existing transportation fuel infrastructures without corrosive consequences (Cascone 2008). Some studies also suggest corn-derived ethanol production consumes more energy than it produces (Farrell, Plevin et al. 2006).

In the natural process of *C. acetobutylicum* fermentation, it produces around 13.0 g/L of butanol under optimal growth conditions (Jones and Woods 1986). Despite the high yield of butanol production, the use of *clostridia* microorganisms as bio-converters have several disadvantages; firstly, it is a spore former that affects butanol-forming abilities; secondly, their low toxic tolerance towards butanol (intolerant to butanol above 1-2%); thirdly, the metabolism shift from acidogenesis to solventogenesis; lastly, their high oxygen sensitivity complicates continuous cultivation (Pfromm, Amanor-Boadu et al. 2010, Jang, Malaviya et al. 2012). Scientists have been trying to find alternative hosts to incorporate the *clostridia* pathway to produce butanol (Atsumi, Cann et al. 2008, Green 2011). Well-studied hosts with genetic engineering tools to accommodate heterologous biosynthetic pathways include *E. coli*, *S. cerevisiae*, *Pseudomonas putida*, *Bacillus subtilis* and *Lactobacillus*

brevis (Atsumi, Cann et al. 2008, Atsumi, Hanai et al. 2008, Steen, Chan et al. 2008, Nielsen, Leonard et al. 2009, Berezina, Zakharova et al. 2010, Branduardi, Longo et al. 2013). All of the organisms have advantages over *Clostridium* species either in higher tolerance to butanol, lack of oxygen sensitivity, or can easily uptake foreign recombinant plasmids. Genetic engineering methods to optimize butanol production include the direct overexpression of butanol biosynthesis genes, or indirectly overexpressed genes involved in increasing glycolytic flux and regenerating NADH (Nielsen, Leonard et al. 2009). Also, deletion of genes responsible for production of by-products such as ethanol and butyrate is used to increase butanol yield (Nielsen, Leonard et al. 2009).

For the fermentation of 1-butanol to have important commercial value, the production of 1-butanol has to exceed 1.0 g/L (Zheng, Li et al. 2009). However, other than the existing *clostridia* pathway in *Clostridium* species, other synthetic pathways don't exceed that concentration **(Table 1)**. In the expression of a heterologous biosynthetic pathway, there are many obstacles to overcome, which include selection of host and enzymes for overexpression, balances of metabolic pathway intermediates and protein levels, and removal of competing pathways without compromising the host organism's viability (Shen and Liao 2008, Zhang, Rodriguez et al. 2011). A well-known difficulty in engineering butanol synthesis pathway in recombinant strains is a functioning butyryl-CoA dehydrogenase complex in the heterologous hosts (Berezina, Zakharova et al. 2010). This enzyme is highly oxygen-sensitive and its low activity in recombinant bacteria limits the amount of butanol production (Boynton, Bennet et al. 1996, Berezina, Zakharova et al. 2010). Hence, elucidation of native pathways for butanol production is of great scientific interest as it can be a potential way to increase conventional butanol production.

1.3 Thermostable ADHs from hyperthermophiles

Alcohol dehydrogenase (ADH) is ubiquitously expressed in all three domains of life including Archaea, Bacteria, and Eukaryotes (Jornvall, Persson et al. 1987). ADHs are classified as as a family of oxidoreductases and catalyze the inter-conversion of alcohol and corresponding aldehydes and ketones (Ciriacy 1975). They are also important biocatalyst for the production of biofuels. They have different physical and enzymatic properties and show a wide variety of substrates specificities (Branden, Jornvall et al. 1975). The ADHs from hyperthermophiles are particularly interesting for study due to their high thermostability and their ability to utilize various substrates.

There are 15 hyperthermophilic ADHs purified and characterized and they have different activities with substrates in both oxidation and reduction reactions (Antoine, Rolland et al. 1999, Ma and Adams 1999, Guy, Isupov et al. 2003, Pennacchio, Giordano et al. 2010, Vitale, Rosso et al. 2010, Ying and Ma 2011, Wu, Zhang et al. 2013). ADHs that have important industrial applications are those that catalyze the production of biofuels including ethanol or butanol or those that have stereoselective specificity with secondary alcohols. Thermostable ADHs can be directly used in biomass fermentation via reduced pressure distillation, and the ability to utilize lignocelluloses, most abundant biomaterial on earth, make them competitive biocatalysts (Aristidou, Baghaei-Yazdi et al. 2011).

1.3.1 Recombinant thermostable ADHs

To gain further insight into the catalytic properties and structures of thermostable ADHs for potential industrial applications, large quantities of pure ADHs are needed. However, it is difficult to obtain native ADHs due to difficulties in cultivation of hyperthermophiles, low basal level expression of ADHs and high oxygen sensitivity of Fe-ADHs that complicates enzyme purification (Demirjian, Morís-Varas et al. 2001). The demonstration

of successful overexpression of hyperthermophilic ADHs with similar catalytic properties in the mesophilic host *E. coli* has facilitated the study of thermophilic ADHs (Cannio, Fiorentino et al. 1996, Antoine, Rolland et al. 1999, van der Oost, Voorhorst et al. 2001, Hirakawa, Kamiya et al. 2004, Kube, Brokamp et al. 2006, Machielsen, Uria et al. 2006, Ying, Grunden et al. 2009). The ability of recombinant ADHs to maintain their catalytic properties suggests that hyperthermophilic proteins can properly fold at temperatures far below their optimal catalytic temperatures (Danson, Hough et al. 1996, Danson and Hough 1998). Expression vectors for the overexpressions of hyperthermophilic ADHs have tRNAs for rare codons to compromise for the different codon usage (Ermolaeva 2001). Hyperthermophiles are mostly archaea and they have greater similarity in codon usage with eukaryotes than bacteria. Archaea also have eukaryotic-like but simpler transcription and translation initiation (Bell and Jackson 1998). However, for translation elongation, archaea resembles that of bacteria and the failure of proper folding into monomeric subunits in the endoplasmic reticulum and into the secretory pathway remains a major obstacle in the use of eukaryotic expression systems (Bell and Jackson 1998). *E. coli* is still the preferred host for heterologous overexpression of thermophilic ADHs and optimization of this heterologous production of thermostable ADHs is essential for biotechnological applications and useful for determination of three-dimensional structures and structure/function studies by site-directed mutagenesis.

1.3.2 Relationship of thermophilic ADHs properties with phenotypic origins

Many microorganisms including hyperthermophiles contain multiple ADHs, two well-characterized examples are 12 putative ADHs from *Sulfolobus sofataricus* and two different types of ADHs from *P. furiosus* (Ma and Adams 1999, Raia, Giordano et al. 2001). It is proposed each ADH may have different physiological functions for survival (Radianingtyas and Wright 2003). It is interesting that properties of thermophilic ADHs are related to the phenotypic origin as almost all marine hyperthermophiles have at least

one Fe-containing ADH while most terrestrial ones have Zn-containing ADH in addition to different types of ADHs (Radianingtyas and Wright 2003). Marine biotopes are of similar kinds of environments, and all hyperthermophiles isolated are anaerobic except for a few including *Pyrobaculum aerophilum* (Radianingtyas and Wright 2003). *P. aerophilum* is the only species in the group that doesn't have Fe-containing ADH (Radianingtyas and Wright 2003). Terrestrial biotopes are more diverse and include both natural water-containing volcanic areas and anthropogenic biotopes. Similarly, the exceptional anaerobic archaeon *Thermococcus zilligii* AN1 from terrestrial biotopes doesn't have Zn-containing ADH. This variation showed that multiple and different types of ADHs can be used to cope with the stress components of the environment and the biotopes of isolation could predict the type(s) of ADH that hyperthermophiles may contain (Radianingtyas and Wright 2003).

1.4 *Hyperthermus butylicus*

H. butylicus produces 1-butanol but the pathway of its production is unknown based solely on previous genome analysis (Zillig, Holz et al. 1990; Brugger, Chen et al. 2007). There is a possibility that a new pathway present in *H. butylicus* for the production of butanol. However, butanol dehydrogenase, the only enzyme known for catalyzing butanol production, must be present. The study of this enzyme serves as an initial step to understand the physiological importance of the pathway. Butanol dehydrogenase can also be a potent industry biocatalyst.

1.4.1 Growth of *H. butylicus*

H. butylicus is a peptide-fermenting and sulfur-reducing archaeon that belongs to the kingdom of *Crenarchaeota* (Zillig, Holz et al. 1990). It was isolated from the sea floor, a solfataric habitat, with temperatures up to 112 ^{o}C on the coast of Sao Miguel, Azores (Zillig, Holz et al. 1990). *H. butylicus* is a neutrophil with sharp optimal pH at 7.0 and optimal salt

concentration of 17 g/L NaCl (Zillig, Holz et al. 1990). It is capable of growing between 80 ^{o}C to 108 ^{o}C with optimal growth temperatures between 95 ^{o}C to 106 ^{o}C (Zillig, Holz et al. 1990). It utilizes peptide mixtures as carbon and energy sources and all the enzymes of the gluconeogenesis pathway were found in the genome sequence (Zillig, Holz et al. 1990, Brugger, Chen et al. 2007). However, it does not utilize amino acid mixtures, various synthetic peptides or undigested protein and any carbohydrates due to the lack of ATP-binding cassette transporters for those substrates (Zillig, Holz et al. 1990, Brugger, Chen et al. 2007). In the genome of *H. butylicus*, there are at least 23 putative peptidases that belong to different families of peptidases including oligopeptidases, metallopeptidases, and carboxypeptidases, and at least five of the peptidases have putative N-terminal signal peptides that induce extracellular secretion (Brugger, Chen et al. 2007).

The major energy metabolism is by fermentation, and elemental sulfur (S^{o}) and H_2 act as accessory energy sources for growth (Zillig, Holz et al. 1990). The addition of S^{o} and H_2 have no major change on the formation of end-products and it is predicted that S^{o} is reduced to sulfide by H_2, which couples the generation of ATP (Zillig, Holz et al. 1990, Noll and Childers 2000). In the natural habitat, large amounts of CO_2 are found but CO_2 is not used as a carbon source (Zillig, Holz et al. 1990).

1.4.2 Metabolic end-products

Major metabolic end-products from fermentation have been detected by gas chromatography-mass spectroscopy and nuclear magnetic resonance spectroscopy (Zillig, Holz et al. 1990). In a 100 L fermenter with cell density of 2.2 x 10^{8} cells per ml, 67 mmol of 1-butanol (collected from the cooled trap of the gas outflow), a similar amount of acetic, propionic and phenylacetic acids, one-tenth the amount of hydroxyphenylacetic acid and trace amounts of propylbenzene, acetophenone, and hydroxyacetophenone were detected (Zillig, Holz et al. 1990). These metabolic end-products suggest they are probably formed

from metabolism of different amino acids. Acetic acid is formed from metabolism of alanine and glycine (Kinoshita, Udaka et al. 1957); propionic acid is from metabolism of leucine, isoleucine or valine (Gao, Oh et al. 1997); phenylacetic acid is from the metabolism of phenylalanine and hydroxyphenylacetic acid is from the metabolism of tyrosine (Christensen 1990). A previous analysis is unable to identify the metabolic pathway for 1-butanol production in *H. butylicus* as no homolog of the bacterial acetoacetate-butyrate / acetate-CoA transferase is found in the genome, which is essential for 1-butanol production in *Clostridium* species (Toth et al. 1999).

1.4.3 ADH in *H. butylicus*

One ADH homolog is annotated in the genome of *H. butylicus*, Hbut_0414 (WP_048061395). It is deduced to have the closest similarity with zinc-containing ADH. The gene has 843 base pairs encoding a protein of 280 amino acid residues. This sequence also has 37.3% and 27.9% identity with Zn-containing ADH from *Pyrolobus fumarii* and *Streptomyces sclerotialus*, respectively. There is a high possibility of this gene as a functional ADH and overexpression of this gene provides characteristics of this ADH and its potential role in 1-butanol production in *H. butylicus*.

H. butylicus is isolated from marine biotopes and there is a high possibility of Fe-containing ADH(s) present. There is no gene annotation of a Fe-containing ADH from the genome sequence. Since 1-butanol is detected as one of the major end-products, and ADH is the only conventional enzyme for catalyzing 1-butanol production *in vivo*. The investigation of an ADH responsible for 1-butanol production in *H. butylicus* may help us to optimize butanol production from microorganisms and advance our understanding of thermostable ADHs in *Crenarchaeota*.

1.5 Objectives

The general goal of this research is to identify the ADH responsible for 1-butanol production in *H. butylicus*. The following are the specific goals:

a) Optimize the growth of *H. butylicus*: cell yield and growth rates under different growth conditions will be measured and compared.
b) Detect metabolic end-products from *H. butylicus* and confirm the production of 1-butanol under the cultivation conditions used. The production of 1-butanol will suggest ADH from *H. butylicus* is functionally expressed.
c) Prepare sufficient biomass for the study of ADH from *H. butylicus*.
d) Clone and overexpress Hbut_0414 in *E. coli, and* purify recombinant Hbut_0414
e) Determine if the recombinant Hbut_0414 is a functional ADH and/or the ADH responsible for 1-butanol production.
f) Detect ADH activity from the cell-free extract of *H. butylicus*. Purify the ADH from the cell-free extract of *H. butylicus*, and identify the gene encoding the purified ADH.
g) Characterize the purified recombinant Hbut_0414 (ADH1) and the ADH purified from the cell-free extract (ADH2), and determine their physiological functions.

Chapter 2 Materials and Methods

2.1 Materials

2.1.1 Microorganisms

H. butylicus (DSM 5456) was obtained from the Deutsche Sammlung von Mikroorganismen und Zellkulturen, Braunschweig, Germany.

E.coli DH5α [(*supE44 ΔlauU 169 Φ80 lazZΔM15*) *hsdR17 recAlgyrA96 thi-1 relA*l] (Biomedical Research Laboratories, CA, USA)

E.coli BL 21 (DE3)-Rosetta [F^-, ompT, hsdSB ($r_B^- m_B^-$) gal dcm lacY1, pRARE (CamR)] (Strategene, CA, USA)

2.2 Growth of *H. butylicus*

2.2.1 Cultivation and growth condition

Growth of *H. butylicus* used medium as described in Zillig (Zillig, Holz et al. 1990) with modifications **(Table 2)**. The preparation of trace elements solution was according to the DSMZ formula with modifications from Balch (Balch, Fox et al. 1979)

Table 2. *H. butylicus* medium composition

Chemicals	(g/L)
NaCl	17.0
$MgSO_4 \cdot 7H_2O$	3.5
$MgCl \cdot 6H_2O$	2.75
KCl	0.325
NaBr	0.05
H_3BO_3	0.0015
$SrCl \cdot 6H_2O$	0.0075
Citric acid	0.005
KI	0.0025
$CaCl_2 \cdot 2H_2O$	0.2
KH_2PO_4	0.5
$NiCl_2 \cdot 6H_2O$	0.002
$(NH_4)_2SO_4$	0.01
Sulfur	10.0
NH_4Cl	0.5
Tryptone	6.0
100x Trace mineral	10.0 ml
Resazurin	0.001
HEPES	5.2
$Na_2S \cdot 9H_2O$ (3%w/v)	10.0 ml

For small scale growth, the medium was prepared as described above without $Na_2S{\cdot}9H_2O$ and the pH was adjusted to 6.6 with 2 M NaOH. 20 ml of medium was dispensed to a 60 ml serum bottle and sealed with a sterile gray butyl stopper (20 mm, Fisher Scientific, Ontario) and crimped with an aluminum seal (20 mm CS/M, Fisher Scientific, Ontario) with a hand crimper (Wheaton, New Jersey). The medium was degassed and pressurized with 3 psi nitrogen gas immediately. For sterilization, the medium was heated in a water bath (ISO Temp 215, Fisher Scientific, Ontario) at 90 ^{o}C for at least one hour on three subsequent days. Before use, the medium was reduced by adding 0.2 ml sterile and anaerobic 3% (w/v) $Na_2S{\cdot}9H_2O$ and was reduced at 95 ^{o}C for 15-20 minutes. The medium was then inoculated with 10% (v/v) fresh, late log phase, seed-culture with a final cell density of around 1 x 10^8 cells/ml and overpressurized with 100% H_2 (by flushing out nitrogen gas in the headspace) at 3 atms. Subsequently, the medium was incubated at 95°C for cultivation. Samples were withdrawn every eight hours using a 1 ml anaerobic sterile gas tight syringe to monitor growth until stationary phase.

Large scale growth was achieved by using a 1 L flask (Pyrex, Mexico) with 500 ml of medium that was prepared as described above. For growth under anaerobic condition, the flask was sealed with a black rubber stopper (size 7) that had an access port fitted with a sterile gray butyl stopper (20 mm) and an aluminum cap (20 mm) (Fisher Scientific, Ontario). The black rubber stopper was secured on the mouth of the flask using an aluminum clamp (Science Shop, University of Waterloo, Waterloo) which is a device fastened with screws and wing nuts. The flask was then connected to the manifold for degassing with a rubber tube (Fisher Scientific, Ontario). Similarly, the medium is sterilized by heating at 90 ^{o}C for at least an hour on three subsequent days in an incubator (Lunaire, Pennsylvania). Prior to inoculation with 10% (v/v) seed culture, 2 ml of 15% (w/v) $Na_2S{\cdot}9H_2O$ was added for reduction at 95 ^{o}C for 15-20 minutes. The medium was overpressurized with 100% H_2 at 5 psi (0.34 atm) and incubated at 98 ^{o}C for cultivation.

Samples were withdrawn at different time intervals for monitoring the growth until late log phase at which the cells were harvested.

2.2.2 Monitoring the growth of *H. butylicus*

H. butylicus cell numbers were monitored over time by direct cell counting using a Petroff-Hausser counting chamber (0.02 mm deep, Hausser Scientific, PA) and a Nikon Eclipse E600 phase-contrast light microscope. Each point in the growth curves is an average of measurement values in triplicate. The growth curves were plotted on a semilogarithmic scale with $\log_{10}$ (cell density) versus time.

2.2.3 Cell mass collection and storage of microorganisms

Cells were harvested using centrifugation. 250 ml Sorvall centrifugation tubes (Kendro Laboratory Products, Connecticut) were used with a Sorvall GSA rotor (Sorvall Instruments, Minnesota) in a Sorvall 6 refrigerated super-speed centrifuge. The culture was cooled down on ice before centrifugation. The temperature was set at 4 °C and the speed was 8,000 rpm (GSA rotor: 10,444 × *g*) for 15 minutes. The cell pellet of *H. butylicus* after harvesting was stored in a 50 ml sterilized falcon tube and immediately frozen in liquid nitrogen and stored at -80 ^{o}C until used.

2.3 Detection of metabolic products under different growth conditions

2.3.1 HPLC standard curves

Standard curves were prepared for acetate, acetone, ethanol, butyrate, 2-propanol and 1-butanol at concentrations of 0.5 mM, 1.0 mM, 2.0 mM, 2.5 mM, and 5.0 mM except for acetate where the concentrations were double the values above. Acetone, ethanol, 1-butanol, and 2-propanol are volatile and each with concentrations at 2.0 mM, 5.0 mM and

10.0 mM were prepared in a master mix solution and subsequently heated at 95 ^{o}C for 30 minutes, 1 hour, 2 hours and 3 hours to compare the loss of alcohol and acetone into head space. Two standard curves were made for acetone, one at 95 ^{o}C and one at 25 ^{o}C.

2.3.2 Detection of metabolic products of *H. butylicus*

Soluble end-products were measured using high performance liquid chromatography (HPLC) (Prominence HPLC, Shimadzu, Japan) equipped with an LC-20AT solvent delivery unit, SIL-20AC autosampler, CBM-20AC column oven and an Alltech organic acid OA-1000, 7.8 x 300 mm column (Fisher Scientific, ON). The mobile phase consisted of 60% Millipore water and 40% 0.02125 M H_2SO_4. The flow rate was 0.4 ml/min using the low pressure gradient flow setting with a column temperature of 60 ^{o}C and pressure between 680 to 720 psi. Acetate, acetone, ethanol, butyrate, 1-butanol and 2-propanol were quantitatively detected using HPLC. Isobutyrate, isovalerate, propionic acid, succinic acid, formic acid and lactic acid were also qualitatively detected.

Different growth conditions included different pH values (pH 6.0, 6.5, 7.0, 7.5 and 8.0) at 3 atm H_2 overpressurized and different overpressure of 100% H_2 (3, 2, 1.5, 1.0, 0.5, 0.34, and 0.2 atm) at pH 7.0. Cultures grown without sulfur or H_2 were also prepared. Media samples of approximately 0.8 ml were withdrawn at the late log phase from the above conditions and were filtered through 0.45 μm 4 mm nylon syringe filters (Thermo Scientific, ON) before aliquoting into HPLC vials (Mandel Scientific, ON). In addition, samples from growth conditions at pH 7.0, 7.5, without sulfur or H_2 were collected at initial, early-log, mid-log, late-log, and stationary phases to monitor end-products of production. Samples of 20 μl were injected into the HPLC and the application software program LC solutions (Shimadzu, Japan) was used for displaying and analyzing the data.

2.4 Cloning and overexpression of Hbut_0414

2.4.1 Preparation of stock solutions of antibiotics and reagents

A Stock solution of chloramphenicol was prepared in a concentration of 0.34 mg/ml in 100% pure ethanol, whereas for kanamycin was at 0.5 mg/ml in deionized water. The stock solutions were 1000 times concentrated and filtered sterilized through 0.2 μm filter membranes (Corning NJ, USA) for storage at -20 ^{o}C until used. IPTG (isopropyl β-D-1-thiogalactopyranoside) was prepared at 0.1 M in deionized water. It was then filter sterilized through a 0.2 μm filter membrane and stored at -20 ^{o}C until used.

2.4.2 Preparation of competent cells

2.4.2.1 *E. coli* DH5α high efficiency competent cells

E. coli DH5α as a non-expression host was used first for transformation. The competent cells were prepared following a standard protocol. *E. coli* DH5α cells were first streaked onto an LB plate and grown overnight at 37 ^{o}C. On the next day, a well-formed colony was picked and transferred into 250 ml LB media. The cells were then grown at 37 ^{o}C at 250 rpm until OD_{600} 0.4 (around 3 to 4 hours) and was immediately chilled on ice for 20 minutes. The cells were harvested at 3,000 x *g* for 10 minutes at 4 ^{o}C and the cell pellets were re-suspended in 15 ml of ice-cold 0.1 M $CaCl_2$ followed by incubation on ice for 30 minutes. The suspension was then centrifuged at 3,000 x *g* for 10 minutes at 4 ^{o}C and the cell pellets were carefully re-suspended in 4 ml of ice-cold 0.1 M $CaCl_2$ containing 15% glycerol. Cells were dispensed into pre-chilled 1.5 ml eppendorf tubes and frozen in liquid nitrogen immediately. Cells were stored at -80^{o}C and used for transformation for approximately 6 months.

2.4.2.2 *E. coli* BL 21 (DE3)-Rosetta competent cells

Competent *E. coli* Rosetta cells were prepared using a similar procedure as described above with the modification of adding 34 µg/ml chloramphenicol onto LB media and LB agar plate for a specific selection.

2.4.3 Preparation of *H. butylicus* genomic DNA

The genomic DNA from *H. butylicus* was isolated from lysis of 0.2 g of whole cells. The cells were grown in degassed media and harvested by centrifugation. The cells were lysed using 100 mg/ml lysozyme and 25% SDS, then was subsequently treated with 1 mg/ml proteinase K and 5 M NaCl. DNA from the mixture was isolated using a solution of phenol, chloroform, and isoamyl alcohol in the ratio of 25:24:1. The genomic DNA was precipitated by 100% isopropanol and desalination with 75% ethanol. The quality and quantity of DNA were measured using a NanoDrop spectrophotometer and run on a 1% agarose gel for visualization.

2.4.4 Primers and PCR conditions

The target gene Hbut_0414 was amplified from genomic DNA using primers, HButF1, HButF2, HButR1, and HButR2 **(Table 3)**. HButF1 and HButR1 were designed at the 5' and 3' region of the gene and HButF2 and HButR2 were designed at the termini of the open reading frame. Primers were designed with software Primer Premier5 (Premier Biosoft, USA) and parameters were optimized. Two rounds of PCR were performed for confirmation of the correct gene being amplified by PCR. The annealing temperature for primers in both rounds was at 55^{o}C and amplified for 35 cycles. *Taq* DNA polymerase was used for amplification of the gene in a volume of 50 µl and all reagents were added according to standard conditions recommended by the suppliers. After PCR amplification, the PCR product was separated by electrophoresis on a 1.5% agarose gel to check for

appropriate size and the PCR products were then purified using QIAquick PCR purification kit (Qiagen, Canada).

Table 3. List of primers used for cloning and sequencing the annotated zinc dehydrogenase gene (Hbut_0414)

Name of Primers	Nucleotide sequence (5'- 3')	Restriction enzyme sites (underlined)
HbutF1	GCGTGCCCAGCATTGTGATT	
HbutF2	GGAATTC**CATATG**CAGCATGTCCAGCCACTAG	*NdeI*
HbutR1	AACGGCGGCGGCAAGAACAC	
HbutR2	GGC**GAGCTC**CTAGCCGAGCCTATACACTAGACCC	*XhoI*
T7 terminator	GCTAGTTATTGCTCAGCGG	

2.4.5 Construction of expression vector

The expression vector for Hbut_0414 was constructed through the following procedures. Hbut_0414 was isolated and amplified by gene specific primers with appropriate restriction enzyme sites. The forward primers HbutF2 was linked to *NdeI* recognition site and the reverse primer HbutR2 was liked to *XhoI* recognition site. The gene was amplified by PCR with initial denaturation at 95 ^{o}C for 5 minutes, followed by 35 cycles of denaturation at 95 ^{o}C for 30 seconds, annealing at 55 ^{o}C for 30 seconds and extension at 72 ^{o}C for 1 minute and a final extension step at 72 ^{o}C for 10 minutes. The PCR products were purified by QIAquick PCR purification kit (Qiagen, ON, Canada) and digested with *NdeI* and *XhoI* to create sticky ends for ligation. The digestion was performed at 37 ^{o}C for 30 minutes to 1 hour using 10-20 U of restriction enzyme per 0.5-1.5 µg DNA. After completion of the restriction digestion, the reaction mixture was analyzed on a 1.5% agarose gel.

The expression vector pET30a, 5630bp, $P_{T7,}$ Kan^{R} (Novagen, WI, USA) with similar cut ends was used for ligation. The insert to vector molar ratio was in 3:1 to optimize the ligation and the ligation was performed using 1U T4DNA ligase (Fermentas, Canada) incubated at 16 ^{o}C overnight.

The ligation mixture (3 µl) was transformed into *E. coli* DH5α by standard heat stock method of heating at 42 ^{o}C for 45 seconds. After recovery on ice for 30 minutes, *E. coli* was plated on an agar plate containing 50 µg/ml of kanamycin. Colony PCR was performed with primers HbutF2 and T7 terminator to select colonies with the inserted plasmid and gene of interest. The same colony was then grown in 5 ml LB media with 50 µg/ml kanamycin for plasmid extraction with a plasmid extraction kit (Bio Basic Inc, Canada) the next day.

After plasmid extraction, the plasmid was digested with the same restriction enzymes used in cloning to verify the gene insert. The recombinant plasmids were sent to The Centre for Applied Genomics at the University of Toronto for Sanger sequencing.

The recombinant plasmid that was confirmed to have the inserted gene was transformed into the *E. coli* Rosetta 2 expression strain using standard heat shock method as described previously. As *H. butylicus* coding genes have a very different codon usage compared to *E. coli*, *E. coli* Rosetta 2 was chosen as it contains 6 tRNAs for rare codons (AGG, AGA, CGG, AUA, CUA, CCC, and GGA). The transformation mixture was spread onto an agar plate supplemented with 50 μg/ml kanamycin and 34 μg/ml chloramphenicol for selection of *E. coli* colonies that contained the constructed plasmids.

2.4.6 Growth of *E. coli*

E. coli was grown in LB media (Difco, New Jersey) with 10 g/L of tryptone, 5 g/L of yeast extract and 10 g/L of NaCl. Deionized water was added to a total volume of 1 L and autoclaved for 30 minutes at 121 ^{o}C. *E. coli* strains were grown in 500 ml LB media at 37 ^{o}C, shaken at 180-200 rpm in 2 L baffled flasks. The inoculum for culture was 12-14 colonies from an agar plate with selective antibiotics or with a previous culture at late exponential phase in 1-2% (v/v). For the recombinant stock of *E. coli*, a single colony was picked from an LB agar plate containing 50 μg/ml kanamycin and inoculated into a 5 ml liquid LB media with the same selective antibiotic. It was then grown at 37 ^{o}C with vigorous shaking until OD_{600} 0.6-0.8. Then an aliquot (0.8 ml) of the bacterial culture was transferred to a sterilized cryo-vial containing 0.5 ml of 50% glycerol. After gently mixing the culture, it was stored at -20^{o}C or -80^{o}C for short and long term storage, respectively.

2.4.7 Optimization of induction conditions

For expression of the cloned gene in *E. coli* Rosetta 2, the transformants were grown in LB medium at 37 ^{o}C before induction. Recombinant protein expression was driven by the T7-lac promoter and the recombinant enzyme was obtained in the periplasmic space when IPTG was added. The concentration of IPTG, temperature of induction and cell density at which the IPTG was added affected the final yield of the recombinant protein. To optimize the yield, the inducer IPTG was added in the exponential phase when the OD_{600nm} of the *E. coli* culture reached 0.4-1.0, and the ideal yield with the highest activity presented is when the cell culture reached OD_{600nm} of 0.8. Different concentrations of IPTG, 0.1 mM, 0.2 mM, 0.4 mM, 0.6 mM, 0.8 mM and 1.0 mM and different temperatures 18 ^{o}C, 25 ^{o}C, 30 ^{o}C and 37 ^{o}C were tested to optimize recombinant protein expression. Whole cells lysates of *E. coli* were run on SDS-PAGE for visualization of recombinant protein overexpression. The culture was then induced with 0.6 mM of IPTG and cultivated at 30 ^{o}C for 12-16 hours prior to harvesting of the cells.

2.5 Enzyme assays

2.5.1 Alcohol dehydrogenase

The assay for alcohol dehydrogenase was based on monitoring the substrate-dependent absorbance change of NADP(H) at 340 nm (ε_{340} = 6.3$mM^{-1}cm^{-1}$). Unless otherwise specified, the enzyme assay was carried out in duplicate using the assay mixture (2 ml) for alcohol oxidation containing 60 mM 1-butanol and 0.4 mM NAD(P) in 100 mM EPPS (4-(2-Hydroxyethyl)-1-piperazinepropanesulfonic acid) buffer (pH 8.5 for ADH1 and 9.0 for ADH2). The assay mixture (2 ml) for reduction of ketone/aldehyde contained 30 mM butyraldehyde and 0.4 mM NAD(P)H in 100 mM citrate acid (pH 5.0) for ADH1 and PIPES (piperazine-N,N'-bis(2-ethanesulfonic acid) (pH 6.0) for ADH2. The addition of

the appropriate amount of purified enzyme (35 μg for ADH1 and 15 μg fir ADH2) initiated the enzyme assay. One unit of activity is defined as 1 μmol of NAD(P)H formed or oxidized per min.

2.6 Purification of ADHs

2.6.1 Preparation of cell-free extract

The steps for preparation of cell-free extracts were carried out anaerobically. Frozen cells were transferred into a degassed serum bottle and immediately sealed with a gray butyl stopper and capped with an aluminum seal. The bottle was immediately degassed for 30 minutes and pressurized by 3 psi N_2 gas. Lysing buffer contained 50 mM Tris-HCl at pH 7.5, 2 mM sodium dithionite, 2 mM dithiothreitol, 0.1 mg/ml lysozyme, and 0.01 mg/ml DNase I (Sigma, Oakville). Lysing buffer was then degassed. The volume of anaerobic lysis buffer was about five times the weight of the cells (v/w). The lysing buffer was then anaerobically transferred with a syringe to the degassed serum bottle containing the cells and the cell suspension was stirred with a magnetic stirrer at 37 ^{o}C for 2 hours. To achieve complete breakage of cells, the cell suspension was then transferred into a French Press cell (Thermo scientific, MA) and lysed at 1,500 psi (25 k psi on cells). The lysis mixture was centrifuged at 8,000 rpm for 15 minutes at 4 ^{o}C to separate the cell-free extract and crude extract. The cell-free extract was then transferred anaerobically into a degassed serum bottle for further experimental use.

2.6.2 Enzyme purification

AKTA^{TM} Fast Performance Liquid Chromatography (FPLC), a liquid chromatography system with P-920 pump (Amersham Pharmacia Biotech) was used to purify the enzymes under anaerobic conditions using Tris-HCl buffer (pH 7.8) at room temperature. Buffer A

consisted of 50mM Tris-Base, 5% (v/v) glycerol, 2mM sodium dithionite and 2mM dithiothreitol. The buffer was filtered using filter paper, degassed and maintained at 3 psi N_2. The eluted samples were collected anaerobically with a needle in degassed 6 ml serum bottles.

2.6.2.1 Purification of ADH1

The recombinant ADH encoded by Hbut_0414 (ADH1) was purified from *E. coli* biomass grown until late log phase. The cell-free extract (CFE) from *E. coli* was prepared anaerobically. Four columns were run in series for the purification of ADH1. The CFE was first loaded on a DEAE-sepharose column (3 cm x 5 cm, column volume [CV] 35 ml) that was equilibrated with 70 ml of buffer A. Buffer B was prepared by dissolving 2 M NaCl in buffer A. The bound proteins were eluted with a gradient of 3 CV buffer B from 12% to 35% and ADH1 was eluted when 0.3 M of buffer B was applied to the column at a flow rate of 2 ml/min. Fractions containing the ADH activity were combined and loaded onto a hydroxyapatite column equilibrated in Buffer A (2.6 cm x 12 cm) at a flow rate of 1.0 ml/min. Buffer B (0.32 M potassium phosphate dibasic and 0.18 M potassium monobasic in buffer A) from 35% to 100% was applied to the column in 3 CV. ADH1 started to elute from the column when 0.5 M potassium phosphate buffer was applied to the column. Fractions containing the ADH activity were then pooled and applied to a phenyl-Sepharose column (5 cm x 10 cm) that had been equilibrated with 2.0 M $(NH_4)_2SO_4$ in buffer A at a flow rate of 2 ml/min. A linear decreased gradient from 0.82 M to 0 M $(NH_4)_2SO_4$ was applied to the column and ADH1 started to elute out when 0.0 M of $(NH_4)_2SO_4$ was applied. Fractions containing the ADH activity were combined, concentrated and desalted with ultrafiltration using a Ultracel PL 10 membrane (EMD Millipore Ultracel, ON).

ADH1 was loaded onto a Superdex 200 gel filtration column (2.6 x 60 cm: Amersham Biosciences) after the phenyl-Sepharose column to determine the molecular mass of its

native form. The column was first equilibrated with 50 mM Tris-HCl (pH 7.8) containing 100 mM KCl. The size of its native form was calculated based on the elution volumes of standard proteins (Pharmacia, NJ, USA) that contained blue dextran (molecular mass, Da, 2,000,000), thyroglobulin (669,000), ferritin (440,000), catalase (232,000), aldose (158,000), bovine serum albumin (67,000), ovalbumin (43,000), chymotrypsinogen A (25,000) and ribonuclease A (13,700).

2.6.2.2 Purification of ADH2

The ADH from the cell-free extract of *H. butylicus* (ADH2) was purified from *H. butylicus* biomass in a similar approach. *H. butylicus* was grown until late log phase before harvesting. The cell-free extract was prepared anaerobically. Three columns, DEAE-sepharose, hydroxyapatite, and phenyl-Sepharose, were run in series for purification. The CFE was first loaded onto a DEAE-sepharose column (3.5 cm x 5 cm) that was equilibrated with buffer A. The bound proteins were eluted with a gradient of 3 CV buffer B from 5% to 50% and ADH2 was eluted when 0.55 M of buffer B was applied to the column at a flow rate of 2 ml/min. Fractions containing ADH activity were combined and loaded onto a hydroxyapatite column (2.6 cm x 12 cm) at a flow rate of 1.0 ml/min. The column was applied with a gradient of buffer B (0.32 M potassium phosphate dibasic and 0.18 M potassium monobasic in buffer A) and ADH2 started to elute from the column when 0.5 M potassium phosphate buffer was applied to the column. Fractions containing the ADH activity were then pooled onto a phenyl-Sepharose column (5 cm x10 cm) that had been equilibrated with 2.0 M $(NH_4)_2SO_4$ in buffer A overnight at a flow rate of 0.5 ml/min. ADH2 started to elute when 0.8 M of $(NH_4)_2SO_4$ was applied. Fractions with ADH activity were collected in 6 ml serum bottles with 3 ml in each bottle.

2.7 Characterization of ADHs

2.7.1 Optimum pH

The optimal pH for alcohol oxidation and aldehyde/ketone reduction of ADH1 and ADH2 were determined by enzyme assay of 1-butanol oxidation and butyraldehyde reduction. The standard enzyme assay was performed with 100 mM buffer at different pH at 60 ^{o}C for ADH1 and 80 ^{o}C for ADH2. The optimal pH for oxidation was determined using buffers HEPES (7.5, 8.0), EPPS (8.0, 8.5, 9.0) and glycine (9.0, 9.5, 10.0) for ADH1 and EPPS (8.0, 8.5, 9.0), glycine (9.0, 9.5, 10.0) and CAPS (10.0, 10.5, 11.0, 11.5) for ADH2. The optimal pH for reduction was determined using citrate (4.5, 5.0, 5.5, 6.0) and PIPES (6.0, 6.5) for ADH1 and citrate (5.5, 6.0) and PIPES (6.0, 6.5) for ADH2.

2.7.2 Temperature dependence

The effect of temperature on the enzyme activity was examined at temperatures between 30 ^{o}C to 80 ^{o}C for ADH1 using the standard enzyme assay described in section 2.5.1. Temperatures ranging from 50 ^{o}C to 90 ^{o}C were used for ADH2. The thermostability of both ADHs was also examined. For ADH1 temperatures of 60 ^{o}C, 75 ^{o}C and 95 ^{o}C were used and for ADH2, temperatures of 85 ^{o}C and 95 ^{o}C were used. Residual activities were measured after different time intervals of incubation and compared to the initial activity before heat treatment.

2.7.3 Oxygen sensitivity

The effect of oxygen on enzyme activity was investigated by exposing the purified ADHs to air at room temperature under stirring and residual activity after exposure to oxygen was determined. The exposure was performed in the presence of 2mM DTT and 2mM SDT.

The residual activities of each sample at different time intervals were measured using the standard assay.

2.7.4 Substrate specificity and enzyme kinetics

Substrate specificity was determined using primary (C1-8) and secondary (C3-C6) alcohols, diols (C3-5) and glycerol at 60 mM or aldehydes (C2-4), benzaldehyde and ketone (C3-4) at 30 mM under optimal enzymatic conditions for both ADH1 and ADH2.

Enzyme kinetic parameters were determined using different substrates and cofactors ($NAD(P)^+$ or NAD(P)H). For the oxidation reaction, 1-propanol, 2-propanol, ethanol, and 1-butanol were used and the corresponding ketone acetone and aldehydes propanal, butyraldehyde and acetaldehyde for reduction were used for determining the respective K_m and k_{cat}. NAD(H) was the cofactor used for ADH1 and NADP(H) was for ADH2. Unless specified, various substrates with concentrations from 0 to $\geq$ 10 K_m unless specified were used to determine the corresponding activity. Substrate was prepared at a concentration of 0.3 M and different volume (2.5 μl, 5 μl, 7.5 μl, 10 μl, 15 μl, 20 μl, 25 μl, 50 μl, 75 μl, 100 μl and 200 μl) of the solution were added into the enzyme mixture to achieve different final concentrations of the substrates. The concentration of the corresponding cofactor was kept constant, which was $\geq$ 10 K_m. Apparent values of K_m and k_{cat} were calculated using the non-linear curve fittings of the Michaelis-Menten equation $V = \frac{V_{max}[S]}{K_m+[S]}$ from GraphPad Prism (GraphPad Software, Inc, CA).

2.8 Protein sequence analysis

ADH2 was purified to homogeneous after the phenyl-Sepharose column and only one band was visible on a SDS-PAGE. The band was cut out precisely and preserved in Millipore water in an eppendorf tube wrapped in parafirm. It was then sent out for peptide identification by mass spectrometry at the Alberta Proteomics and Mass Spectrometry Facility, University of Alberta (AB, Canada).

ADHs protein sequences used in sequence alignments were from the database available at http://www.ncbi.nlm.nih.gov/guide/proteins/ and listed in the Appendix. Protein alignments were done using the online software Clustal Omega (http://www.ebi.ac.uk/Tools/msa/clustalo/). Conserved domains were identified from the conserved domains database (http://www.ncbi.nlm.nih.gov/cdd/).

2.9 Other methods

2.9.1 Protein determination

The Bradford assay was used to measure protein concentrations in solutions using a spectrophotometer (Bradford 1976). Bio-Rad reagent (200 µl) was added into 800 µl of diluted protein solution and a control was set by replacing the protein solution with 800 µl deionized water. A linear calibration curve was constructed with known concentrations of standard protein bovine serum (BSA, albumin fraction V) from 1 mg to 20 mg/ml standard solution. The protein reading was taken at 595 nm based on the λ_{max} of coomassie blue dye binding to proteins.

2.9.2 SDS-PAGE

SDS-PAGE was performed using a Hoefer Mighty Small 250 mini system (Amersham Biosciences, Montreal) based on the methods by Laemmli (Laemmli 1970). Protein samples for SDS-PAGE were prepared by heating in boiling water for 10 minutes in 1x sample loading buffer (0.1 M sodium phosphate buffer, 4% SDS, 10% 2-mercaptoethanol, 20% glycerol, pH 6.8). The protein samples were loaded onto an SDS-PAGE (12.5 % acrylamide) and was run under a constant voltage of 150 V. The gel was then stained with Coomassie Brilliant Blue R250 for at least one hour on a shaker at approximately 100-150 rpm. It was followed by destaining with a destaining solution (15% methanol, 10% glacial acetic acid and 75% deionized water) until protein band(s) started to become visible. The molecular mass of the enzyme under denaturing conditions was estimated by using medium range markers phosphorylase B (97.4 kDa), BSA (66 kDa), ovalbumin (43 kDa), carbonic anhydrase (31 kDa), soybean trypsin inhibitor (20.1 kDa), and lysozyme (14.3 kDa) (Sigma, Oakville)

Chapter 3 Results

3.1 Growth of *H. butylicus*

3.1.1 Growth of *H. butylicus* in two mediums

H. butylicus is only able to grow on peptides mixture, and tryptone (6.0 g/L) was used as the substrate for growth. It is reported that sulfur and hydrogen are required for growth (Zillig, Holz et al. 1990). In addition to the sulfur (10 g/L) and high pressure of H_2 (3 atmosphere overpressure), 20 mM of HEPES (5.2 g/L) was added as a buffer to maintain a constant pH of 7.0 at 95 ^{o}C. In comparison to the media without HEPES, the maximum cell densities obtained in the media with HEPES were doubled from around 5.0 x 10^7 cells/ml to 1.0 x 10^8 cells/ml **(Fig 3)**.

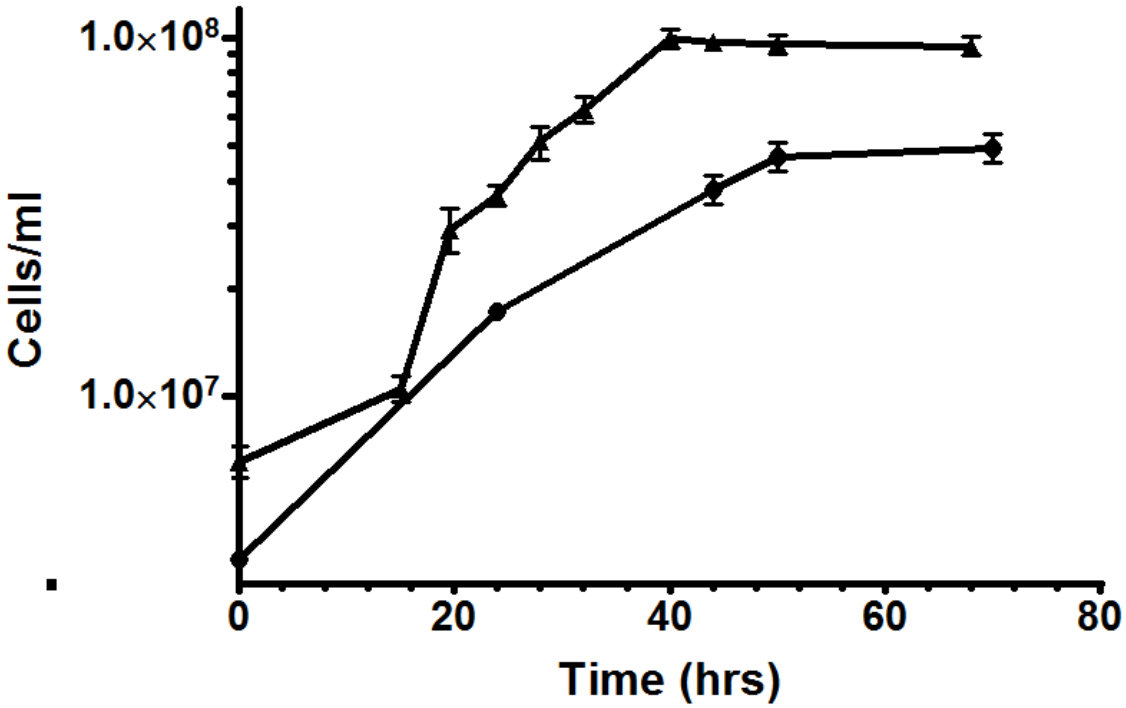

Figure 3. Growth of *H. butylicus* in two different mediums. Filled triangles (n=3) represented the growth of *H. butylicus* in media with HEPES (5.2 g/L), and the filled circles (n=8) represented the growth in media without HEPES. Cultures were grown in the same volume of media under the same initial conditions. Data were presented as mean ± standard deviation.

3.1.2 Effect of pH, hydrogen pressure and sulfur on the growth of *H. butylicus*

The effect of pH, hydrogen pressure and sulfur on growth was tested. To better understand the effect of pH on growth, the pH of the media was adjusted to 6.0, 6.5, 7.0, 7.5 and 8.0 respectively, keeping other conditions the same. The pH of the medium was measured at room temperature before inoculation. pH was monitored throughout growth and measured by pH papers (Millipore, CA) and showed similar pH as initial. Based upon a comparison of the final cell density, the optimal pH was 7.0, followed by 7.5, 8.0, 6.5 and 6.0 **(Fig 4)**. The growth curve for medium at pH 8.0 exhibited a slower initial growth rate but had the greatest growth rate in the mid log phase that resulted in an increase in the final cell density.

The maximum cell density in media without sulfur at pH 7.0 had around 5 times lower cell density and a shorter log phase than the same media without sulfur **(Fig 4)**.

Different pressures of H_2 were used in the head space of 60 ml serum bottles with 20 ml media to examine the effect of H_2 pressure on growth. The growth curves showed that the higher the H_2 pressure, the higher the final cell density **(Fig 5)**. The growth curves also showed that cells grown at lower H_2 pressures (pressure $\leq$ 1.0 atmosphere overpressure) had longer lag phases but similar duration of exponential phases as the ones at higher H_2 pressure. Cells could still grow without H_2 but the final cell density was around 5 times lower than that obtained at 3 atmosphere overpressure and similar to that without sulfur in media.

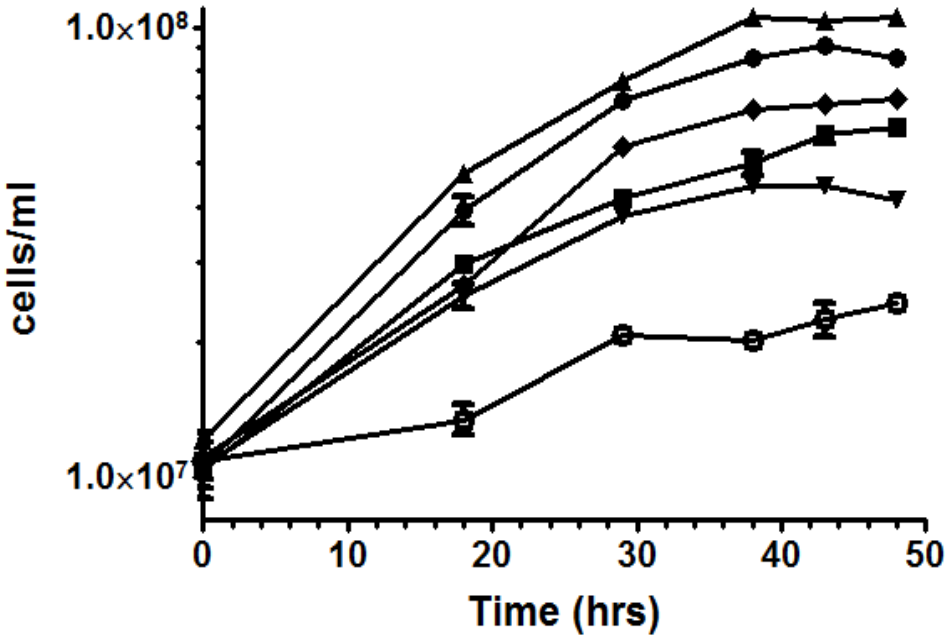

Figure 4. pH dependent growth of *H. butylicus*. pH 6.0 (inverted filled triangles), pH 6.5 (filled squares), pH 7.0 (filled triangles), pH 7.5 (filled circles), pH 8.0 (filled diamonds), and media without sulfur at pH 7.0 (open circles) were monitored in triplicate. Cells were grown in same volume and pressure of H_2 (3 atmosphere overpressure). Data were presented as mean $\pm$ standard deviation.

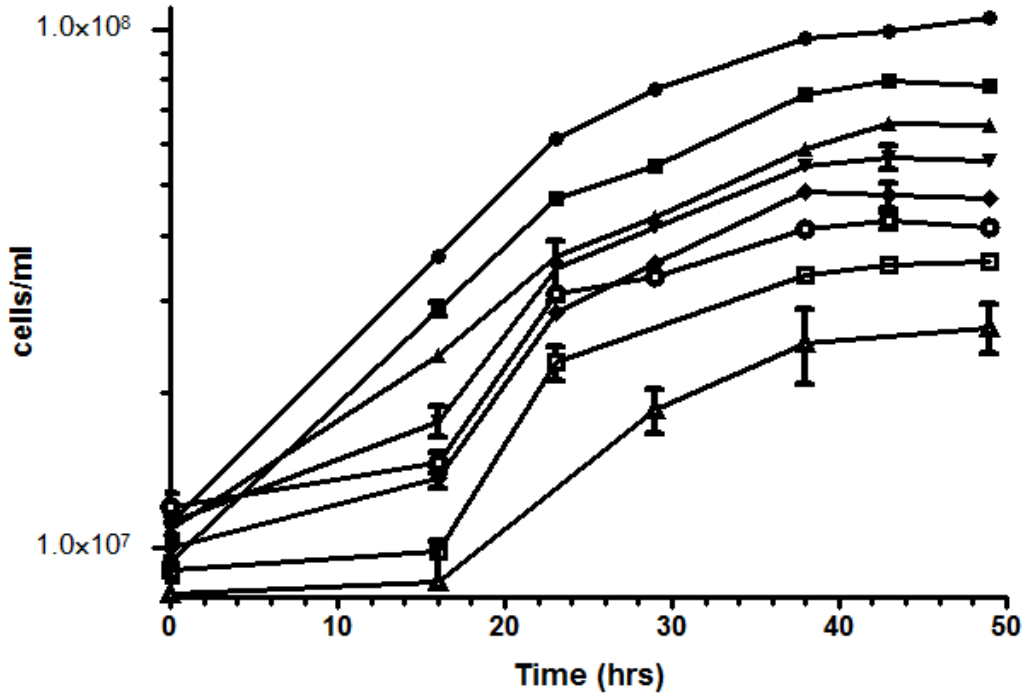

Figure 5. Growth of *H. butylicus* under different pressures of hydrogen. Growth under 3 atmosphere overpressure (filled circles), 2 atmosphere overpressure (filled squares), 1.5 atmosphere overpressure (filled triangles), 1.0 atmosphere overpressure (inverted triangles), 0.5 atmosphere overpressure (filled diamonds), 0.34 atmosphere overpressure (open circles), 0.2 atmosphere overpressure (open squares) and 100% nitrogen gas at 0.2 atmosphere overpressure (open triangles). Growth curves were monitored in triplicate and all cells were grown at pH 7.0 with 10 g/L of sulfur. Data were presented as mean $\pm$ standard deviation.

3.2 Metabolic end products

3.2.1 Standard curves for HPLC

The standard curves shown were used for determining concentrations of respective substrates **(Fig 6)**.

A. acetate

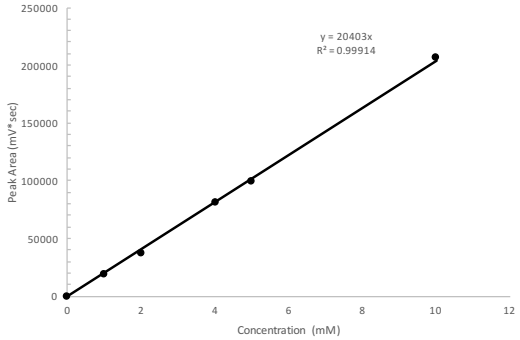

B. acetone

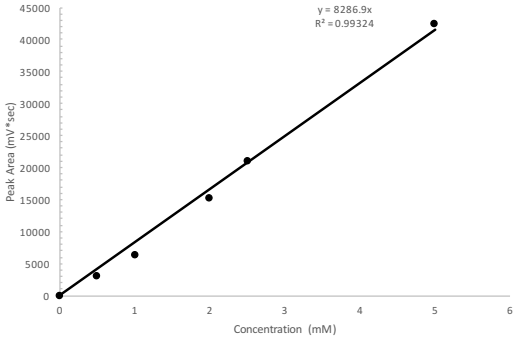

C. 1-butanol

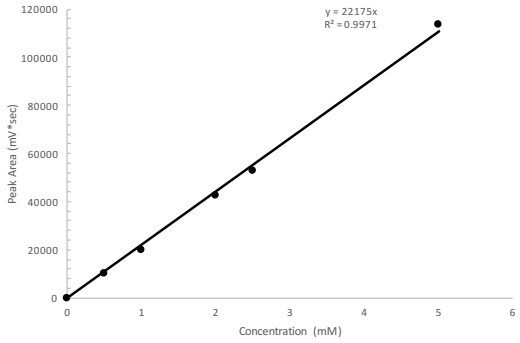

D. butyrate

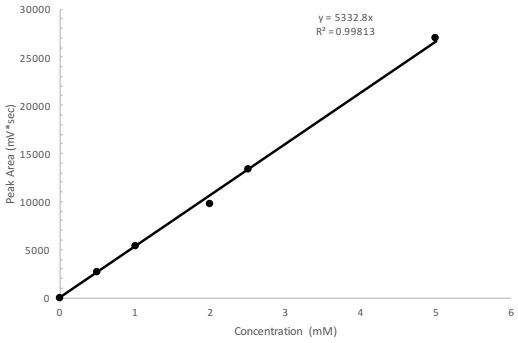

E. ethanol

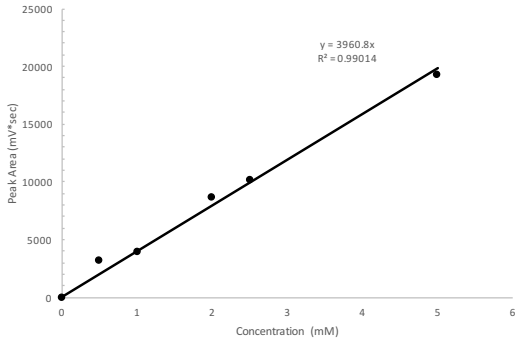

F. isopropanol

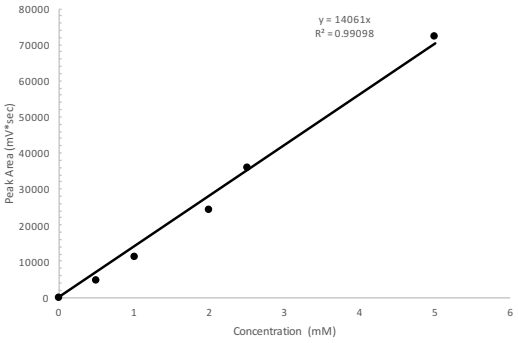

Figure 6. Standard curves for determination of (A) acetate, (B) acetone, (C) 1-butanol, (D) butyrate, (E) ethanol and (F) isopropanol using HPLC.

3.2.1.1 Comparison of acetone, 1-butanol, ethanol and 2-propanol concentration at room temperature and at 95^{o}C

As acetone, 1-butanol, ethanol, and 2-propanol are volatile and *H. butylicus* cultures were incubated at 95^{o}C, the loss of those end-products into the head space had to be considered for an accurate measurement of the actual concentration of metabolic end-products in the media. To do so, acetone, 1-butanol, and ethanol in concentrations of 2 mM, 5 mM or 10 mM was mixed and heated at 95 ^{o}C for 0.5 hours, 1 hour, 2 hours and 3 hours respectively in a sealed serum bottle for determining the time for equilibrium and the concentration lost into the head space. As cultures were grown at high pressure, the master mix was prepared in duplicate with one set at 1 atmosphere pressure and another set at 3 atmosphere overpressure. After reaching equilibrium at approximately 1 hour, the acetone concentration significantly decreased but ethanol and 1-butanol had no apparent changes **(Fig 7 A, B, and C)**. Standard solutions of 2-propanol were prepared at 5 mM at high pressure and there was no apparent loss into the head space. At an initial concentration of 2 mM, acetone concentration decreased by around 80%. At a concentration of 5 mM, acetone decreased by around 70%, whereas, at a concentration of 10 mM, it decreased by around 60% **(Fig 7 A, B, and C)**. The same changes were observed in the set incubated at high pressure. The acetone concentration at room temperature was plotted against its concentration at 95 ^{o}C **(Fig 7D)** and the equation from the line of best fit (y=1.5246x) was used for a better estimation of acetone produced from *H. butylicus*. The concentration of acetone at 95 ^{o}C (x) represented the concentration detected in the HPLC and the concentration of acetone at 25 ^{o}C (y) resembled what was actually produced in the culture by *H. butylicus*.

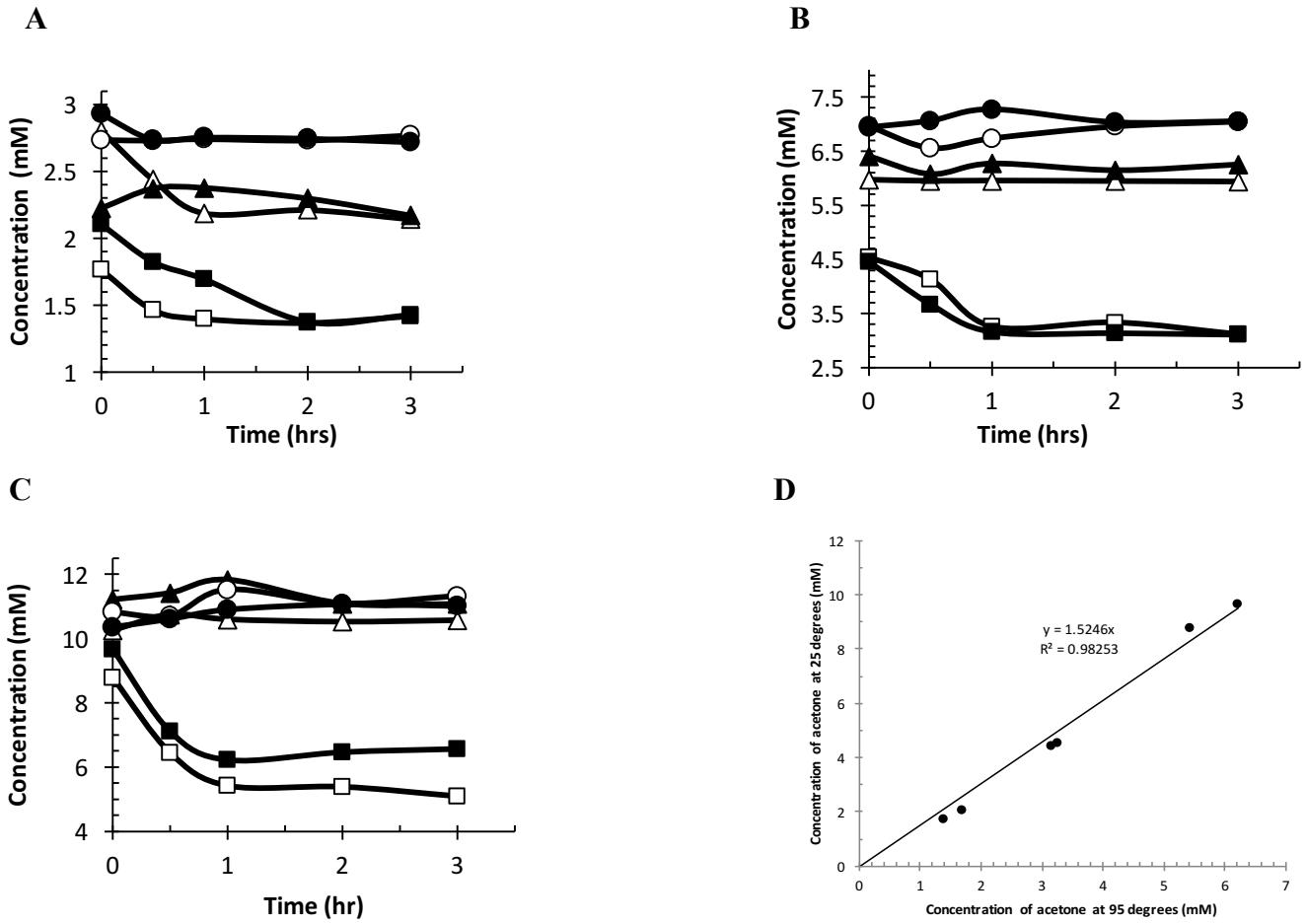

Figure 7. Comparison of acetone, 1-butanol and ethanol concentrations determined at room temperature and 95°C (A) 2 mM, (B) 5 mM and (C) 10 mM. (D) different concentrations of acetone at 25 °C and 95 °C. Acetone at 1 atmosphere (open squares), at 3 atmosphere overpressure (filled squares); ethanol at 1 atmosphere pressure (open triangles), at 3 atmosphere overpressure (filled triangles); 1-butanol at 1 atmosphere pressure (open circles), at 3 atmosphere overpressure (filled circles).

3.2.2 Metabolic end-products summary for *H. butylicus* under different growth conditions

Major metabolic end products from *H. butylicus* in culture media were detected using HPLC. As 1-butanol and acetate were detected as one of the major end products (Zillig, Holz et al. 1990), other end-products from the *Clostridium*'s butanol production pathway including butyrate, ethanol, 2-propanol and acetone were considered to be possible metabolites. Metabolic products from amino acid metabolism including propionic acid, isovaleric acid, and isobutyric acid; and from carbohydrate metabolism such as succinic acid, formic acid, and lactic acid were also qualitatively measured to give a comprehensive profile of *H. butylicus* metabolism. Metabolic end-products produced in cultures at late log phase, which was 39 hours after initiation of growth (growth of cells were monitored and growth curves were compared to determine late log phase), were determined (**Table 4**). All metabolic end-products from the *Clostridium* pathway except for ethanol were detected in more than one of the growth conditions. The HPLC peaks were identified by comparing the retention times of different known substrates. The media with and without inoculation showed a peak similar to that of the retention time of acetone. Using the same standard curve for acetone, the concentration was calculated to be around 0.3 mM. The concentrations detected in the cultures were well above this minor peak (0.3 mM) and production of acetone by *H. butylicus* was valid. The HPLC detection peaks of various metabolites in the media with inoculation and cultures grown under optimal conditions at different growth phases including early log phase, mid-log phase, late-log phase and stationary phase are included in the Appendix.

It was observed that the production of 1-butanol and acetone was directly correlated to the cell density (**Fig. 8 A and B**). Cells grown under 3 atmosphere overpressure at pH 7.0 had the highest production of 1-butanol while cells grown without sulfur showed no butanol production. The mean production of acetone and 1-butanol were the highest at pH 7.5 and pH 7.0 (**Fig. 8 C**). The production of acetone and 1-butanol decreased at pH 8.0. Butyrate

was not detected in some growth conditions probably due to a limitation in the detection of low butyrate. Acetate was detected in all growth conditions and conditions with higher cell densities had more acetate production than conditions with lower cell densities. It is interesting to note that 2-propanol was only detected in cultures grown at pH 7.0 and 7.5 with the highest production observed at pH 7.5. Isovaleric acid was also detected in the culture. Although the peak corresponded to formic acid was already present in the media before cultivation, the area increased along with the growth, indicating formic acid might be produced by *H. butylicus*. Propionic acid, isobutyric acid, succinic acid and lactic acid were not detectable.

Table 4. Metabolic end-product summary for *H. butylicus* under different growth conditions

Growth Condition	End product (mM)				
	Acetate	Acetone [a]	Butanol	Butyrate	2-propanol
Medium	-	0.290 ± 0.093 (n=2)	-	-	-
Medium with inoculation	-	0.302 ± 0.053 (n=2)	-	-	-
Without S	0.163 ± 0.010 (n=3)	0.729 ± 0.190 (n=6)	-	-	0.410 ± 0.094 (n=6)
Without H_2	0.189 ± 0.019 (n=3)	0.570 ± 0.036 (n=3)	0.213 ± 0.010 (n=3)	-	0.416 ± 0.048 (n=3)
0.34 atm	0.274 ± 0.044 (n=2)	1.159 ± 0.169 (n=2)	0.180 ± 0.008 (n=2)	-	-
0.5 atm	0.427 ± 0.040 (n=2)	1.174 ± 0.050 (n=3)	0.226 ± 0.042 (n=3)	0.432 ± 0.025 (n=2)	0.379 ± 0.048(n=3)
1.0 atm	0.381 ± 0.117 (n=3)	1.246 ± 0.109 (n=3)	0.264 ± 0.091 (n=3)	0.420 ± 0.016 (n=2)	0.349 ± 0.023 (n=2)
1.5 atm	0.360 ± 0.100 (n=3)	1.293 ± 0.028 (n=3)	0.287 ± 0.039 (n=3)	-	0.372 ± 0.035 (n=3)
2.0 atm	0.364 ± 0.088 (n=3)	1.459 ± 0.0487 (n=3)	0.301 ± 0.077 (n=3)	0.420 (n=1)	0.348 ± 0.023 (n=3)
3.0 atm	0.495 ± 0.119 (n=9)	1.542 ± 0.0432 (n=9)	0.414 ± 0.0410 (n=9)	0.538 ± 0.105 (n=6)	0.456 ± 0.056 (n=7)
pH 6.0	0.202 (n=1)	1.086 ± 0.071 (n=3)	0.183 ± 0.011 (n=2)	-	-
pH 6.5	0.202 ± 0.021 (n=3)	1.226 ± 0.112 (n=3)	0.228 ± 0.017 (n=2)	-	-
pH 7.5	0.431 ± 0.088 (n=6)	1.725 ± 0.222 (n=6)	0.403 ± 0.123 (n=6)	0.543 ± 0.069 (n=3)	0.587 ± 0.0223 (n=6)
pH 8.0	0.240 ± 0.016 (n=3)	1.329 ± 0.209 (n=3)	0.208 ± 0.0184 (n=3)	-	-

Concentrations of acetate, acetone, butanol, butyrate, ethanol and 2-propanol were determined from the standard curve of the respective end product and above the detection limit of HPLC. Medium with inoculation was inoculated with the same amount of seed culture as other growth conditions but without initiation of growth. At all H_2 pressures, the growth was at pH 7.0. At all pH values, the growth was at 3 atmosphere overpressure of H_2. Abbreviation S: sulfur; H_2: hydrogen gas; atm: atmosphere overpressure; n: number of samples. Data were presented as mean ± standard deviation. [a] concentration of acetone shown was calculated from the equation displayed in Figure 7d with background detection of 0.3mM subtracted.

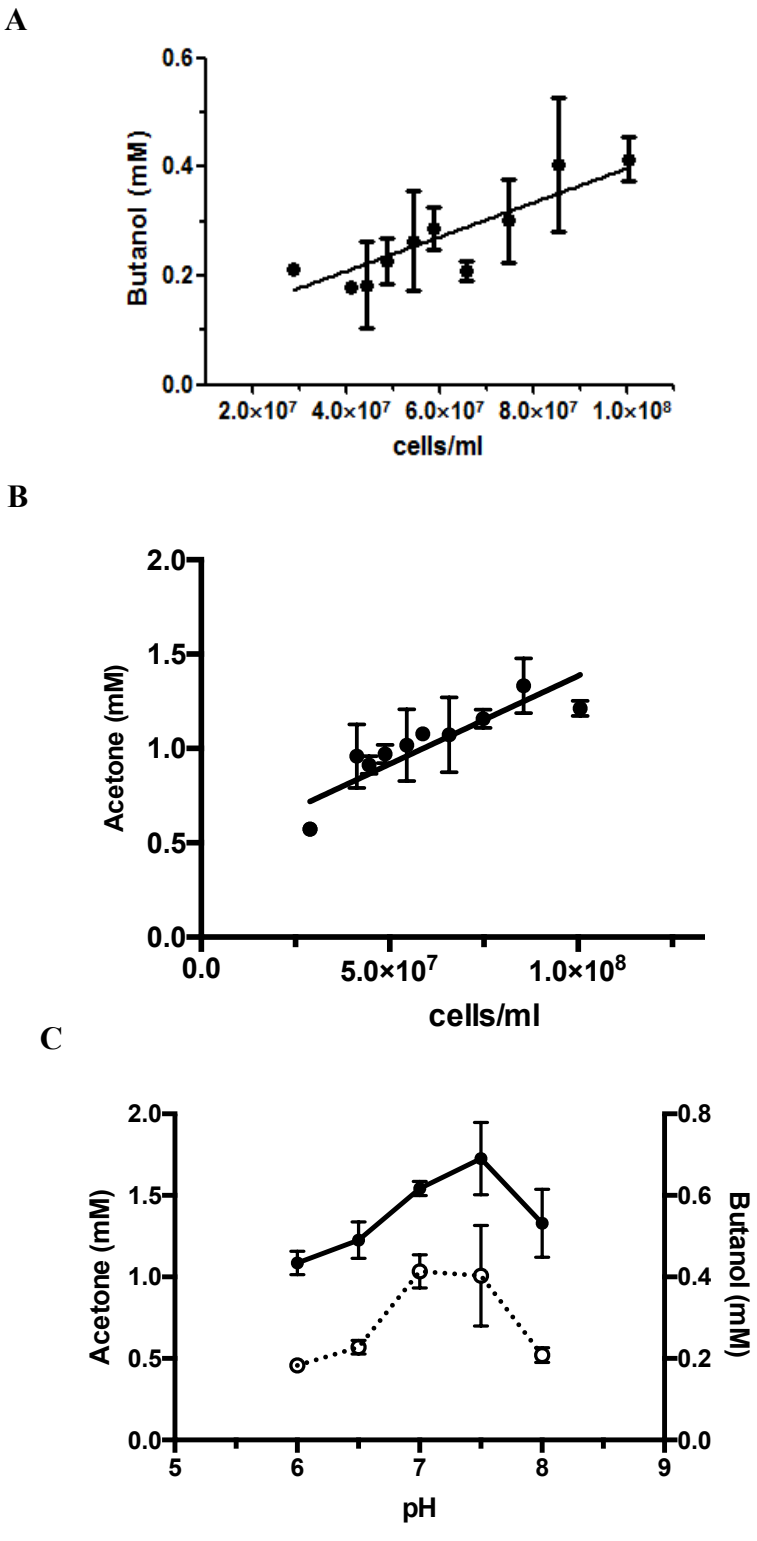

Figure 8. Cell density and pH dependent production of 1-butanol and acetone. (A) the mean production of 1-butanol plotted against cell density; (B) the mean production of acetone plotted against cell density; (C) the mean production of acetone (filled circles) and 1-butanol (unfilled circles) plotted against the pH of the culture. Cell density is the cells/ml at the time the metabolic end-product was measured. Data are presented as mean ± standard deviation.

3.2.3 Production of acetone, 1-butanol and 2-propanol at different growth phases

The production of 1-butanol, acetone and 2-propanol were monitored by withdrawn of an aliquot of culture at different times corresponding to different growth phases. Four growth conditions were chosen for monitoring the production, which included growth at pH 7.0 or pH 7.5 at 3 atmosphere overpressure of H_2 and with 10 g/L of sulfur, growth at pH 7.0 with the absence of sulfur or H_2. The different time points corresponded to early log phase, mid log phase, late log phase, and stationary phase.

Acetone was produced in early log phase and production continued to increase until late log phase only for cells grown with 10 g/L of sulfur and 3 atmosphere overpressure of H_2 **(Fig. 9)**. As mentioned previously, the small peak in the media with the same retention time as acetone was subtracted from the measured values. The difference in pH value (7.0 and 7.5) resulted in no significant difference in the production of acetone **(Fig. 9)**. Without either sulfur or H_2, the production of acetone stops at mid log phase and shows a similar pattern in production **(Fig. 9)**. The total production is much lower than that in cultures with sulfur and H_2.

Under optimal growth conditions at pH 7.0 and 7.5, the production of butanol started at early log phase and production decreased at mid log phase **(Fig. 10)**. A paired t-test between butanol production in cells grown at pH 7.0 and pH 7.5 showed that there was a significant difference (probability of difference due to a random error less than 0.05) in butanol production in the two growth conditions. There was no butanol production in cells grown in culture media without sulfur. It also showed that without H_2 in the media, butanol production starts at mid-log phase and the production was significantly lower **(Fig. 10)**. For both the production of 1-butanol and acetone, it was correlated with the growth.

2-propanol is a major metabolic product in the butanol production pathway of *C. beijerinckii* and it is produced from acetone reduction catalyzed by an ADH (Ismaiel et al 1993). In all of the growth conditions tested, the production of 2-propanol began at

mid log phase, which was later than the time of acetone production. The maximum 2-propanol production was in cultures grown at pH 7.5 **(Fig 11)**. The concentration of 2-propanol in cultures decreased after late log phase except in cultures grown at pH 7.0 with sulfur and at high pressure of H_2. Similar to the production of acetone, cultures grown without sulfur or H_2 showed similar patterns and concentrations of 2-propanol production. It is interesting to note that the production of acetone was much lower in cultures without sulfur or H_2 but the difference in 2-propanol production was smaller.

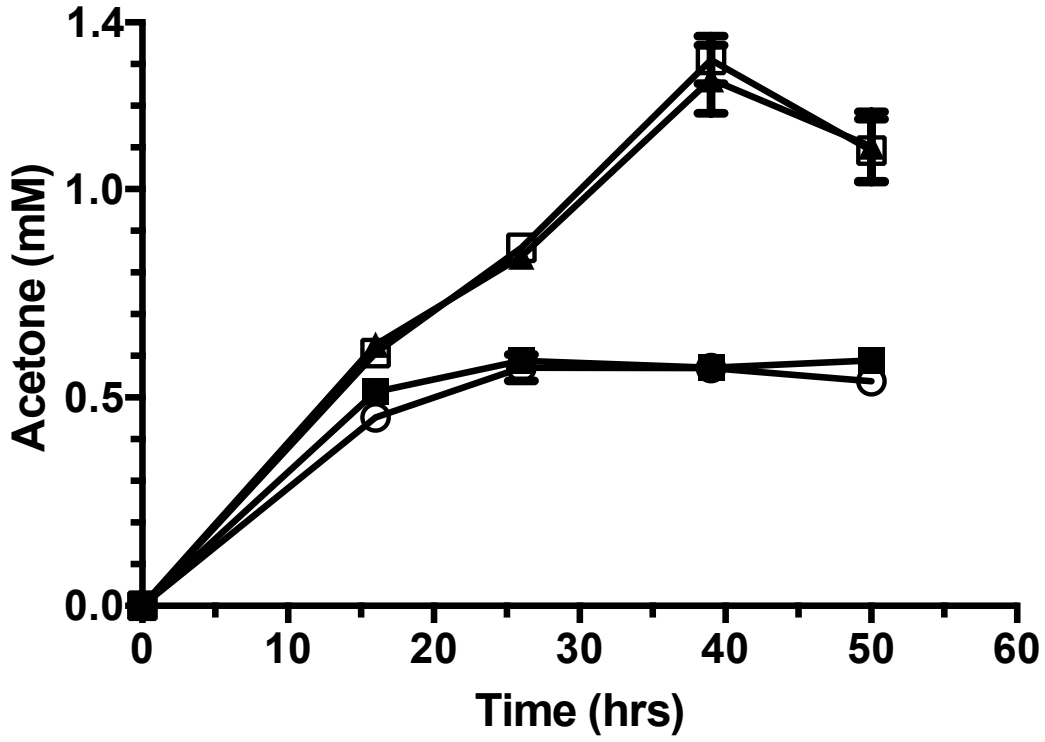

Figure 9. Production of acetone from *H. butylicus* under different growth conditions. Acetone concentrations at pH 7.0 (unfilled squares) and pH 7.5 (filled triangles) from culture grown at 3 atmosphere overpressure of hydrogen gas and 10 g/L of sulfur, in the absence of sulfur (open circles) or hydrogen gas (filled squares). Data were averages from triplicate, and presented as mean $\pm$ standard deviation.

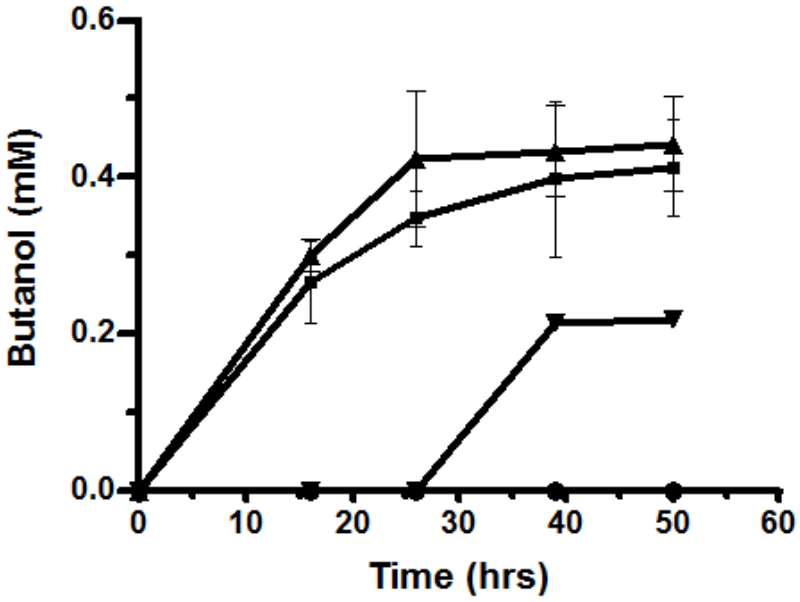

Figure 10. Production of 1-butanol from *H. butylicus* under different growth conditions. Production of 1-butanol in culture grown at pH 7.0 (filled triangles) and pH 7.5 (filled squares) under 3 atmosphere overpressure of hydrogen gas in 10 g/L of sulfur, without sulfur (filled circles) or without hydrogen gas (inverted filled triangles). Date were average of triplicate and presented as mean $\pm$ standard deviation.

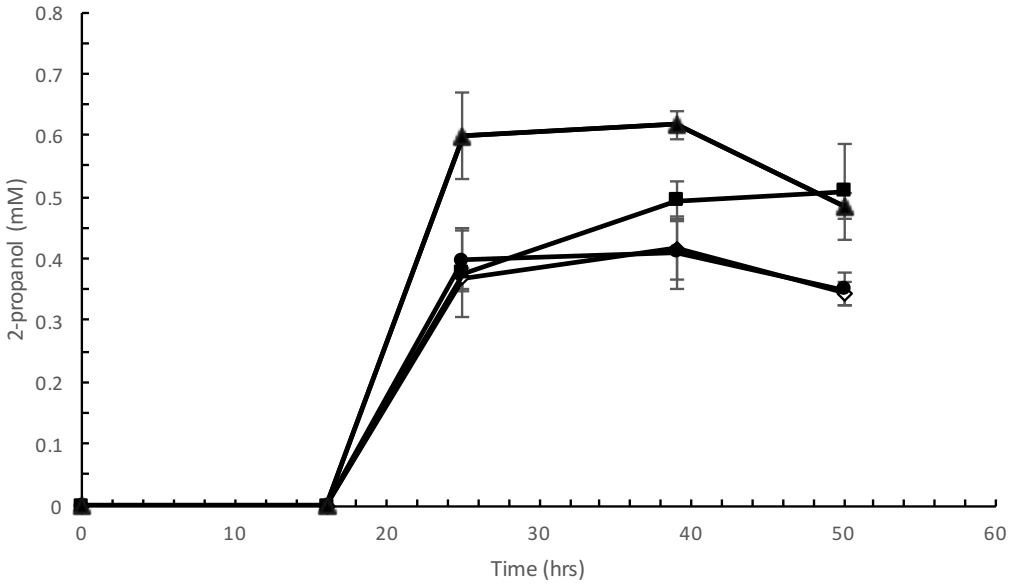

Figure 11. Production of 2-propanol from *H. butylicus* under different growth conditions. Production of 2-propanol from cultures grown at pH 7.0 (filled squares) and pH 7.5 (filled triangles) and under 3 atmosphere overpressure of hydrogen gas in 10 g/L of sulfur, without sulfur (filled circles) or without hydrogen gas (open diamonds). Data were average of triplicate and presented as mean $\pm$ standard deviation.

3.2.3.1 Confirmation of acetone production

Acetone has not been reported as one of the end products of *H. butylicus*. To confirm the production of acetone, it was tested if the acetone detected in the cultures would have similar chemical behavior as the acetone in the standard solutions prepared from section 3.2.1.1. The concentrations of acetone in standard solutions should increase after cooling down to room temperature (around 25 ^{o}C) from a higher temperature (95 ^{o}C) as the solubility of acetone increases at a lower temperature. The concentration of acetone in the standard solution increased around 30 $\pm$ 12.8% **(Table 5)**. Compared to its initial concentration before heating, it was decreased by a mean value of 18 $\pm$ 9.1% except for the 2 mM acetone solution stored under 1 atmosphere pressure. In the cultures that were grown at pH 7.0, the acetone detected also increased by 30 $\pm$ 4.3% after the cultures were cooled down to room temperatures **(Table 5)**. However, acetone concentration in cultures grown at pH 7.5 only increased by 10 $\pm$ 2.5% (**Table 5**), which might be caused by a leak of the stopper.

Table 5. Percentage increase in acetone concentration at a lower temperature

Conditions (acetone)	95°C (mM)	25°C (mM)	Initial (mM)	Increase in acetone (%)
2mM	1.416	2.107	1.762	48.8
2mM (high pressure)	1.424	2.052	2.102	44.1
5mM	3.112	3.553	4.540	14.2
5mM (high pressure)	3.112	3.678	4.457	18.2
10mM	5.101	7.026	8.789	37.7
10mM (high pressure)	6.571	8.512	9.669	29.5
Culture at pH 7.0	1.038	1.384	-	33.3
Culture at pH 7.0	1.242	1.631	-	31.3
Culture at pH 7.0	0.998	1.232	-	23.5
Culture at pH 7.5	0.990	1.088	-	9.89
Culture at pH 7.5	1.265	1.359	-	7.43
Culture at pH 7.5	1.052	1.194	-	13.5

High pressure was at 3 atmosphere overpressure of N_2, which was the same pressure used for the two pH conditions. The increase in acetone was calculated by the difference in concentration at 95°C and 25°C

3.3 Alcohol Dehydrogenase 1

3.3.1 *H. butylicus* Hbut_0414 sequence analysis

The entire gene Hbut_0414 has 843 bp with a deduced 280 amino acids sequence. The molecular weight was calculated to be 30,581 Da. It belongs to the superfamily of Zn-dependent alcohol dehydrogenase. This classification is based on a 29.4% overall identity between the sequence (amino acid 33 to 234) and the conserved domain (cd05188) corresponding to Zn-dependent alcohol dehydrogenase-like family **(Fig 12)**. The sequence also has the lowest e-value with Zn-dependent alcohol dehydrogenase-like family **(Fig 13)**. Members of this family have two signature domains including a C-terminal NAD(P) binding-Rossmann fold domain of a β-α form and an N-terminal catalytic GroES-like domain. ADHs in this superfamily contain zinc metals, some have binding motifs for both catalytic and structural zinc while others have only the binding motif for catalytic zinc.

Blast tool available at http://blast.ncbi.nlm.nih.gov/Blast.cgiPROGRAM showed the Hbut_0414 protein sequence had relatively low overall identities (24.9 % to 37.3 %) with other Zn-containing ADHs in hyperthermophiles. It is said to have relatively low identities because the other thermophiles ADHs that belong to the same group of Zn-containing ADH can have an overall identity in the range of 70 to 80% (Uria, Machielsen et al. 2006). Through blast search, the sequence showed comparative higher overall identities with ADHs from *Crenarchaeota*, the same phylum as *H. butylicus* and interestingly with mesophilic bacteria as well. These included ADHs from *Pyrolobus fumarii (*37.3% identity, WP_014026672.1), *Staphylothermus hellenicus* (27.9%, WP_013143693.1), *S. solfataricus* (26.8%, WP_009988924.1), *Pyrobaculum islandicum* (25.0%, WP_014026672.1) and *Desulfurococcus fermentans* (24.9% identity, WP_048815804.1) and ADHs from mesophilic bacteria *Streptomyces sclerotialus* (28.8% identity, WP_030623043.1) and *Vibrio* sp. EJY3 (29.3% identity, WP_014232168). In the sequence alignment with the mesophilic and hyperthermophilic ADHs, amino acids from Hbut_0414 had the conserved cofactor

NAD(P) binding motif ($GXGX_2G$, residues 130-135) but the catalytic zinc binding motif is modified from $GHEX_2GX_5GX_2V$ to $GCSX_2GX_5GX_2A$ (residues 41-55) (Ying and Ma 2011). This catalytic Zn-binding motif is also modified in the other ADHs compared **(Fig. 14)**. Cysteine is also an amino acid for coordinating Zn and the replacement of glutamic acid by serine and valine by alanine are semi-conserved substitutions. Moreover, a structural Zn-binding motif site was not found in all the sequences compared.

The amino acid composition of Hbut_0414 and its mesophilic and thermophilic ADH homologs were compared. As the Hbut_0414 protein has 100 fewer amino acids than the other Zn-containing ADHs compared, the percentage of each amino acid was used for comparison **(Table 6)**. The primary amino acid analyzes revealed that Hbut_0414 and ADH from its thermophilic homolog *P. fumarii* had apparent higher percentages of hydrophilic amino acid Val, Leu and lower percentages of Phe and Ala than ADH from mesophilic homolog *Vibrio* sp. EJY3. Also, Hbut_0414 had noticeable higher percentages of small hydrophobic amino acid Arg, Pro, and Tyr than *P. fumarii* ADH. The Hbut_0414 amino acid composition was also compared to well-characterized hyperthermophilic Zn-containing ADHs from *S. solfataricus* P2 (28.7% identity, WP_009988924) and *T. guaymasensis* (23.4% identity). Both ADHs had characterized to have optimal enzyme activity above 80 ^{o}C (Raia, Giordano et al. 2001, Ying and Ma 2011). *T. guaymasensis* is from the phylum *Euryarchaeota,* whereas *S. solfataricus* P2 is from the phylum *Crenarchaeota*. In comparison, Hbut_0414 had higher percentages of hydrophobic amino acids Val, Leu, Ala, and Pro but a lower percentage of charged amino acid Lys compared to both *S. solfataricus* P2 and *T. guaymasensis* ADHs **(Table 6)**.

```
Cd05188          EVLVRVEAAGLCGTDLHIRRGGYPPPPKLPLILGHEGAGVVVEVGPGVTGVKVGDRVVVL
H.butylicus      WVLLRVKLARWCSIDGFAA---W-WPLSRQRIAGCSGAGVVAEHGVDADTDLPGRQVV-L
                  **:**: *  *. * .     :  * .   * * .*****.* *  .     * :** *

Cd05188          PNLGCGTCELCRELCPGGGILGEGLDGGFAEYVVVPADNLVPLPDGLSLEEAALLPEPLA
H.butylicus      GGY-------SPEY-----LPPLNVNGWLAEYTSAPSSLLIPVGR--LEPRLVFYPDAVT
                           . *      :    ::* :***. .*:. *:*:       . .: *: ::

Cd05188          TAYHALRRAGVLKPGDTVLVLGAGGVGLLAAQLAKAAGARVIVTDRSDEKLELAKELGAD
H.butylicus      AC---SVAEELEAAGRSVLVYGAGFYGLSAAHLALDAGLDVDIVTNVKEATRIAREMGAR
                 :.        :   * :*** ***  ** **:**  **  * :. . .*  .:*:*:**

Cd05188          HVIDYKEEDLEEELRLTGGGGADVVIDAVGGPETLAQALRLLRPGGRIV
H.butylicus      VYTRPPSGRHYDAIVLAAA-----SANAIGVVETYSPSLIVLHPLHTIA
                       .    : : *:..       :*:*  ** : :* :*:*   *.
```

Figure 12. Amino acid sequences alignment of Hbut_0414 and conserved domain Cd05188. The sequences were aligned using Clustal Omega (Larkin, Blackshields et al. 2007). *H. butylicus* represented the Hbut_0414 amino acids sequence from 33 to 234. "*", residues that are identical in the alignment; ":", conserved substitutions; ".", semi-conserved substitutions; "-", no corresponding amino acid.

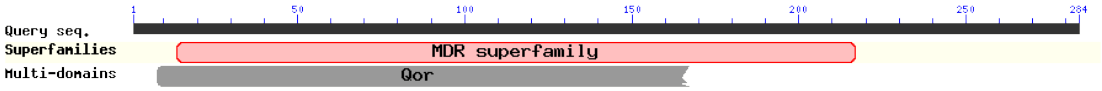

Figure 13. Putative conserved domains of *H. butylicus* Hbut_0414

MDR, medium chain reductase/dehydrogenase/ zinc-dependent alcohol dehydrogenase-like family, Qor, NADPH:quinone reductase or related Zn-dependent oxidoreductase

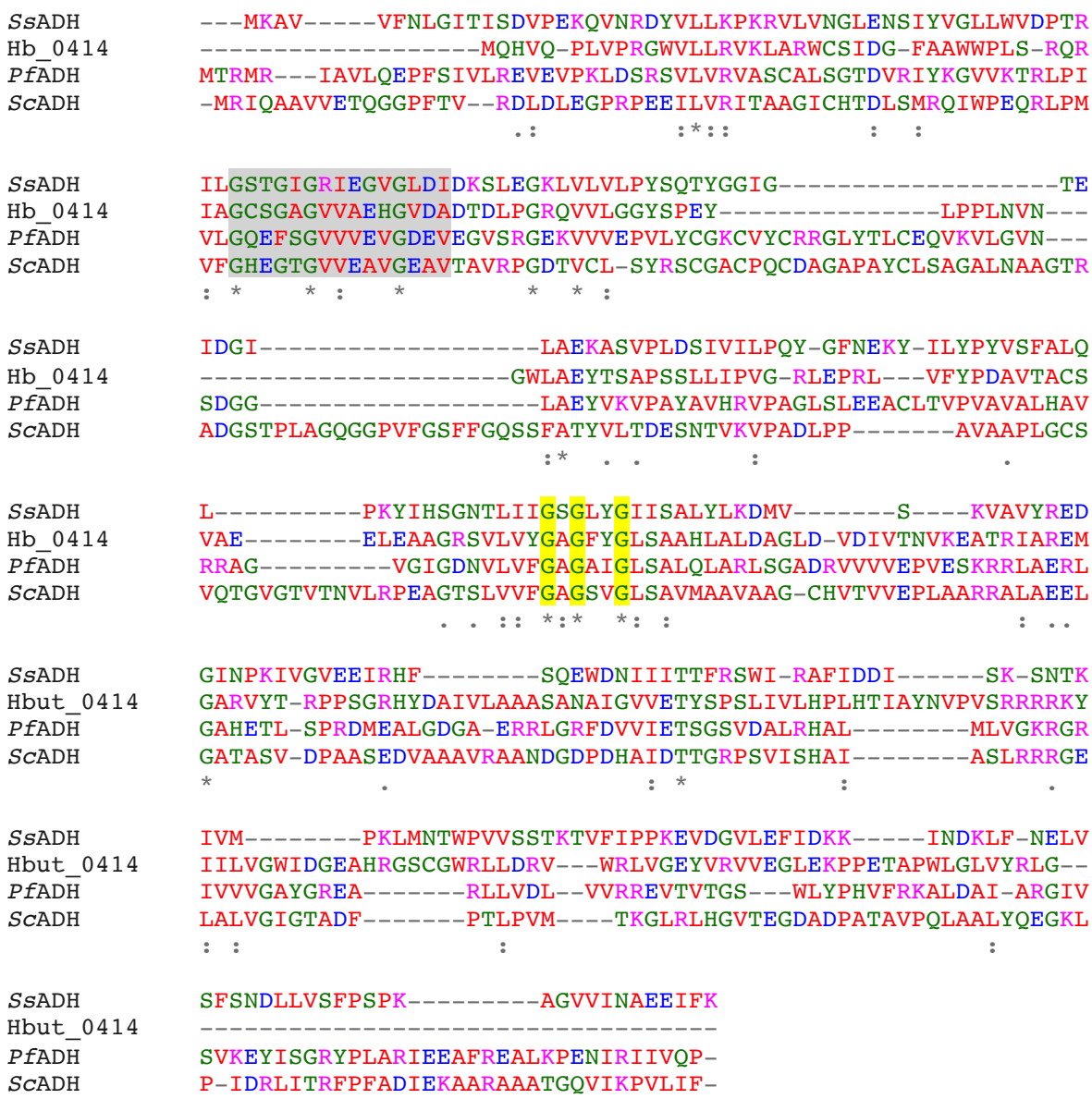

Figure 14. Amino acid sequences alignment of Hbut_0414 and its homologues

The sequences were aligned using Clustal Omega (Larkin, Blackshields et al. 2007). *Ss*ADH, ADH from *S. solfataricus*; Hbut_0414, annotated zinc-containing ADH from *H. butylicus*; *Pf*ADH, ADH from *P. fumarii* 1A; *Sc*ADH, ADH from *S. sclerotialus*. "*", amino acid residues that are identical in all sequences in alignment; ":", conserved substitutions; ".", semi-conserved substitution; "-", no corresponding amino acid. Highlighted in grey, conserved putative binding sites of catalytic zinc; highlighted in yellow, conserved putative motif of cofactor binding site. Red: small and hydrophobic amino acids and tyrosine; Blue: acidic amino acids; Magenta: basic amino acids and histidine; Green: amino acids with hydroxyl, sulfhydryl or amine group and glycine.

Table 6. Comparison of the typical amino acids between Hbut_0414 and its thermophilic and mesophilic homologs

Amino acid	Hbut_0414	*Pf*ADH	*Vs*ADH	*Ss*ADH	*Tg*ADH	ΔHbut_0414 and *Vs*ADH	Δ*Pf*ADH and *Vs*ADH	ΔHbut_0414 and *Ss*ADH	ΔHbut_0414 and *Tg*ADH
Aromatic									
Phe	1	2	4	2	4	-2	-2	0	-3
Hydrophobic									
Val	14	17	12	10	10	2	5	4	4
Leu	14	11	9	9	6	5	2	5	7
Met	1	1	2	3	4	-1	-1	-2	-3
Small hydrophobic									
Ala	13	9	19	10	9	-6	-10	3	4
Pro	8	4	8	4	7	0	-4	4	1
Gly	12	9	12	10	12	0	-3	2	0
Charged									
Glu	6	8	6	7	6	0	2	-1	0
Lys	2	4	2	7	7	0	2	-5	-5
Hydrophilic									
Ser	7	5	6	4	2	1	-1	3	5
Asn	2	1	1	3	2	1	0	-1	0
Gln	2	1	4	3	1	-2	-3	-1	1
Total	234	337	313	347	364				

The numbers are represented in percentage of individual amino acid over total amino acids. *Pf*ADH, ADH from hyperthermophilic *P. fumarii; Vs*ADH, ADH from mesophilic *Vibrio* sp. EJY3; *Ss*ADH, ADH from hyperthermophilic *S. solfataricus* P2 and *Tg*ADH, ADH from hyperthermophilic *T. guaymasensis.;* amino acid highlighted in yellow and grey are amino acids obviously higher in comparison and lower in comparison, respectively.

3.3.2 Cloning of *H. butylicus* Hbut_0414

Based on the method as described in section 2.4.3, the genomic DNA (gDNA) from *H. butylicus* strain was isolated with a high purity **(Fig 15 A)**. The isolated gDNA had a concentration of 1,028 ng/µl. It was then used as the template for the amplification of Hbut_0414 gene directly by two rounds of PCR for gene specificity. The first round PCR directed by primers HBADHF1 and HBADHR1, which produced a single band on a 1% agarose gel with an approximate size of 1000 bp **(Fig 15 B)**. The second round PCR directed by primers HBADHF2 and HBADHR2 also produced a single band on a 1% agarose gel with a size of around 900 bp **(Fig 15 B)**.

The gene after amplification from PCR was cloned into the expression vector pET30a. The amplified gene with *NdeI* and *XhoI* restriction sites at the 5' and 3' terminals were digested with respective restriction enzymes to create overhang regions which was inserted into the *NdeI* and *XhoI* double digested pET-30a expression vector **(Fig 16 A)**. The recombinant plasmids were selected from colonies grown on an agar plate with 50 µg/ml kanamycin. The selected colonies were then confirmed by colony PCR **(Fig 16 B)** and DNA sequencing and they contained the inserted Hbut_0414 gene in the recombinant plasmids in the correct orientation and without a mutation.

The codon usage of *E. coli* and *H. butylicus* were compared to assess *E. coli* capability to express protein from *H. butylicus*. It showed that codons AGG (codon for arginine), CTA and CTC (codons for leucine), ATA (codon for isoleucine) and CCC (codon for proline) are rare codons in *E. coli* but commonly used in *H. butylicus*. Hence, *E. coli* Rosetta 2 that co-expresses the tRNAs for these rare codons including AGG, CTA, ATA and CCC was used for the expression of the protein encoded by Hbut_0414. However, *E. coli* Rosetta 2 doesn't have tRNA for the codon CTC.

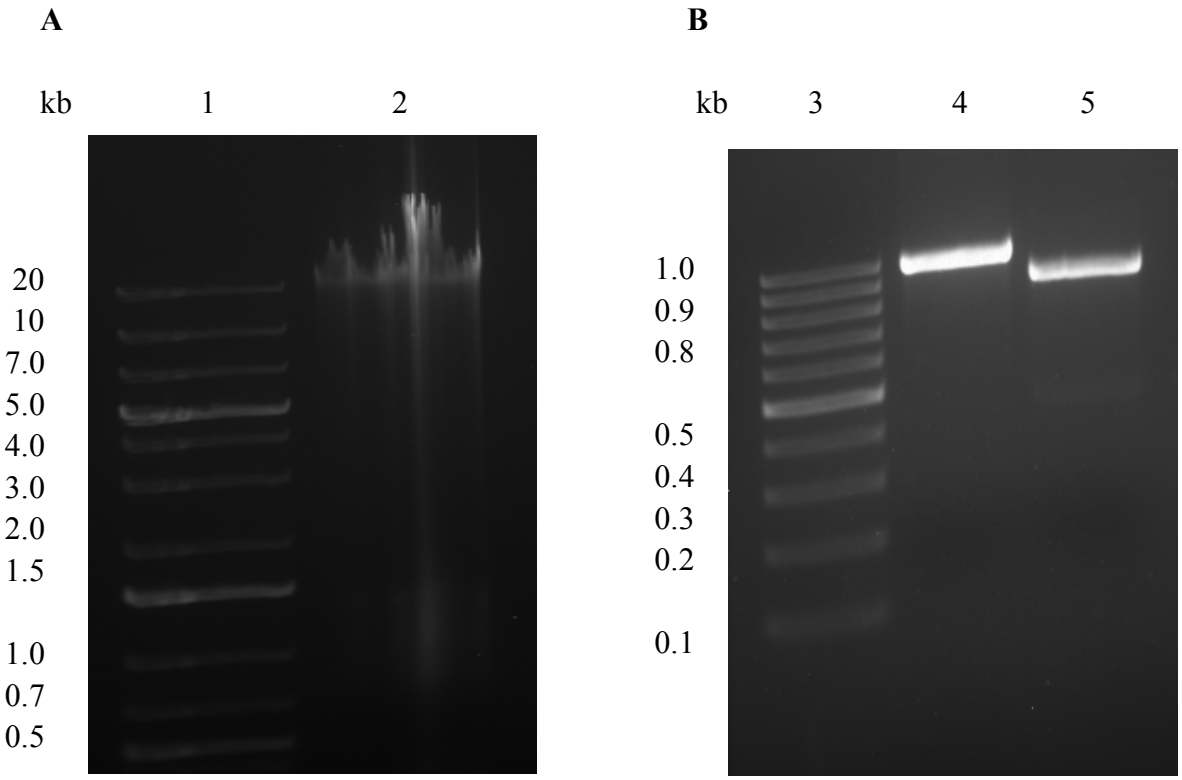

Figure 15. *H. butylicus* genomic DNA isolation and PCR amplification of the gene encoding *H. butylicus* Hbut_0414. (A) 0.8% agarose gel showing the isolated *H. butylicus* genomic DNA; (B) 1% agarose gel showing the PCR products using different primers. (A) Lane 1, 1kb plus DNA ladders (Novogan, WI, USA); lane 2, *H. butylicus* genomic DNA; (B) lane 3, 100bp DNA ladders (Fermentase Canada Inc., ON, Canada); lane 4, PCR product with primers HBADHF1 and HBADHR1; lane 5, PCR product with primers HBADHF2 and HBADHR2.

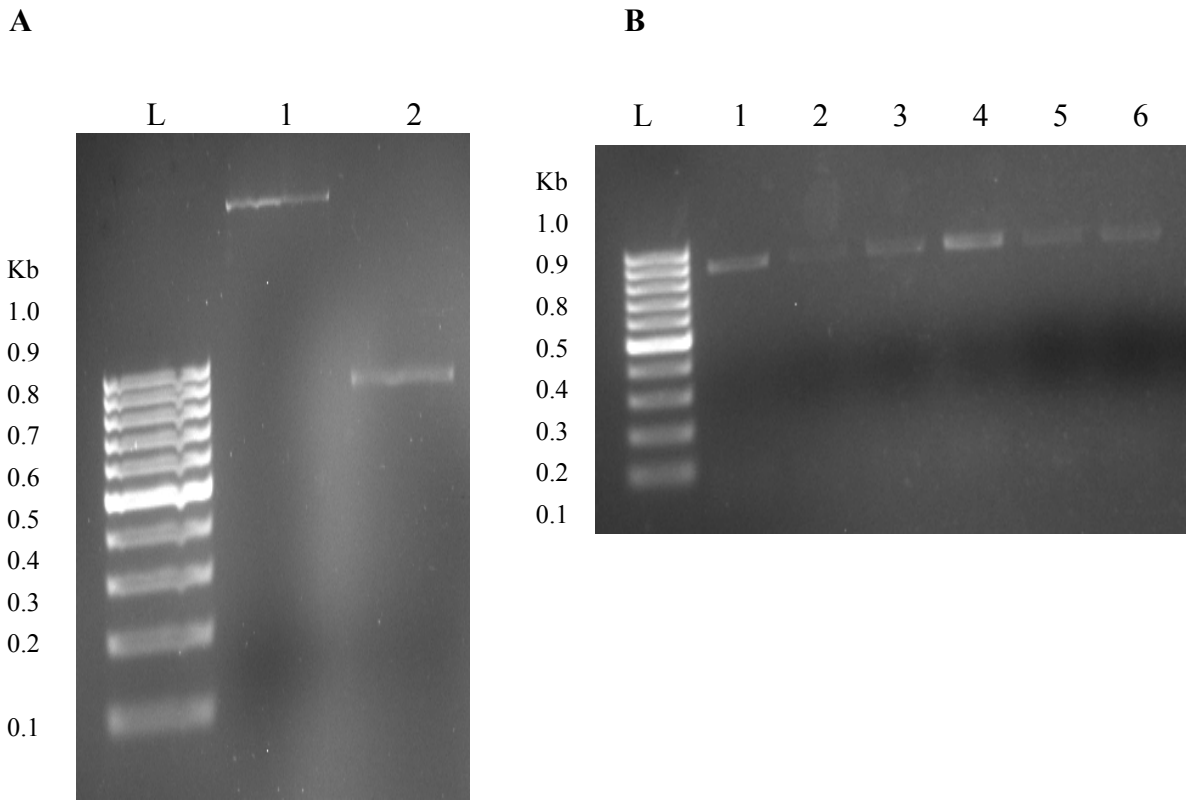

Figure 16. Agarose gel showing the double enzymes digestion of PCR product and expression vector and colony PCR. (A) L: Ladder 100 pb DNA ladders (Fermentase Canada Inc., ON, Canada); lane 1, the complete digestion of the expression vector pET30a by *NdeI* and *XhoI* ; lane 2, digestion of the PCR product from the amplification of gene encoding Hbut_0414 by the two restriction enzymes and did not cut the gene internally. (B) Colony PCR with primers HBADHF2 and T7 terminator (lanes 1-6) showed that all selected colonies contain the gene with a band of appropriate size (~880bps) and in the correct orientation. L: Ladder 100 pb DNA ladders (Fermentase Canada Inc., ON, Canada).

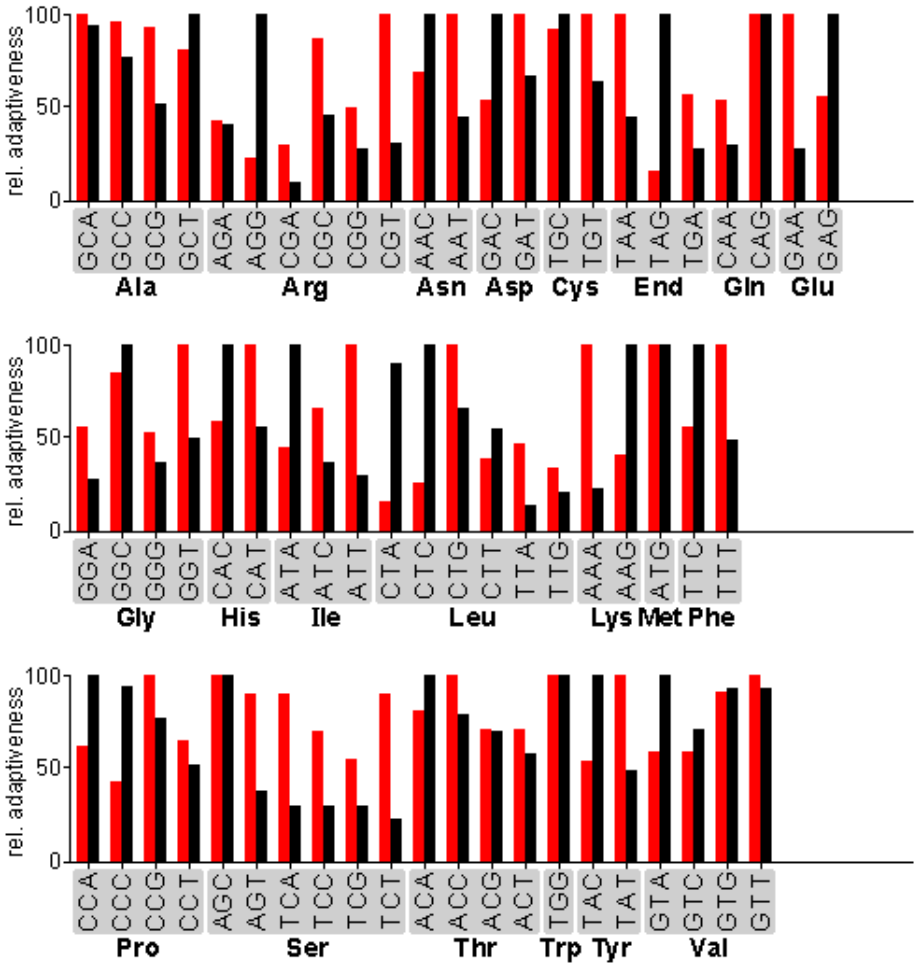

Figure 17. Codon usage comparison between *H. butylicus* and *E. coli.* Codon usage analysis was conducted using Graphical codon usage analyzer at http://gcua.schoedl.de/ (Nakamura, Gojobori et al. 2000). Columns in red, codon usage pattern of *E. coli*; columns in black, codon usage pattern of *H. butylicus*. The numbers of most frequently used codons for the specific amino acid was defined as 100.

3.3.3 Over-expression of ADH1

The expression vector pET-30a is driven by T7-lac promoter, and overexpression of Hbut_0414 was induced by IPTG. The recombinant Hbut_0414 showed ADH activity with NAD as a cofactor and would be described as ADH1 in the following sections. The 12.5% SDS-PAGE showed that ADH1 was around 32 kDa and expressed only in the presence of IPTG as an inducer **(Fig 18)**. The use of *E. coli* Rosetta 2 strain as the expression host showed better expression than *E. coli* BL21. *E. coli* Rosetta 2 contains extra tRNAs for rarely used codon (amino acid) included AGG/AGA/CGG (arginine), AUA (isoleucine), CUA (leucine), CCC (proline) and GGA (glycine) to overcome codon bias. In comparison to *E. coli* BL21, it has only three extra tRNAs for codons CGG, CCC, and GGA.

From small scale growth (5 ml), the optimal expression of ADH1 was when the concentration of induced IPTG reached 0.6 mM, and at 30 ^{o}C for induction **(Fig 18 and 19)**. The large scale (0.5-1 L) culture with recombinant *E. coli* was incubated in LB medium with 50 µg/ml kanamycin at 37^{o}C until OD_{600nm} 0.8 before induction, which took 4-5 hours. It was then moved to a 30 ^{o}C incubation room and 0.6 mM of IPTG was added for induction.

Recombinant *E. coli* without IPTG induction and with empty vector inserted were grown in the same conditions as the induced *E. coli*. Their cell-free extracts (0.3 mg) were used for measuring ADH activity in uninduced *E. coli* in 100 mM of EPPS at pH 8.5 and 60 ^{o}C with 1-butanol as substrate. The specific activity of *E. coli* without IPTG induction was 0.064 U/mg and for *E. coli* with empty vector was 0.059 U/mg total protein. The specific activity was lower than the specific activity of the cell-free extract with overexpression of ADH1 (0.87 U/mg). In *E. coli* genome, there is also no annotated ADH gene with similar molecular size as the recombinant ADH1 encoded by Hbut_0414.

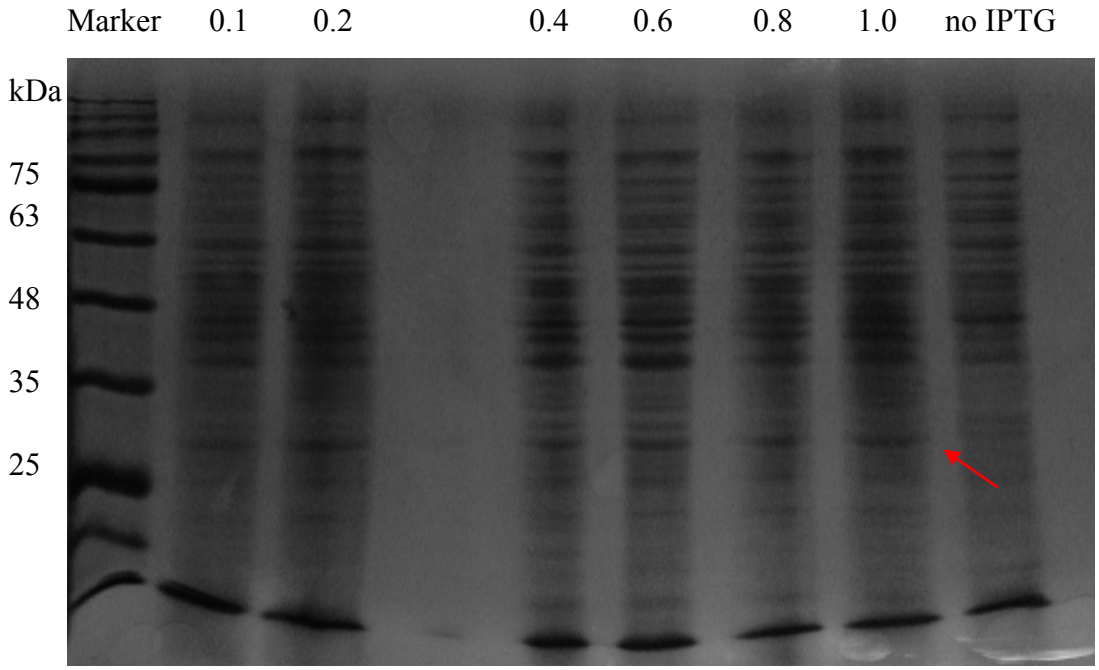

Figure 18. SDS-PAGE (12.5%) showing the expression of ADH1 in *E. coli* induced at different concentration of IPTG. Marker, low molecular weight protein marker (Bio-rad Inc, ON, Canada); lane 0.1, 0.2, 0.4, 0.6, 0.8 and 1.0 corresponding to *E.coli* induced at 0.1 mM, 0.2 mM, 0.4 mM, 0.6 mM, 0.8 mM and 1.0 mM of IPTG, respectively. No IPTG was added for the *E. coli* host cells in the last lane. 15 µl of cell crude extract was loaded for each lane. Red arrow indicates the over-expressed ADH1.

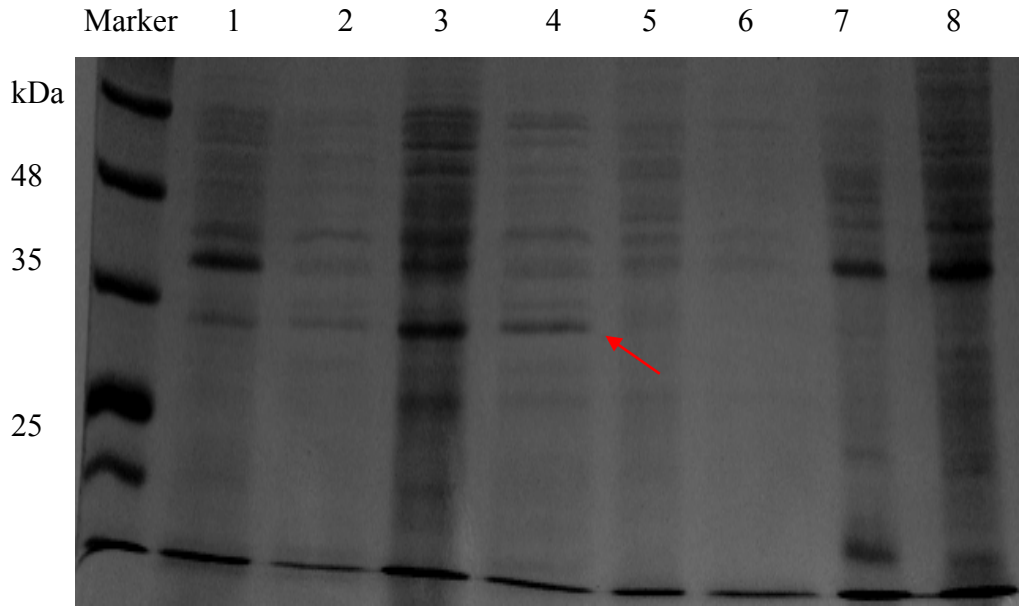

Figure 19. SDS-PAGE (12.5%) showing the expression of ADH1 in *E. coli* induced at different temperatures. Marker, low molecular weight protein marker (Bio-rad Inc, ON, Canada); lane 1,3 and 5: cell-free extract of *E. coli* induced at 25^{o}C, 30^{o}C and 37 ^{o}C respectively; lane 2, 4 and 6: cell-free extract of *E. coli* induced at 25^{o}C, 30^{o}C and 37 ^{o}C after heat treatment at 60^{o}C for 30 minutes respectively; lane 7 and 8, cell-free extract of *E. coli* without IPTG induction. 30 µl of the cell-free extract was loaded per lane. Red arrow indicates the over-expressed ADH1.

3.3.4 Purification of ADH1 from *E. coli*

H. butylicus ADH1 was purified from *E. coli* proteins through a series of chromatography columns **(Table 7)**. The cell-free extract from *E.coli* with 201 U of ADH activity was first loaded onto a DEAE column. Most of the *E. coli* proteins did not bind to the DEAE column and eluted out with buffer A (50mM Tris-HCl (pH7.8), 2mM DTT, 2mM SDT, 5% glycerol). The partially purify ADH1 was then loaded onto a HAP column followed by a phenyl-Sepharose column. ADH1 bound strongly to the phenyl-Sepharose column, by which a further purification of ADH1 was achieved. Gel-filtration chromatography resulted in the purification of ADH1 to homogeneity **(Fig 20)** and the purified ADH1 has a specific activity of around 9 U/mg toward 1-butanol. The yield of the purification was 57 %. The purified ADH1 was stored at -20^{o}C for further characterization experiments.

The molecular weight of ADH1 under denaturing condition was estimated to be 33 kDa on a 12.5% SDS-PAGE using the low range molecular weight protein marker. The native molecular weight was determined by size exclusion chromatography with Superdex-200 column. ADH1 was eluted with an effective volume (V_e) of 165 ml at a flow rate of 2 ml/min. The molecular weight of its native form is around 130 kDa and ADH1 was found to be a homotetramer, similar to the other ADHs from hyperthermophiles (Radianingtyas et al. 2003) **(Fig 21)**.

Table 7. Purification of ADH1

	Total protein (mg)	Total activity (U)	Specific Activity (U/mg)	Purification fold	Yield (%)
Cell-free extract	230	201	0.874	1.0	100
DEAE	80	172	2.157	2.5	86
HAP	52	140	2.698	3.1	70
Phenyl-sepharose	28	128	4.573	5.2	64
Gel-filtration	13	117	9.032	10.3	57

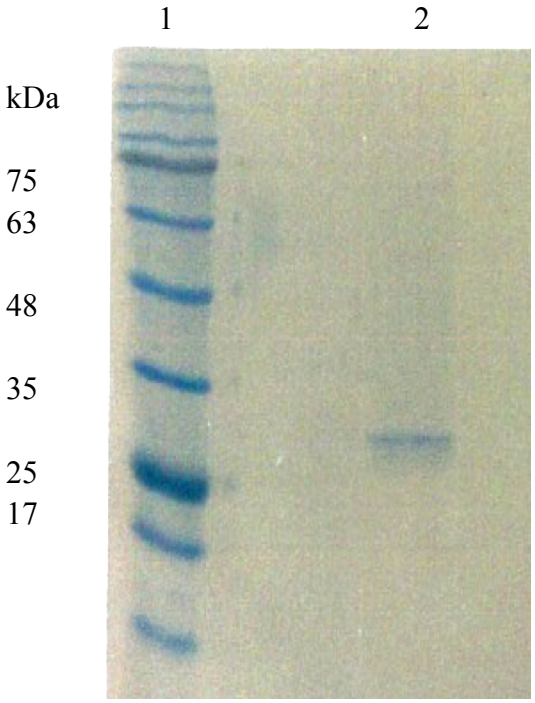

Figure 20. SDS-PAGE (12.5%) for purified ADH1

Lane 1, Low molecular weight protein marker; lane 2, 15 µg of the purified ADH1 was loaded

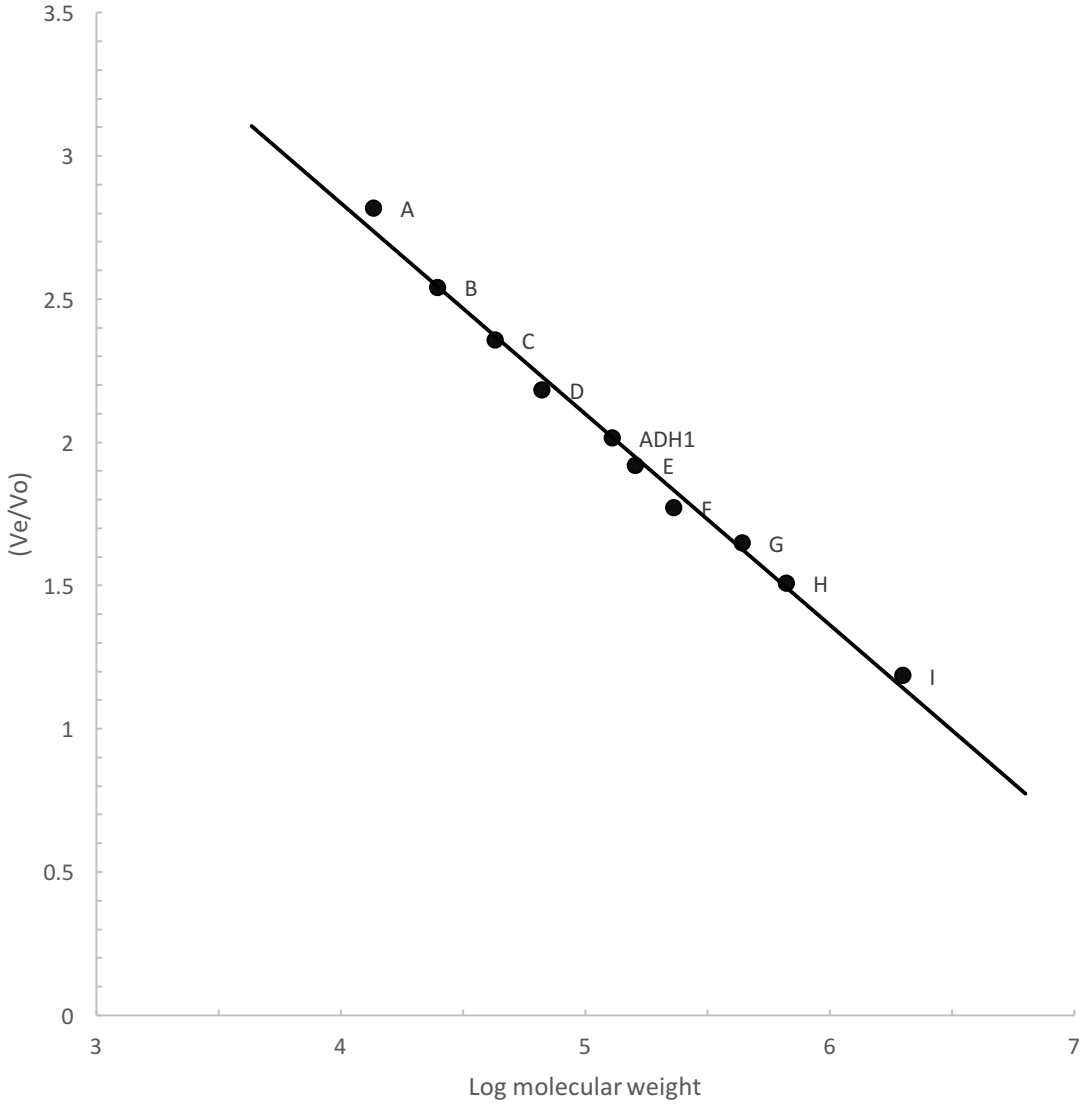

Figure 21. Calibration curve for the determination of ADH1 molecular weight at pH 7.8 by gel filtration on Superdex 200. Marker proteins used for calibration: A: ribonuclease A (13,700); B: chymotrysinogen A (25,000); C: ovalbumin (43,000); D: bovine serum albumin (67,000); E: aldose (158,000); F: catalase (232,000); G: ferritin (440,000); H: thyroglobulin (669,000); I: blue dextran (2,000,000); ADH1: alcohol dehydrogenase encoded by Hbut_0414 in *H. butylicus*

3.3.5 Properties of ADH1

3.3.5.1 Protein concentration dependent enzyme activity

The appropriate protein concentrations for the characterization of ADH1 were determined by initiating the enzyme activity with different protein concentrations of purified enzyme. ADH1 had no activity when NADP(H) was used as a cofactor and NAD(H) was used as the cofactor for all the enzyme assays. The substrate with the highest activity in the oxidation reaction, 1-propanol, was used for measuring the enzyme activities. Different protein amounts from 6 µg to 96 µg were tested and protein amounts from 24 µg to 60 µg showed a relatively constant specific activity. 35 µg of protein was used for the enzyme assays as it also fell in the range of the highest proportionality between the activity and protein amount **(Fig 22)**. Protein less than 25 µg did not initiate the enzyme activity fully and no enzyme assay was performed with protein less 30 µg. It was observed that enzyme concentrations greater than 60 µg experienced a drop in the specific activity. This might be because enzyme concentration was no longer a limited factor in the reaction. The limiting factor could be the substrate concentration.

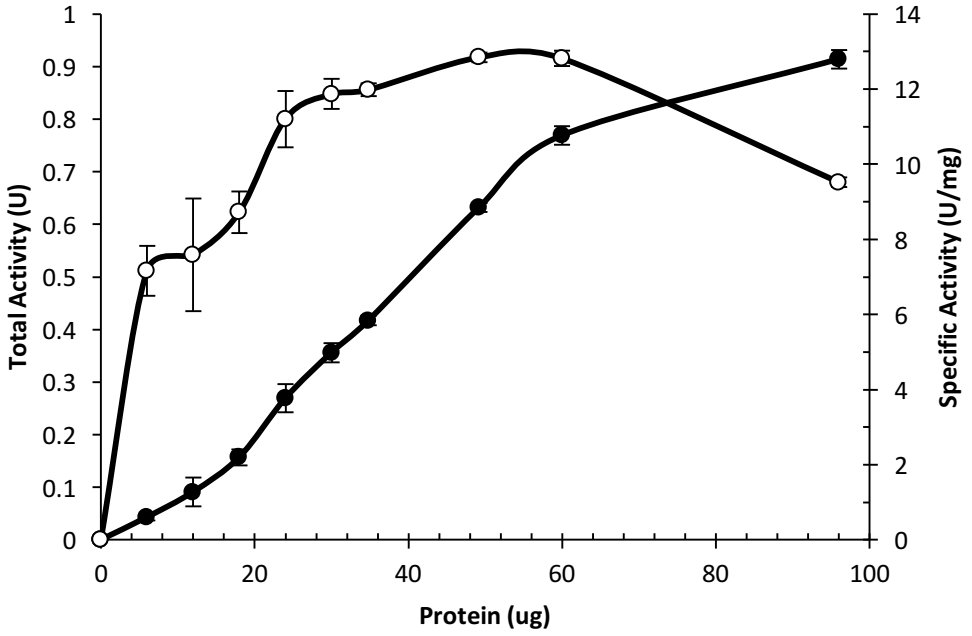

Figure 22. Protein concentration dependent activity of ADH1. Enzyme assay was performed in 100 mM EPPS at pH 8.5 with 60 mM of 1-propanol, 0.4 mM of NAD at 60^{o}C, the reaction was initiated with different amount of ADH1. Total activity was displayed in filled circles and specific activity is displayed in unfilled circles. Data were presented as mean $\pm$ standard deviation

3.3.5.2 Optimal pH

The optimal pH was determined with various 100 mM buffers from pH 4.5 to 6.5 for reduction and pH 7.5 to 10 for oxidation. The optimal pH for 1-butanol oxidation was at 8.5 **(Fig 23A)** and for butyraldehyde reduction was at 5.0 **(Fig 23B)**. The oxidation activity decreased dramatically when pH increased to higher than 9.0 and reduction activity decreased sharply when pH was higher than 5.

3.3.5.3 Optimal temperature

The optimal temperature for ADH1 activity was measured from 30 ^{o}C to 80 ^{o}C. The activity increased from 30 ^{o}C to 60 ^{o}C and decreased at higher temperatures **(Fig 24)**. The optimal temperature was at 60 ^{o}C, which was lower than other characterized hyperthermophilic ADHs. The relative activity was less than 20% when activity was measured at 80 ^{o}C, the temperature where other hyperthermophilic ADHs are relatively thermostable.

3.3.5.4 Thermostablity

Thermostability of ADH1 was measured at 60 ^{o}C, 75 ^{o}C, and 95 ^{o}C, respectively. The optimal growth temperature for *H. butylicus* is at 95 ^{o}C. The time for the loss of 50% of the activity at 60 ^{o}C was about 3 hours, and it decreased to 20 minutes at 75 ^{o}C and the activity was lost more than 80% after incubation at 95 ^{o}C for 5 minutes (**Fig 25**). This showed ADH1 had low resistance to heat. Inactivation kinetic for the resistant portion of the activity was determined. The semi-log plot of the residual activities versus heating time were linear at 60 ^{o}C and 75 ^{o}C **(Fig 26)**. From the slopes of these lines, inactivation rate constant was 3.2 times higher at 75 ^{o}C compared to that at 60 ^{o}C. ADH1 was almost immediately inactivated at a heating temperature of 95 ^{o}C.

3.3.5.5 Oxygen sensitivity

ADH1 sensitivity toward oxygen was measured by exposing the enzyme to oxygen for 5 hours. Residual activity was measured at different time intervals. ADH1 was not oxygen sensitive and activity was only decreased by less than 20% after 5 hours exposure to air in the presence of reducing agents **(Fig 27)**.

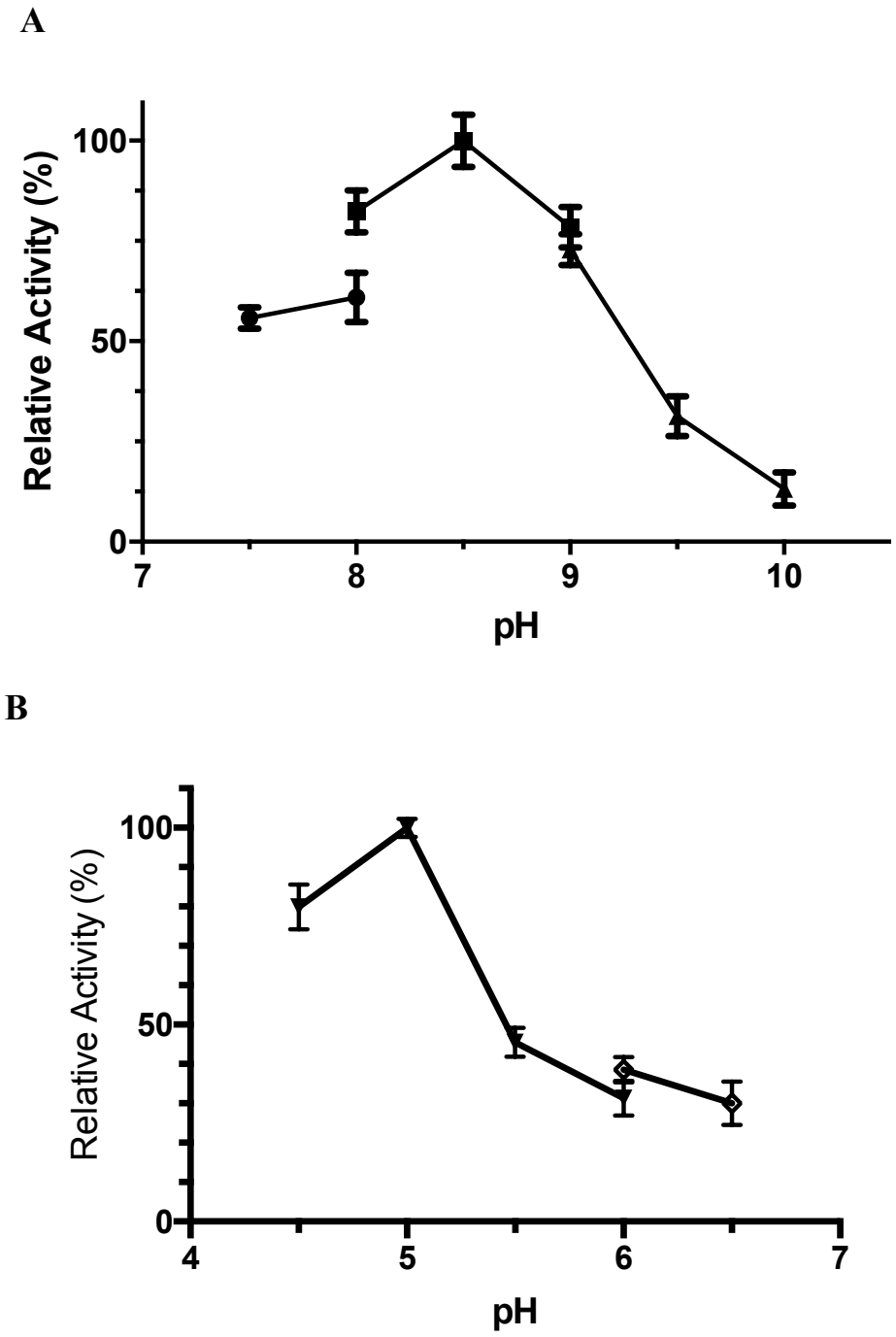

Figure 23. Optimal pH of ADH1. (A) optimal pH for alcohol oxidation. Activities were measured with 60 mM 1-butanol and buffers (100 mM) used were HEPES (filled circles), EPPS (filled squares), and glycine (filled triangles). The relative activity of 100% referred to 9.56 U/mg of alcohol oxidation activity. (B) optimal pH for aldehyde/ketone reduction. Activities were measured with 60 mM butyraldehyde and buffer (100mM) used were citrate (inverted filled triangles) and PIPES (open diamonds). The relative activity of 100% referred to 3.56 U/mg of aldehyde reduction activity. Data were presented as mean $\pm$ standard derivation. pH values of buffers were measured at room temperatures.

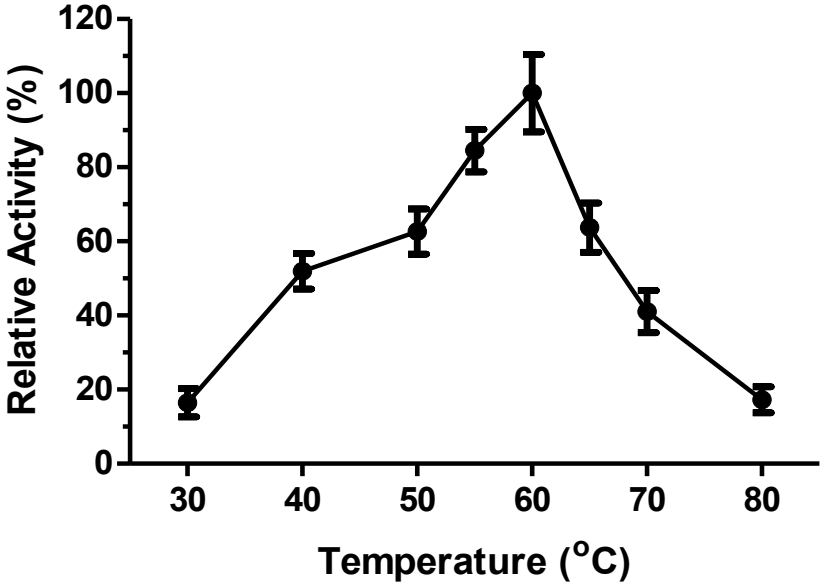

Figure 24. Temperature dependence of ADH1. The activities were measured in the standard assay conditions with temperatures varied from 30 to 80 ^{o}C. The relative activity 100% was defined as the highest activity value at 60 ^{o}C, which was 10.6 U/mg with 60mM 1-propanol as substrate. Data were presented as mean $\pm$ standard derivation.

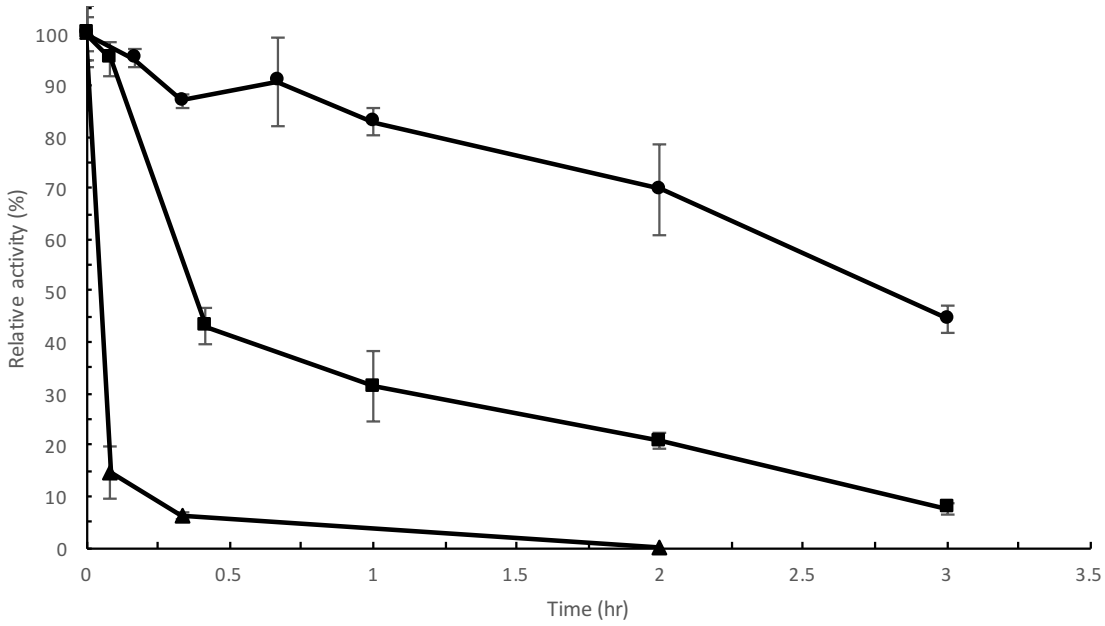

Figure 25. Thermostability of ADH1. Incubation at 60 ^{o}C (filled circles); incubation at 75 ^{o}C; (filled squares), incubation at 95 ^{o}C (filled triangles). The relative activity of 100% equaled to the initial ADH activity without heat treatment, which was measured with 60mM 1-propanol (10.6 U/mg). Data were presented as mean $\pm$ standard derivation.

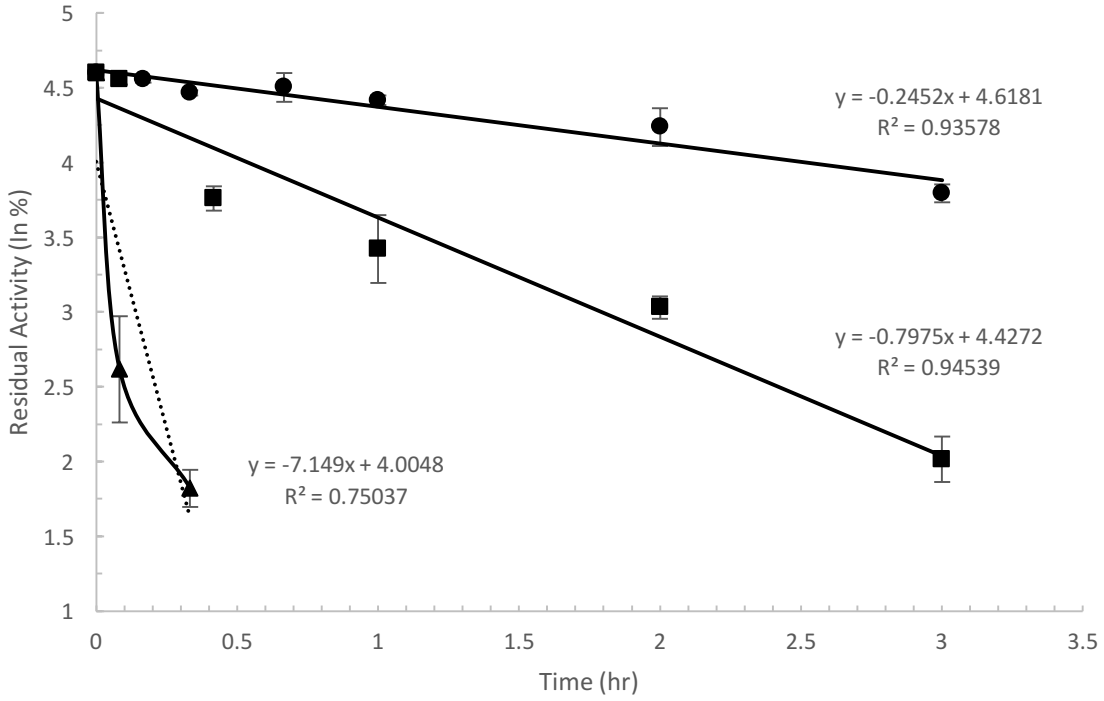

Figure 26. Inactivation of ADH1 at different temperatures. Inactivation rate at 60 ºC (filled circles); inactivation rate at 75 ºC (filled squares); and inactivation rate at 95 ºC (filled triangles). Residual activities (in the natural log of respective percentages of remaining activities) were plotted against time of incubation at different temperatures. The residual activities were compared to initial ADH1 activity without heat treatment, which was measured using 60 mM 1-propanol as substrate (10.6 U/mg). Data were presented as mean $\pm$ standard deviation.

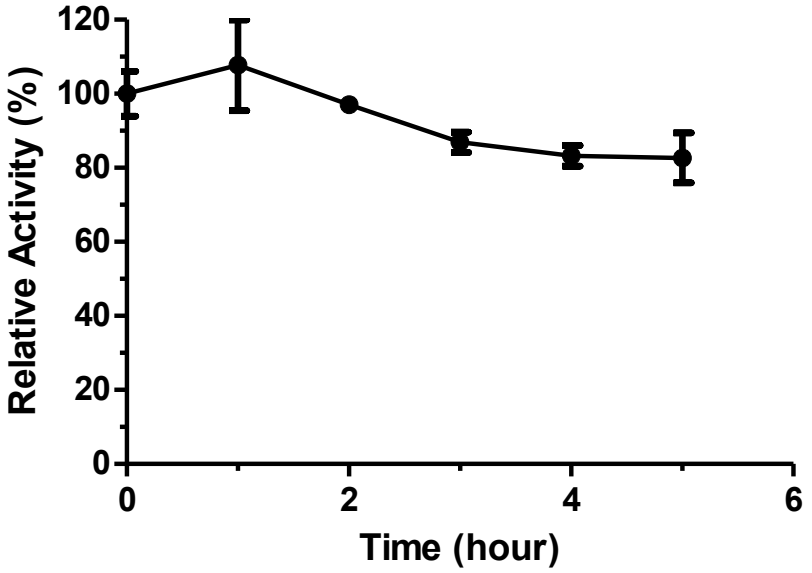

Figure 27. Oxygen sensitivity of ADH1. The activities were measured in the presence of 2 mM DTT and 2 mM SDT. The relative activity of 100% equaled to the ADH activity before oxygen exposure with 60mM 1-propanol as substrate (10.6 U/mg). Data were represented as mean $\pm$ standard derivation.

3.3.5.6 Substrate specificity

The substrate specificity of ADH1 was determined using a set of alcohols, aldehydes, and ketones **(Table 8 and 9)**. In the oxidation reactions, ADH1 was able to oxidize a broad range of primary alcohols except for methanol **(Table 8)**. ADH1 was also reactive with secondary alcohols but with lower activities, suggesting ADH1 was a primary/secondary ADH. It was also able to oxidize diols with higher activities towards primary diols than secondary diols. ADH1 showed no activity toward the polyol-glycerol examined. In the reduction reactions, ADH1 exhibited the ability to reduce various aldehydes and ketones **(Table 9)**. The activities were higher toward aldehydes than ketones. For the oxidation reaction, the substrate with the highest activity was 1-propanol and for the reduction reaction, propanal supported the highest activity.

3.3.5.7 Enzyme kinetics

The apparent K_m values for substrates in the reduction reaction was lower than that for the corresponding alcohols in the oxidation reaction **(Table 10)**. The apparent K_m value for propanal was 5.6 times lower than 1-propanol, and apparent K_m value for acetone was 3.4 times lower than 2-propanol. The specificity constant k_{cat}/K_m for propanal was the highest (15,975 $s^{-1}M^{-1}$) and about 8 times higher than propanol. The k_{cat}/K_m specificity constants were similar for the primary alcohols examined. The k_{cat}/K_m specificity constant for 1-propanol was around 35 times higher than that for acetone **(Table 10)**. These catalytic properties suggest ADH could play an important role in the reduction of aldehyde especially propanal *in vivo*.

Table 8. Substrate specificity of ADH1 in the oxidation reaction

Substrate	Relative Activity (%)
Alcohols (60mM)	
Methanol	0
Glycerol	0
Ethanol	88 ± 6
1-propanol	100 ± 3 [a]
1-butanol	88 ± 2
1-pentanol	74 ± 3
1-hexanol	62 ± 5
1-heptanol	60 ± 4
1-octanol	27 ± 3
2-propanol	43 ± 1
2-butanol	12 ± 3
2-pentanol	39 ± 4
2-phenylethanol	6 ± 0.7
1,3-propanediol	21 ± 0.9
1,2-butanediol	10 ± 2
1,3-butanediol	12 ± 0.8
2,3-butanediol	4.7 ± 1.2
1,4-butanediol	11 ± 0.9
1,5-pentanediol	31 ± 6
2,4-pentandiol	7.9 ± 0.6

Enzyme assay was performed under standard conditions at pH 8.5 and 60 ^{o}C with various substrates. The ADH activity was initiated with the addition of purified enzyme. The oxidation activity was measured with 0.4 mM NAD^{+}. [a] A relative activity of 100% in alcohol oxidation was 9.85 ± 0.3 U/mg.

Table 9. Substrate specificity of ADH1 in the reduction reaction

Substrates	Relative Activity (%)
Aldehydes or ketones (30mM)	
Benzaldehyde	0.5 ± 0.06
Acetaldehyde	73.3 ± 2
Propanal	100 ± 4 [a]
Butyraldehyde	26.1 ± 3
Acetone	9.4 ± 1
Butanone	12.1 ± 2

Enzyme assay was performed under standard conditions at pH 5.0 and 60 ^{o}C with various substrates. The ADH activity was initiated with the addition of purified enzyme. The reduction activity was measured with 0.2 mM NADH. [a] A relative activity of 100% in aldehyde/ketone reduction was 11.85 ± 0.5 U/mg

Table 10. Kinetic parameter values for ADH1

Substrates (mM)	Cofactors (mM)	Apparent K_m (mM)	k_{cat} (s^{-1})	k_{cat} / K_m ($s^{-1}M^{-1}$)
Ethanol (0.36-26.43)	NAD (0.4)	1.79 ± 0.17	4.36 ± 0.12	2436 ± 706
1-Propanol (0.36-26.43)	NAD (0.4)	2.30 ± 0.24	5.18 ± 0.18	2252 ± 750
2-Propanol (0.36-48.58)	NAD (0.4)	4.85 ± 0.21	1.56 ± 0.21	322 ± 100
Butanol (0.36-26.43)	NAD (0.4)	1.68 ± 0.15	4.36 ± 0.08	2595 ± 533
Acetaldehyde (0.36-13.82)	NADH (0.2)	0.61 ± 0.11	4.79 ± 0.21	7852 ± 1909
Propanal (0.36-13.82)	NADH (0.2)	0.41 ± 0.07	6.55 ± 0.22	15,975 ± 3143
Acetone (0.36-26.43)	NADH (0.2)	1.41 ± 0.19	0.64 ± 0.03	454 ± 158
Butyraldehyde (0.36-26.43)	NADH (0.2)	1.75 ± 0.29	1.96 ± 0.10	1120 ± 345

Various concentrations of alcohols (0.36, 0.72, 1.08, 1.44, 2.16, 2.87, 3.58, 7.08, 13.82, 26.43 and 48.58 mM) were used for the determination of oxidation kinetics parameters (**Fig 28**), and various concentrations of aldehydes/ketones (0.36, 0.72, 1.08, 1.44, 2.15, 2.87, 3.58, 7. 08, 13.82 and 26.43 mM) were used for the determination of reduction kinetics parameters (**Fig 29**)

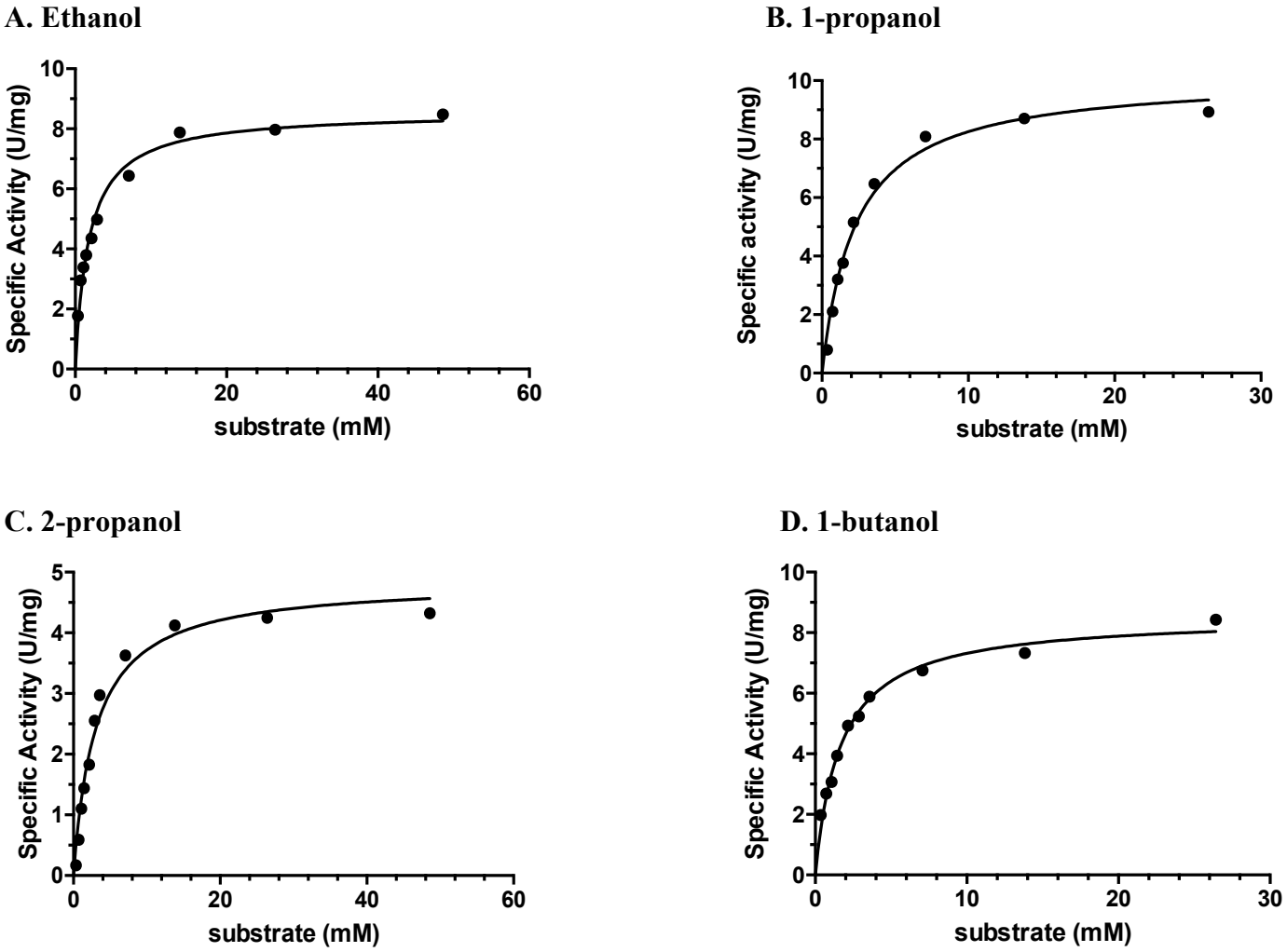

Figure 28. Substrate dependent alcohol oxidation activities of ADH1. Figures showing (A) ethanol; (B) 1-propanol; (C) 2-propanol and (D) 1-butanol. The curves displayed non-linear regression fit of the Michaelis-menten equation of specific activities against different concentrations of substrates.

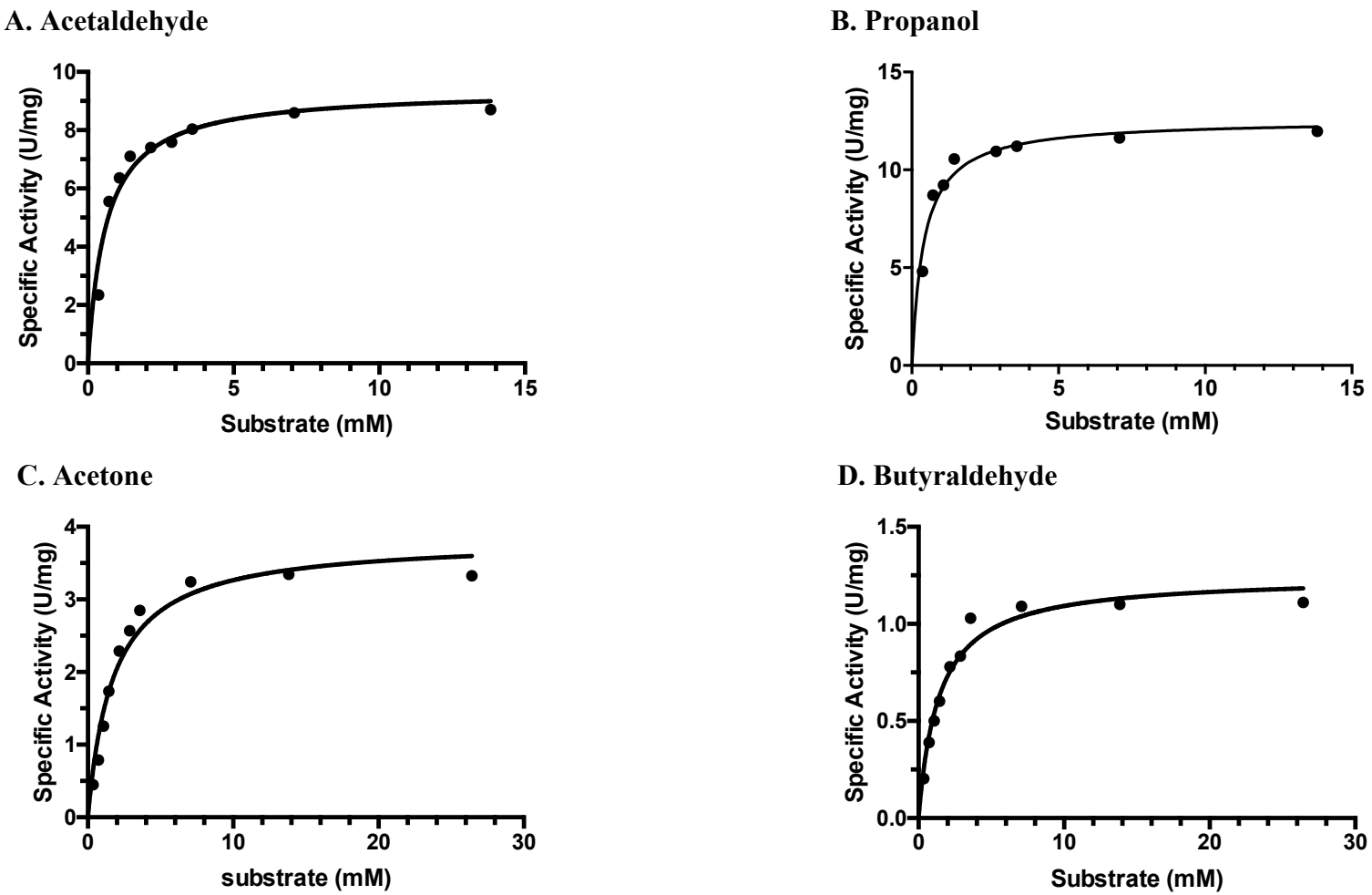

Figure 29. Substrate dependent aldehydes/ketones reduction activities of ADH1. Figures showing (A) acetaldehyde; (B) propanal; (C) acetone and (D) butyraldehyde. The curves displayed non-linear regression fit of the Michaelis-Menten equation of specific activities against different concentrations of substrates

3.4 Alcohol dehydrogenase 2

3.4.1 Purification of ADH2 from H. *butylicus*

The presence of ADH activity in the cell-free extract of *H. butylicus* was first verified with 1-butanol and butyraldehyde as substrates before a purification was carried out. The ADH from the cell-free extract showed activities toward both NADP(H) and NAD(H), which was different from the ADH1 encoded by Hbut_0414. This would suggest there is another ADH (ADH2) presence in *H. butylicus* and it has not been annotated. ADH2 was purified from other proteins through a series of chromatography columns **(Table 11)**. Around 6.5 mg of total proteins were obtained from 1.0 g (wet weight) of cells harvested and 1 L of *H. butylicus* culture yielded 0.6 g of cells biomass.

The cell-free extract of *H. butylicus* with 41 U of ADH2 activity was first loaded onto a DEAE column. Most of other *H. butylicus* proteins bound to the DEAE column similarly to ADH2 and there was only a 1.1-fold purification. ADH2 bound strongly to a HAP column and eluted out after most of the other *H. butylicus* proteins were eluted out. The HAP column resulted in a 4.3-fold purification. The partially purified ADH2 was then loaded onto a phenyl-Sepharose column and it was weakly bound to the column and eluted out before the other *H. butylicus* proteins. The SDS-PAGE showed ADH2 was purified to homogeneity after loading through the phenyl-Sepharose column. The yield of the purification was 52%. ADH2 was stored anaerobically under 5 psi of nitrogen gas at -20^{o}C until further characterization was carried out.

The band corresponded to ADH2 protein was cut out and sent for peptides identification by mass spectrometry at the University of Alberta, AB, Canada.

Table 11. Purification of ADH2 from *H. butylicus*

	Total protein (mg)	Total activity (U)	Specific Activity (U/mg)	Purification fold	Yield (%)
Cell-free extract	30	41	1.367	1.0	100
DEAE	23	36	1.565	1.1	88
HAP	5.1	29	5.854	4.3	71
Phenyl-sepharose	2.6	21	8.236	6.0	52

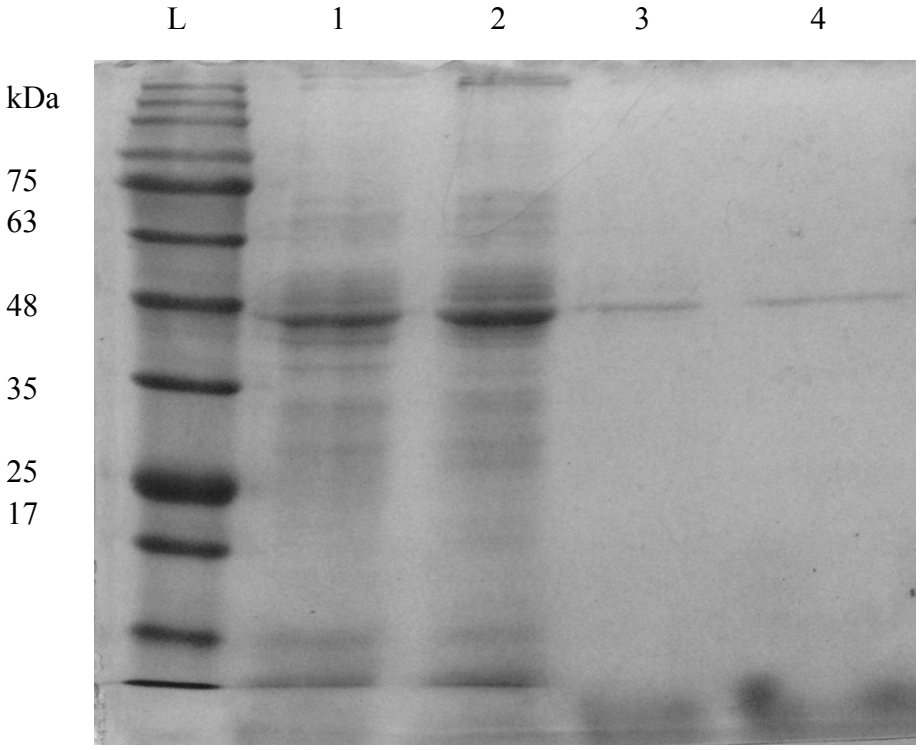

Figure 30. SDS-PAGE (12.5%) for purified ADH2

L; Low molecular weight protein marker; lane 1, *H. buylicus* cell-free extract; lane 2 , combined fractions with ADH2 activity eluted from the DEAE column; lane 3, combined fractions with ADH2 activity eluted from the HAP column; lane 4, purified ADH2 from the phenyl-Sepharose (10 μg of the purified protein was loaded)

3.4.2 Protein concentration dependent enzyme activity

The appropriate protein concentrations for the characterization of purified ADH2 were determined by initiating the enzyme activity with different protein concentrations. Protein amount from 3 μg to 30 μg was used for examining the activity. The specific activities of ADH2 with different protein amounts did not show an apparent constant range, from 6 μg to 18 μg the specific activities increased then decreased slightly. An enzyme amount of 15 μg was used for the following enzyme assays as it was in the range of the highest specific activity **(Fig 31)**. Protein amounts less than 10 μg did not initiate the ADH2 to full activity and no enzyme assay was performed with protein less than 10 μg. Protein amounts greater than 20 μg experienced a decrease in the specific activity. This could be because enzyme at a higher concentration was not under saturated substrate concentration.

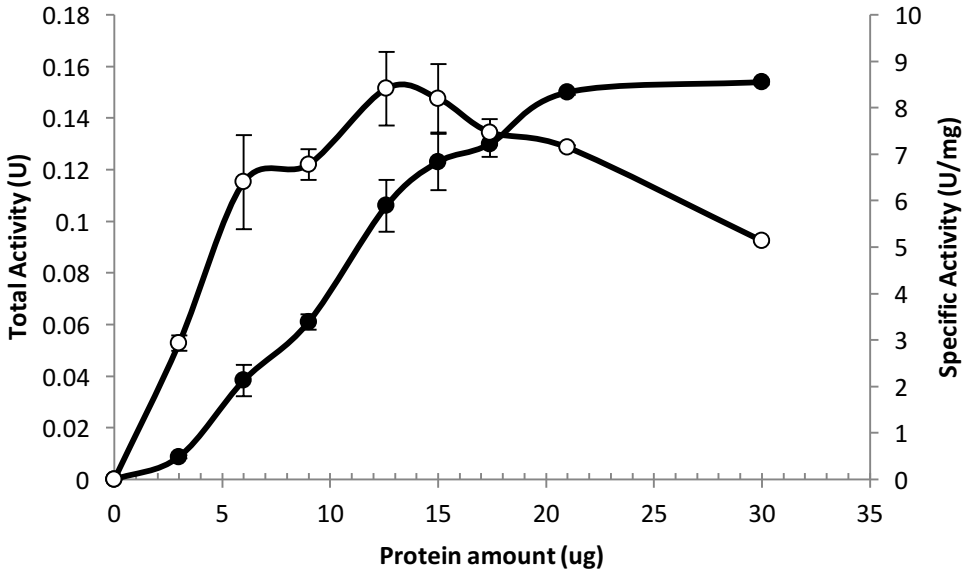

Figure 31. Protein concentration dependent activity of ADH2. Enzyme assay was performed in 100 mM EPPS at pH 9.0 with 60 mM of 1-butanol, 0.4 mM of $NADP^+$ at 80 ^oC, the reaction was initiated with different amount of purified ADH2. Total activity is displayed in filled circles and specific activity is displayed in unfilled circles.

3.3.5.2 Optimal pH

The optimal pH was determined using various 100 mM buffers from 5.5 to 6.5 for the reduction reaction and 8.0 to 11.5 for the oxidation reaction. The optimal pH for 1-butanol oxidation was at 9.0 **(Fig 32A)** and for butyraldehyde reduction was at 6.0 **(Fig 32B).** The reduction activity showed a sharp pH optimal at 6.0 and for the oxidation activity, it decreased dramatically when pH increased to higher than 9.5.

3.3.5.3 Optimal temperature

The optimal temperature for ADH2 activity was measured from 50 ^{o}C to 90 ^{o}C with 1-butanol as substrate. The activity continuously increased from 60 to 90 ^{o}C and no activity was shown from 50 to 60 ^{o}C **(Fig 33)**. Temperatures higher than 90 ^{o}C was not measured due to the instability of the cofactor NADP at higher temperatures. The optimal temperature was expected to be above 90 ^{o}C. The relative activity was around 50% when measured at 75 ^{o}C and around 75% when measured at 85 ^{o}C.

3.3.5.4 Thermostability

Thermostability of ADH2 was measured at the optimal temperature of growth 95 ^{o}C and at 85 ^{o}C to examine the thermostability at high temperature. ADH2 showed remarkable thermostability at 85 ^{o}C. After incubation at 85 ^{o}C for 25 hours, the relative activity was only decreased to 90% of initial activity. The half-life ($t_{1/2}$) at 95 ^{o}C is about 25 hours, and the rate of decreased in activity was faster at the initial 5 hours. The residual activity decreased to 75% of initial after incubation for 5 hours **(Fig 34)**. The semi-log plot of the residual activities versus heating time were linear at both 85 ^{o}C and 95 ^{o}C **(Fig 35)**. The slopes of these lines showed the inactivation rate constant at 95 ^{o}C was 4 times higher than that at 85 ^{o}C.

3.3.5.5 Oxygen sensitivity

ADH2 sensitivity toward oxygen was measured by exposing the enzyme to oxygen for 1 hour and residual activities were measured at different time intervals. ADH2 was very oxygen sensitive and the residual activity decreased to 50% after ten-minute exposure to oxygen in the presence of 2 mM DTT and 2 mM SDT **(Fig 36)**. After 30 minutes, the residual activity was less than 25%. The semi-log graph of residual activity against time of exposure to oxygen showed an inactivation constant of 0.0524 and they were in a linear relationship **(Fig 37)**.

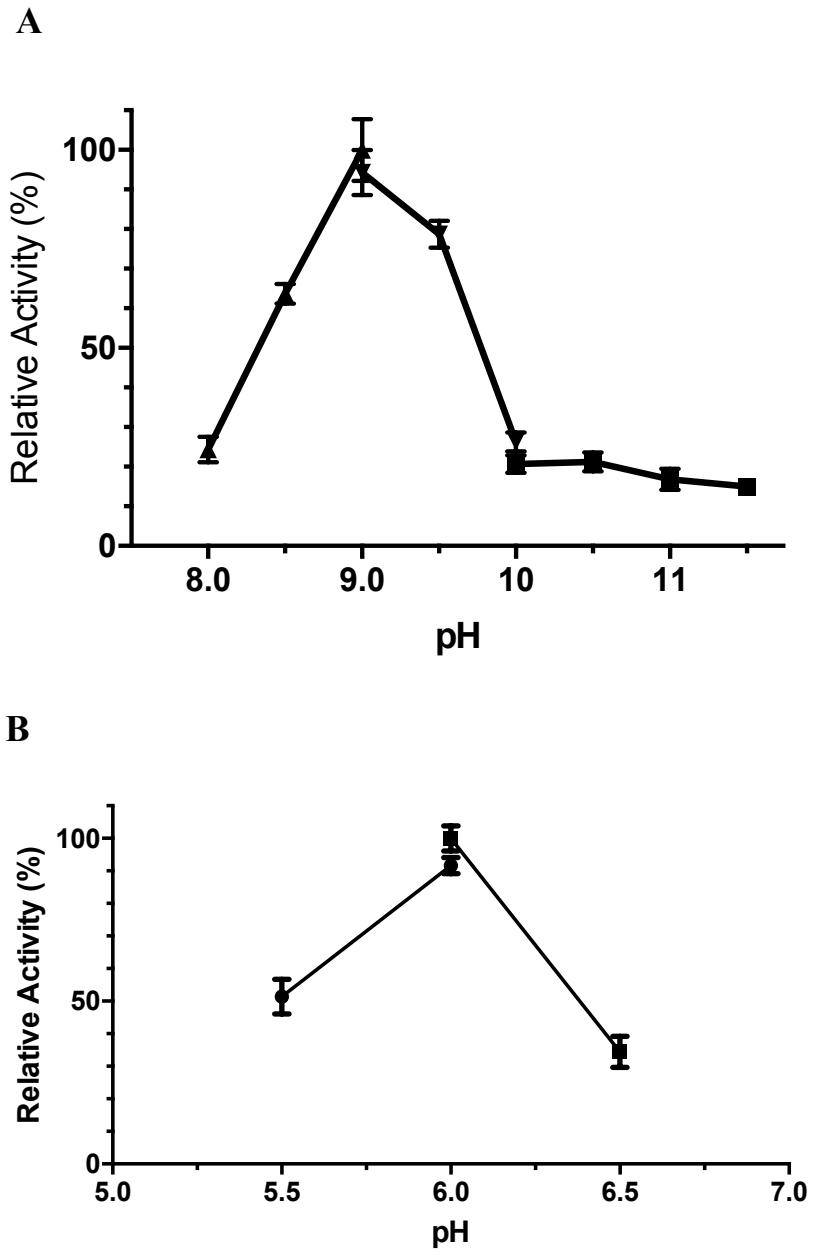

Figure 32. Optimal pH of ADH2. (A) optimal pH for alcohol oxidation. Activities were measured with 60 mM 1-butanol and buffer (100 mM) used were EPPS (filled triangles), glycine (filled inverted triangles), and CAPS (filled diamonds). The relative activity of 100% referred to 8.2 U/mg of alcohol oxidation activity. (B) optimal pH for aldehyde/ketone reduction. Activities were measured with 60 mM butyraldehyde and buffer (100 mM) used were citrate (filled circles) and PIPES (filled squares). The relative activity of 100% referred 11.7 U/mg of aldehyde reduction activity. Data were represented as mean $\pm$ standard derivation. pH values of buffers were measured at room temperatures.

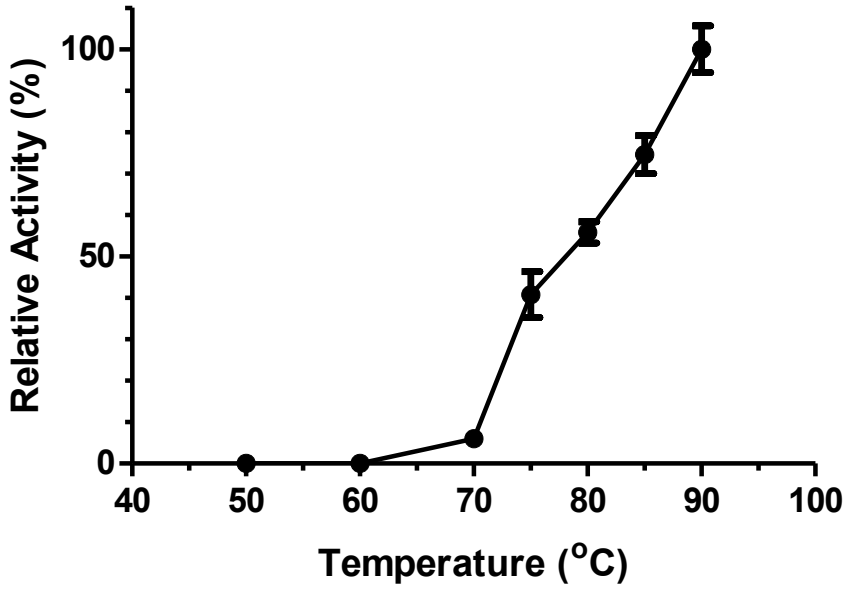

Figure 33. Temperature dependence of ADH2. The activities were measured in the standard assay conditions with temperatures varied from 50 to 90 ^{o}C. The relative activity 100% was defined as the highest activity value at 90 ^{o}C, which was 13.6 U/mg with 60 mM 1-butanol as substrate. Data were presented as mean $\pm$ standard derivation.

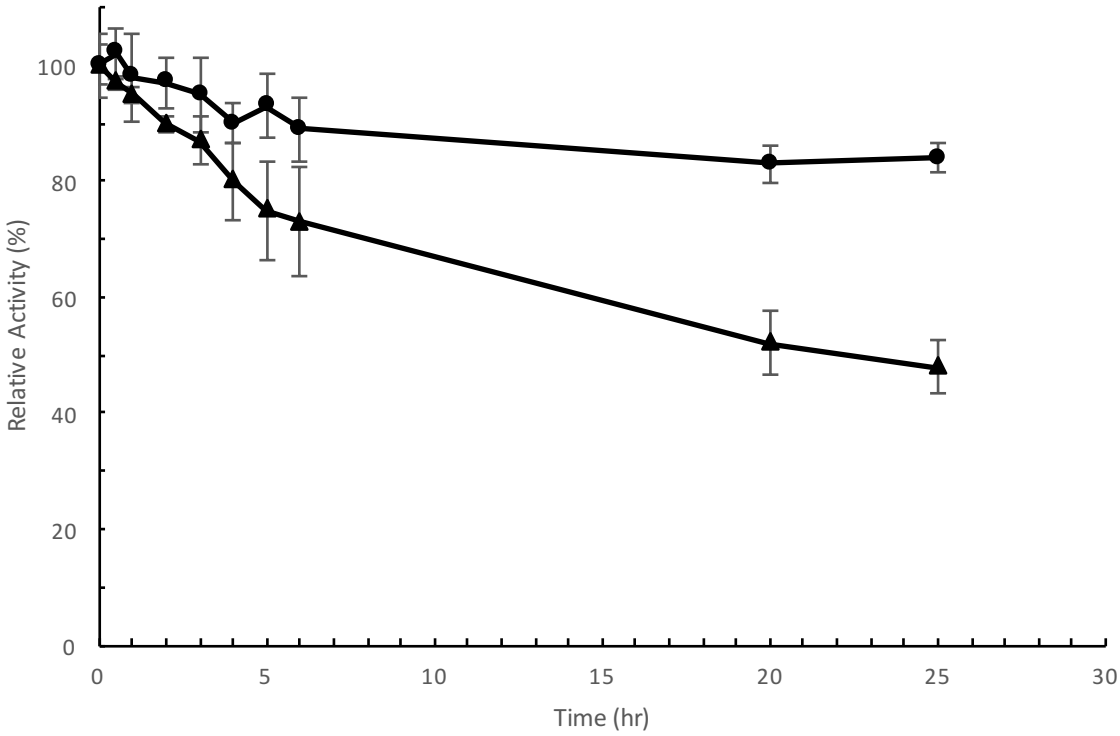

Figure 34. Thermostability of ADH2. Incubation at 85 ^{o}C (filled circles); Incubation at 95 ^{o}C (filled triangles). The relative activity of 100% referred to the initial ADH2 activity without heat treatment with 60 mM 1-butanol as substrate (8.2 U/mg). Enzyme assays were performed at 80 ^{o}C. Data were presented as mean $\pm$ standard derivation

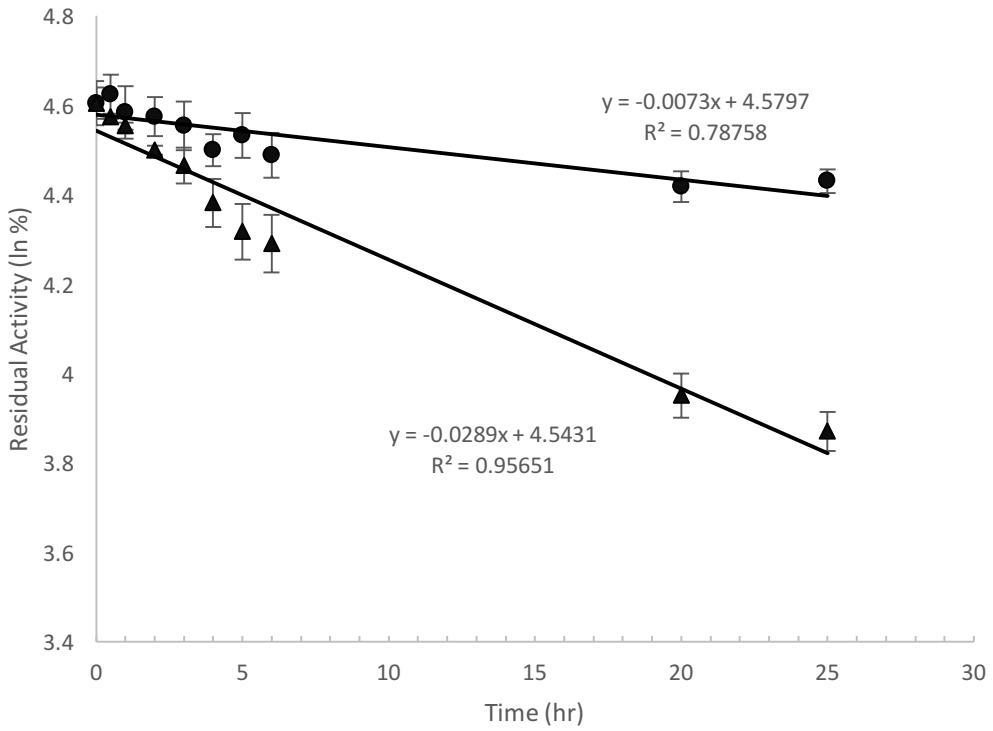

Figure 35. Inactivation of ADH2 at different temperatures. Inactivation rate at 85 ºC (filled circles); inactivation rate at 95 ºC (filled triangles). Residual activities (in the natural log of respective percentages of remaining activities) were plotted against time of incubation at different temperatures. The residual activities were compared to initial ADH2 activity without heat treatment, which was measured using 60 mM 1-butanol as substrate (8.2 U/mg). Data were presented as mean $\pm$ standard deviation.

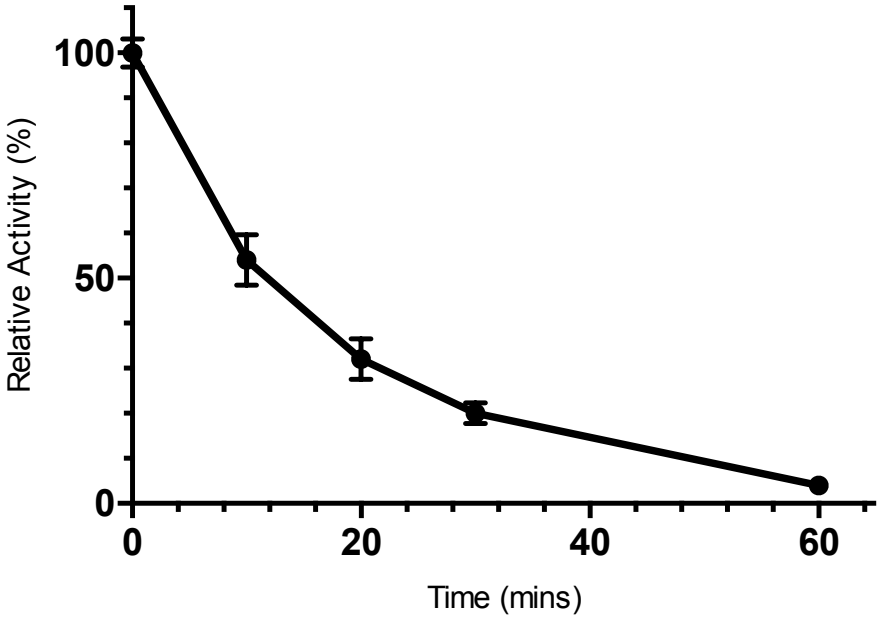

Figure 36. Oxygen sensitivity of ADH2. The activity was measured in the presence of 2 mM DTT and 2 mM SDT. The relative activity of 100% referred to the ADH2 activity before oxygen exposure to air with 60 mM 1-butanol as substrate (8.2 U/mg). Data were presented as mean ± standard derivation.

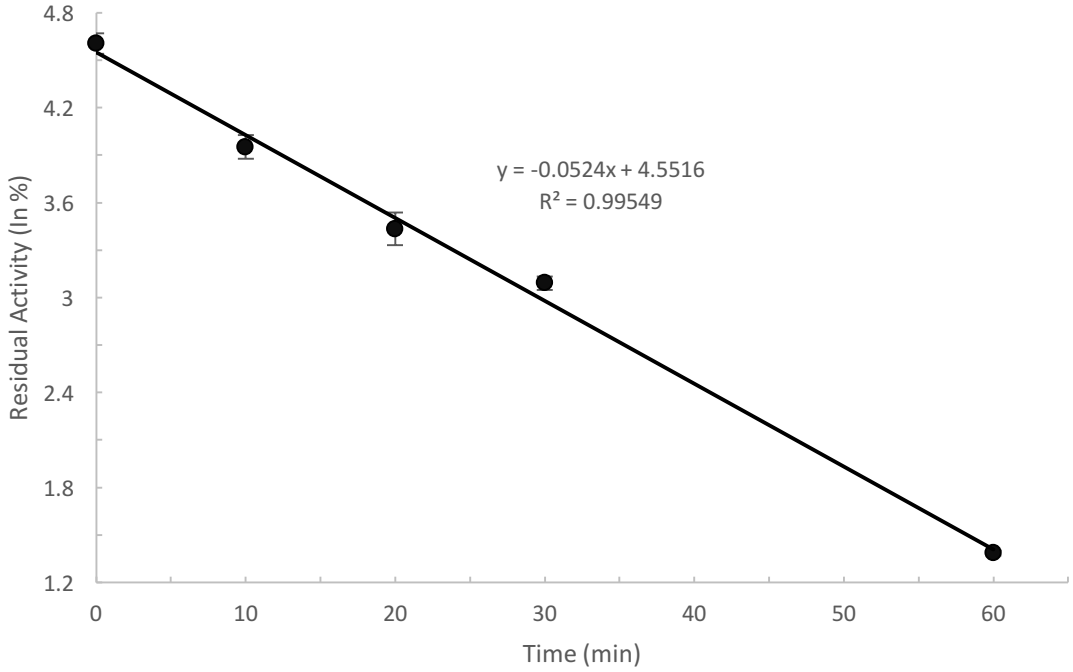

Figure 37. Oxygen inactivation of ADH2. Inactivation rate of ADH2 when exposed to oxygen. The activity was measured in the presence of 2 mM DTT and 2 mM SDT. Residual activities (in the natural log of respective percentages of remaining activities) were plotted against time of exposure to air. The relative activity of 100% referred to the ADH2 activity before oxygen exposure to air with 60 mM 1-butanol as substrate (8.2 U/mg). Data were presented as mean ± standard derivation.

3.4.7 Substrate specificity

The substrate specificity of ADH2 was determined with a set of alcohols, aldehydes, and ketones **(Table 12)**. The highest activity for oxidation was 1-butanol, and for reduction was its corresponding aldehyde butyraldehyde. In the oxidation reaction, ADH2 was able to oxidize a broad range of primary alcohols and secondary alcohols except for methanol. The activities toward primary alcohols were higher than secondary alcohols, suggesting ADH2 was a primary/secondary ADH. The relative activities toward diols were much lower than alcohols and the activities with primary diols were slightly higher than secondary diols. ADH2 showed no activity toward the polyol-glycerol examined. In the reduction reactions, ADH2 exhibited the ability to reduce various aldehydes and ketones **(Table 13)**. The relative activity was higher with acetone than propanal but higher with butyraldehyde than butanone. In general, the activities were higher with aldehydes than ketones.

3.4.8 Enzyme kinetics

The apparent K_m values for substrates in the reduction reaction were around 4 times lower than for the corresponding alcohols in the oxidation reaction **(Table 14)**. The apparent K_m value for acetone was 5.5 times lower than 2-propanol, and that for butyraldehyde was 4 times lower than 1-butanol. For all the substrates examined, the lowest K_m value was with butyraldehyde. The specificity constant k_{cat}/K_m for butyraldehyde was the highest (13,559 $s^{-1}M^{-1}$) and around 2.5 times higher than that for acetaldehyde and 4.8 times higher than that for 1-butanol. The k_{cat}/K_m specificity constant for 2-propanol was 8.7 times lower than that for acetone. The k_{cat}/K_m specificity constants were higher for aldehydes and ketone reduction than those for alcohols oxidation **(Table 14)**. These catalytic properties suggest ADH2 could play an important role in the reduction of butyraldehyde *in vivo*.

Table 12. Substrate specificity of ADH2 in the oxidation reaction

Substrate	Relative Activity (%)
Alcohols (60mM)	
Methanol	0
Glycerol	0
Ethanol	53 ± 3
1-propanol	64 ± 5
1-butanol	100 ± 2 [a]
1-pentanol	57 ± 1
1-hexanol	20 ± 1.3
1-heptanol	6 ± 0.7
1-octanol	2 ± 0.08
2-propanol	48 ± 2.3
2-butanol	75 ± 4
2-phenylethanol	44 ± 1.2
1,3-propanediol	8 ± 0.04
1,2-butanediol	10 ± 0.5
1,3-butanediol	9 ± 0.06
2,3-butanediol	3 ± 0.02
1,4-butanediol	14 ± 1.2
1,5-pentanediol	7 ± 0.8
2,4-pentandiol	2 ± 0.03

Enzyme assay was performed at standard conditions at pH 9.0 and 80 ^{o}C with substrate varied. ADH2 activity was initiated with the addition of purified enzyme. The oxidation activity was measured with 0.4 mM of $NADP^{+}$. [a] A relative activity of 100% in alcohol oxidation was 8.4 ± 0.2 U/mg

Table 13. Substrate specificity of ADH2 in the reduction reaction

Substrate	Relative Activity (%)
Aldehydes or ketones (30mM)	
Benzaldehyde	49 ± 2
Acetaldehyde	78 ± 3
Propanal	20 ± 1
Butyraldehyde	100 ± 5 [a]
Acetone	45 ± 2
Butanone	3.9 ± 0.5

Enzyme assay was performed at standard conditions at pH 6.0 and 80 ^{o}C with substrate varied. ADH2 activity was initiated with the addition of purified enzyme. The reduction activity was measured with 0.2 mM of NADPH. [a] A relative activity of 100 % in aldehydes/ketones reduction was 8.4 ± 0.2 U/mg

Table 14. Kinetic parameter values for ADH2

Substrates (mM)	Cofactors (mM)	Apparent K_m (mM)	k_{cat} (s^{-1})	k_{cat} / K_m ($s^{-1}M^{-1}$)
Ethanol (0.36-48.58)	NADP (0.4)	4.36 ± 0.42	4.00 ± 0.13	915 ± 310
1-Propanol (0.36-48.58)	NADP (0.4)	4.69 ± 0.41	4.40 ± 0.12	938 ± 293
2-Propanol (0.36-48.58)	NADP (0.4)	3.74 ± 0.46	3.47 ± 0.13	928 ± 413
Butanol (0.36-48.58)	NADP (0.4)	2.44 ± 0.30	6.84 ± 0.24	2803 ± 800
Acetaldehyde (0.36-13.82)	NADPH (0.2)	1.27 ± 0.18	7.00 ± 0.31	5512 ± 1722
Propanal (0.36-26.43)	NADPH (0.2)	1.55 ± 0.20	1.79 ± 0.06	1155 ± 300
Acetone (0.36-26.43)	NADPH (0.2)	0.68 ± 0.04	3.84 ± 0.06	8074 ± 1500
Butyraldehyde (0.36-13.82)	NADPH (0.2)	0.59 ± 0.07	8.00 ± 0.22	13,559 ± 3142

Various concentrations of alcohols (0.36, 0.72, 1.08, 1.44, 2.16, 2.87, 3.58, 7.08, 13.82, 26.43 and 48.58 mM) were used for the determination of oxidation kinetics parameters (Fig 34), and various concentrations of aldehydes/ketones (0.36, 0.72, 1.08, 1.44, 2.15, 2.87, 3.58, 7. 08, 10.50, 13.82 and 26.43 mM) were used for determination of reduction kinetics parameters (Fig 35).

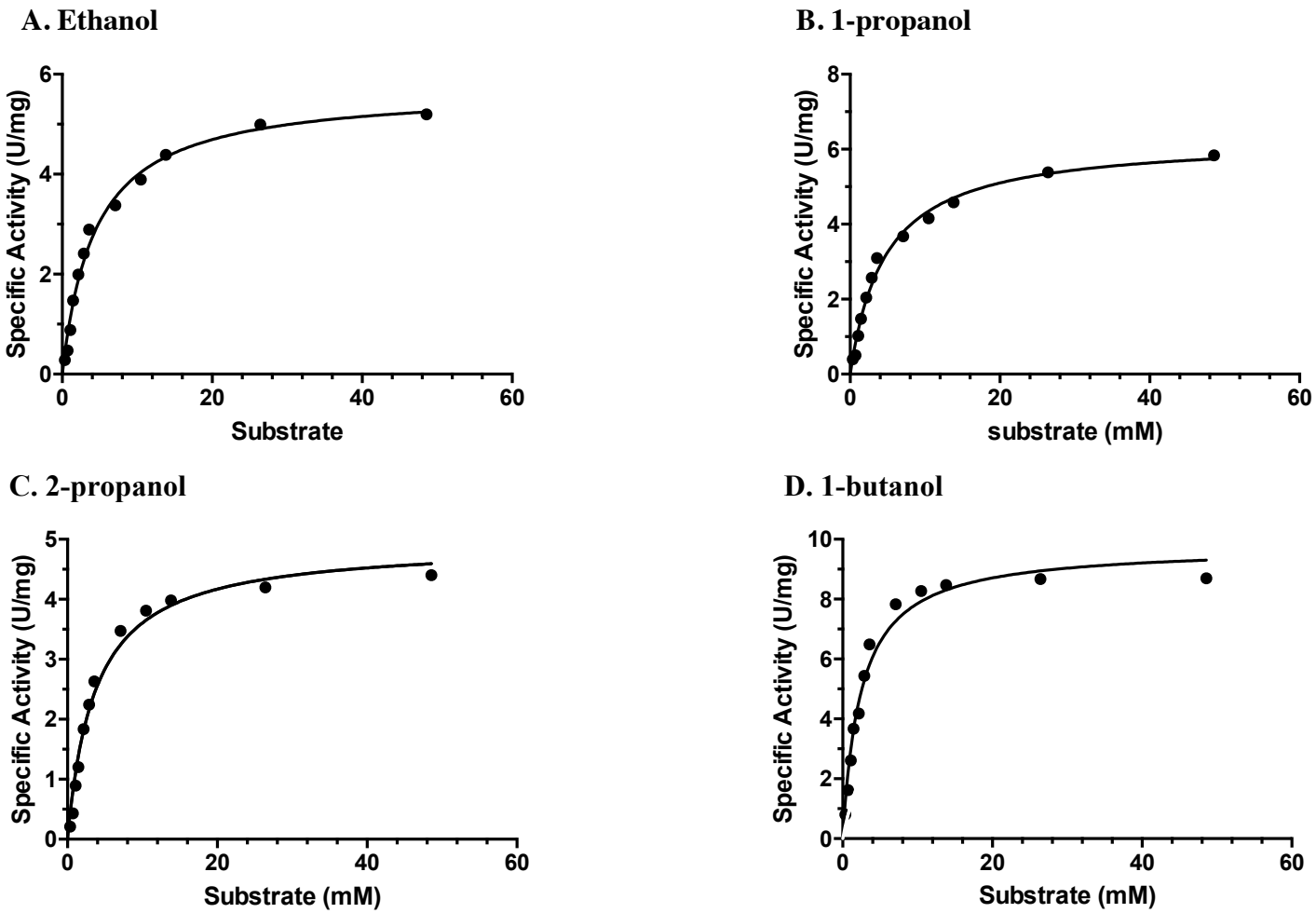

Figure 38. Substrate dependent alcohol oxidation activities of ADH2. Figures showing (A) ethanol; (B) 1-propanol; (C) 2-propanol and (D) 1-butanol. The curves displayed non-linear regression fit of the Michaelis-menten equation of specific activities against different concentrations of substrates.

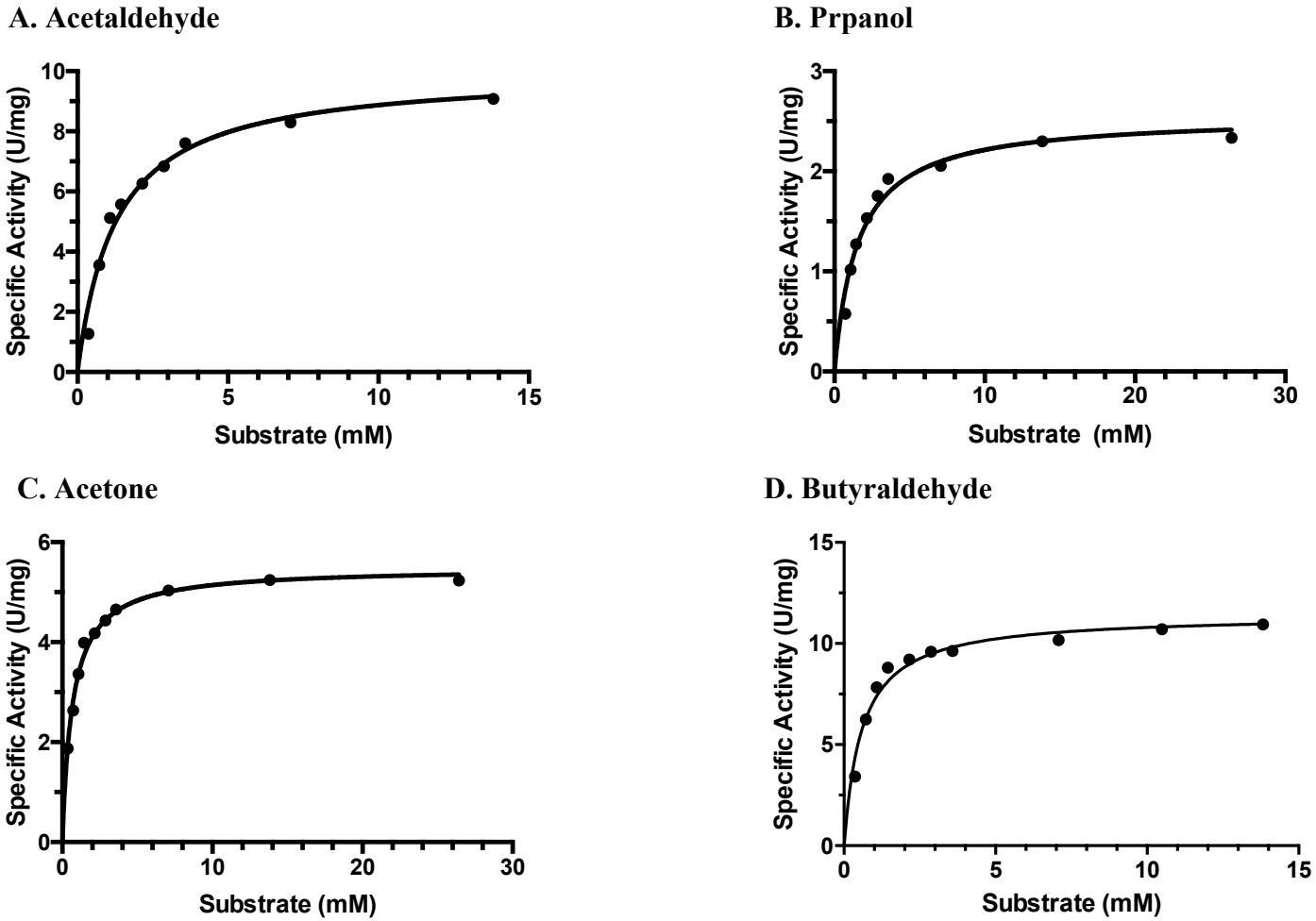

Figure 39. Substrate dependent aldehyde/ketones reduction activities of ADH2. Figures showing (A) acetaldehyde; (B) propanal, (C) acetone and (D) butyraldehyde. The curves displayed non-linear regression fit of the Michaelis-Menten equation of specific activities against different concentrations of substrate

3.4.9 Identification of gene encoding ADH2

The purified ADH2 was sent out for mass spectrometry analysis at the University of Alberta. There were five proteins identified from the band by a mass spectrometer (**Table 15**). Proteins with a similar size in the denatured form could not be separated out by running on an SDS-PAGE. A Size-exclusion column can help to separate proteins with a similar size in the denatured form as it is unlikely they would have the same molecular weight in the native form. However, the protein amount of ADH2 that was eluted out from the phenyl-Sepharose column was only about 2.6 mg. The further purification of ADH2 by the size-exclusion column was not carried out to prevent a further dilution of ADH2 and ensure enough proteins for running an SDS-PAGE that could produce a protein band for peptide identification.

Four proteins identified are already annotated as other enzymes in the *H. butylicus* genome **(Table 15)**. Hbut_0873 is annotated as 4-aminobutyrate aminotransferase with e-value of 2.49 e^{-113}, Hbut_1589 is annotated as aspartate aminotransferase with e-value of 1.69 e^{-157}, Hbut_0503 is annotated as ribulose bisphosphate carboxylase with e-value of 0 and Hbut_0451 is annotated as Xaa-Pro aminopeptidase with e-value of 1.53. The low e-value scores might indicate their presence in the sample prepared, but surely none of them could be an ADH, which could be further supported by the protein scores indicating there might be approximately 80% purity (**Table 15**). The protein encoded by Hbut_0924 has the highest score from the mass spectrometer data and is annotated as a hypothetical protein. The sequence was further analyzed and compared with other annotated ADHs from genomes of hyperthermophiles available from NCBI (http://www.ncbi.nlm.nih.gov).

Nucleotide blast of the Hbut_0924 sequence for a highly similar sequence (megablast) against all genomes showed no significant similarity hit. Blastn search against all genomes also showed no hit with e-value lower than 0.01. Blastp search for similar protein sequence also showed no significant hit. However, DELTA-BLAST for domain enhanced lookup

time accelerated blast against all genomes showed Hbut_0924 had the lowest e-value of 1 e^{-33} with a hypothetical protein from *Pyrodictium Delaneyi* (WP_055409879). The comparison showed 30% in identity but similarly no conserved domain could be identified from this protein.

Since *H. butylicus* is closely related to *Desulfurococcus mucosus* DSM2162 (Brugger, Chen et al 2007), a species from the phylum *Crenarchaeota*, an attempt was made to search its genome. Blastn search showed Hbut_0924 had the lowest e-value of 7 e^{-4} with an iron-containing ADH in *D. mucosus* genome. Reversely, using the gene (DESMU_RS01575) encoding the iron-containing ADH from *D. mucosus* to search the *H. butylicus* genome, the blastn search hit the Hbut_0924 gene with the lowest e-value of 9 e^{-4}.

Although the Blastp search using Hbut_0924 did not find any iron-containing ADH homolog from the NCBI database, the Blastp search using the gene encoding *D. mucosus* iron-containing ADH (DESMU_RS01575) hit five iron-containing ADHs from hyperthermophilic *Crenarchaeota* including *Desulfurococcus fermentans*, *Archaeoglobus profundus*, *Pyrobaculum Islandicum*, *Thermogladius cellulolyticus* and *Thermosphaera Aggregans* with very low e-values (from 0 to 1 e^{-91}). These ADHs belong to the same protein family with conserved domains for $NAD(P)^+$ binding motif and iron metal binding motif. The protein sequence of Hbut_0924 was then aligned with these ADHs to identify its cofactor $NAD(P)^+$ binding motif and Fe ion binding motif.

Table 15. Mass spectrometry data with peptides from *H. butylicus*

Description	Score	Coverage	# Proteins	# Unique Peptides	# Peptides
Hbut_0924	767.88	75.36	1	29	29
Hbut_0873	69.51	39.21	1	13	13
Hbut_1589	60.67	46.49	1	13	13
Hbut_0503	16.88	16.55	1	6	6
Hbut_0451	13.33	18.98	1	5	5

Protein score is the sum of the ion scores of all peptides that were identified; Coverage is the percentage of the protein sequence covered by identified peptides; # proteins is the number of identified proteins in a protein group; #unique peptides is the number of peptide sequences that are unique to a protein group. # peptides is the total number of distinct peptide sequences identified in the protein group

The entire gene encoding Hbut_0924 has 1104 bp with a deduced 367 amino acid residues. The molecular weight was calculated to be 40,694 Da. It is annotated as a hypothetical protein and there is no conserved domain identified in the sequence from NCBI.

The protein sequence of Hbut_0924 was aligned with six annotated Fe-containing ADHs from hyperthermophilic *Crenarchaeota* and sequences identities were compared. The protein sequence from *H. butylicus* has around 20% identity with all the ADHs while the other ADHs compared to each other has more than 40% identity. The highest percent identity was with ADH from *T. cellulolyticus* (WP_014737928), which was 23.3%, followed by ADH from *A. profundus* (WP_012939782.1) with 22% identity.

In the sequence alignment with the hyperthermophilic ADHs, it was found that Hbut_0924 had the three glycine residues in its putative conserved cofactor NAD(P) binding motif ($G_{63}G_{64}G_{65}XXI_{68}$), and the iron binding motif had a slight motification **(Fig 40)**. There were three histidine residues ($H_{130}H_{223}H_{231}$) in the putative iron binding motif but the aspartic acid was replaced with a semi-conserved substitution glutamic acid. ADH2 from *H. butylicus* was highly oxygen sensitive and most likely due to its metal iron. The putative Fe binding motif site in the amino acid sequence and the similarity with other hyperthermophilic Fe-ADHs indicate Hbut_0924 to be an NAD(P)H dependent Fe-containing ADH.

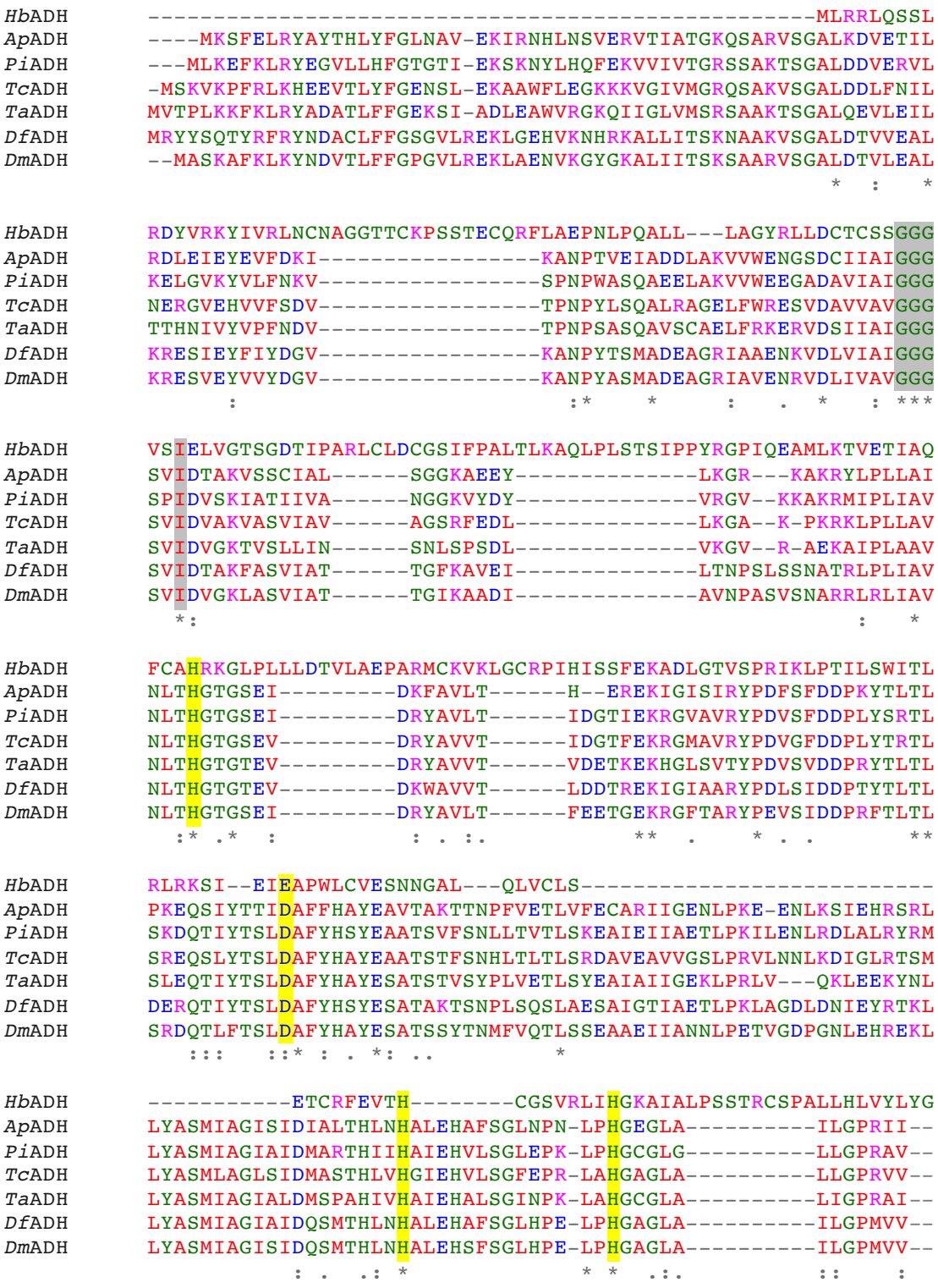
HbADH ----------MLRRLQSSL
ApADH ----MKSFELRYAYTHLYFGLNAV-EKIRNHLNSVERVTIATGKQSARVSGALKDVETIL
PiADH ---MLKEFKLRYEGVLLHFGTGTI-EKSKNYLHQFEKVVIVTGRSSAKTSGALDDVERVL
TcADH -MSKVKPFRLKHEEVTLYFGENSL-EKAAWFLEGKKKVGIVMGRQSAKVSGALDDLFNIL
TaADH MVTPLKKFKLRYADATLFFGEKSI-ADLEAWVRGKQIIGLVMSRSAAKTSGALQEVLEIL
DfADH MRYYSQTYRFRYNDACLFFGSGVLREKLGEHVKNHRKALLITSKNAAKVSGALDTVVEAL
DmADH --MASKAFKLKYNDVTLFFGPGVLREKLAENVKGYGKALIITSKSAARVSGALDTVLEAL
RDYVRKYIVRLNCNAGGTTCKPSSTECQRFLAEPNLPQALL---LAGYRLLDCTCSSGGG
RDLEIEYEVFDKI----------KANPTVEIADDLAKVVWENGSDCIIAIGGG
KELGVKYVLFNKV----------SPNPWASQAEELAKVVWEEGADAVIAIGGG
NERGVEHVVFSDV----------TPNPYLSQALRAGELFWRESVDAVVAVGGG
TTHNIVYVPFNDV----------TPNPSASQAVSCAELFRKERVDSIIAIGGG
KRESIEYFIYDGV----------KANPYTSMADEAGRIAAENKVDLVIAIGGG
KRESVEYVVYDGV----------KANPYASMADEAGRIAVENRVDLIVAVGGG
VSIELVGTSGDTIPARLCLDCGSIFPALTLKAQLPLSTSIPPYRGPIQEAMLKTVETIAQ
SVIDTAKVSSCIAL------SGGKAEEY----------LKGR---KAKRYLPLLAI
SPIDVSKIATIIVA------NGGKVYDY----------VRGV--KKAKRMIPLIAV
SVIDVAKVASVIAV------AGSRFEDL----------LKGA--K-PKRKLPLLAV
SVIDVGKTVSLLIN------SNLSPSDL----------VKGV--R-AEKAIPLAAV
SVIDTAKFASVIAT------TGFKAVEI----------LTNPSLSSNATRLPLIAV
SVIDVGKLASVIAT------TGIKAADI----------AVNPASVSNARRLRLIAV
FCAHRKGLPLLLDTVLAEPARMCKVKLGCRPIHISSFEKADLGTVSPRIKLPTILSWITL
NLTHGTGSEI---------DKFAVLT------H--EREKIGISIRYPDFSFDDPKYTLTL
NLTHGTGSEI---------DRYAVLT------IDGTIEKRGVAVRYPDVSFDDPLYSRTL
NLTHGTGSEV---------DRYAVVT------IDGTFEKRGMAVRYPDVGFDDPLYTRTL
NLTHGTGTEV---------DRYAVVT------VDETKEKHGLSVTYPDVSVDDPRYTLTL
NLTHGTGTEV---------DKWAVVT------LDDTREKIGIAARYPDLSIDDPTYTLTL
NLTHGTGSEI---------DRYAVLT------FEETGEKRGFTARYPEVSIDDPRFTLTL
RLRKSI--EIEAPWLCVESNNGAL---QLVCLS----------
PKEQSIYTTIDAFFHAYEAVTAKTTNPFVETLVFECARIIGENLPKE-ENLKSIEHRSRL
SKDQTIYTSLDAFYHSYEAATSVFSNLLTVTLSKEAIEIIAETLPKILENLRDLALRYRM
SREQSLYTSLDAFYHAYEAATSTFSNHLTLTLSRDAVEAVVGSLPRVLNNLKDIGLRTSM
SLEQTIYTSLDAFYHAYESATSTVSYPLVETLSYEAIAIIGEKLPRLV---QKLEEKYNL
DERQTIYTSLDAFYHSYESATAKTSNPLSQSLAESAIGTIAETLPKLAGDLDNIEYRTKL
SRDQTLFTSLDAFYHAYESATSSYTNMFVQTLSSEAAEIIANNLPETVGDPGNLEHREKL
----------ETCRFEVTH--------CGSVRLIHGKAIALPSSTRCSPALLHLVYLYG
LYASMIAGISIDIALTHLNHALEHAFSGLNPN-LPHGEGLA----------ILGPRII--
LYASMIAGIAIDMARTHIIHAIEHVLSGLEPK-LPHGCGLG----------LLGPRAV--
LYASMLAGLSIDMASTHLVHGIEHVLSGFEPR-LAHGAGLA----------LLGPRVV--
LYASMIAGIALDMSPAHIVHAIEHALSGINPK-LAHGCGLA----------LIGPRAI--
LYASMIAGIAIDQSMTHLNHALEHAFSGLHPE-LPHGAGLA----------ILGPMVV--
LYASMIAGISIDQSMTHLNHALEHSFSGLHPE-LPHGAGLA----------ILGPMVV--

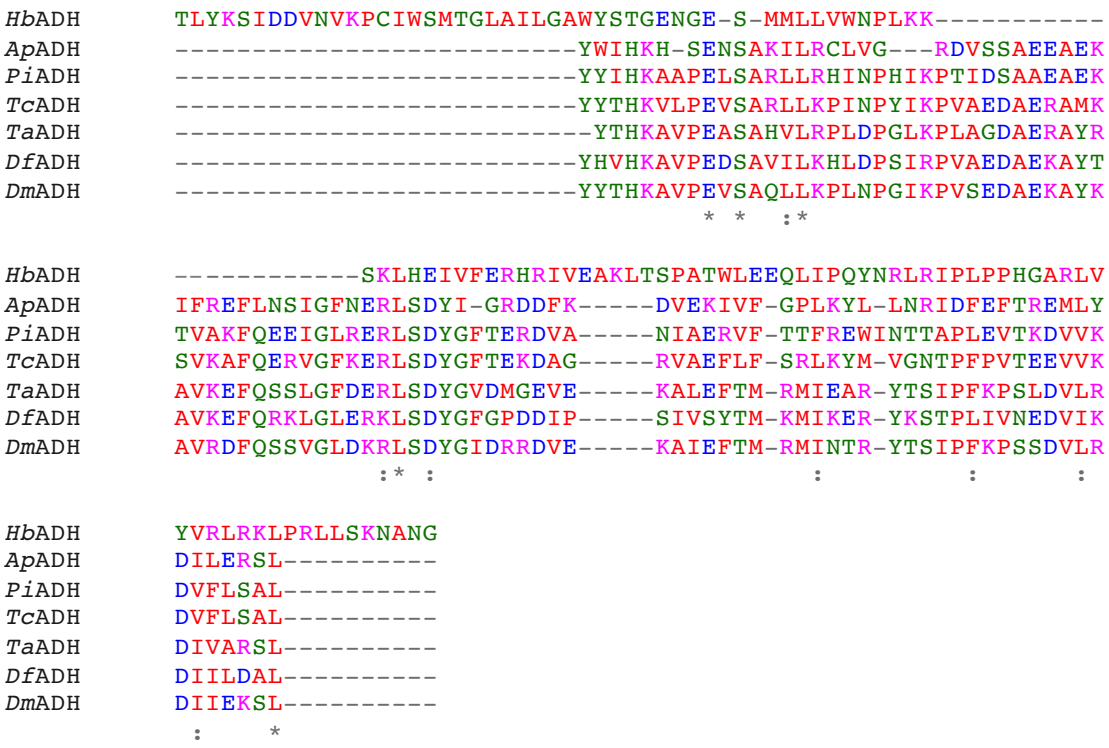

Figure 40. Amino acid sequences alignment of ADH2 and its homologous

The sequences were aligned using Clustal Omega (Larkin, Blackshields et al. 2007). *Hb*ADH, ADH2 encoded by Hbut_0924 from *H. butylicus* (WP_011822090); *Ap*ADH, ADH from *A. profundus* (WP_012939782.1); *Df*ADH, ADH from *D. fermentans* (WP_014767018); *Dm*ADH, ADH from *D. mucosus* (WP_013561843); *Ta*ADH, ADH from *T. aggregans* (WP_013129339); *Pi*ADH, ADH from *P. islandicum* (WP_011763330.1); *Tc*ADH, ADH from *T. cellulolyticus* (WP_014737928). "*", amino acid residues that are identical in all sequences in alignment; ":", conserved substitutions; ".", semi-conserved substitutions; "-", no corresponding amino acid. Highlighted in grey, conserved putative motif of cofactor binding sites; Highlighted in yellow, conserved putative motif of iron binding sites. Red: small and hydrophobic amino acids and tyrosine; Blue: acidic amino acids; Magenta: basic amino acids and histidine; Green: amino acids with hydroxyl, sulfhydryl or amine group and glycine.

Chapter 4. Discussion

4.1 Growth of *H. butylicus*

H. butylicus is a hyperthermophilic peptide-fermenting archaeon growing optimally from 95 ºC to 106 ºC at pH 7.0 (Zillig, Holz et al. 1990). Reported growth conditions of *H. butylicus* include the use of a high pressure (2,000 kPa) fermenter and continue gassing with CO_2 or N_2 (Zillig, Holz et al. 1990). In this study, the growth of *H. butylicus* was studied in small closed serum bottles, which is operational in a conventional laboratory.

In this study, it was found that the addition of buffer, HEPES, in the culture media enhanced the maximum cell density of *H. butylicus* by 2-fold. CO_2 in the fermenter can act as a buffer for the culture and stabilize the pH. The study of the growth of *H. butylicus* at different pH values also showed that it had a sharp pH optimal at 7.0. The maximum cell density obtained in this study was around 1.3 x 10^8 cells/ml, which was less than the maximum cell density of 2.0 x 10^8 cells/ml reported previously (Zillig, Holz et al. 1990). This was probably due to the requirement of H_2 for the maximum growth of *H. butylicus*, which can only be achieved using a high pressure resistant fermenter (Zillig, Holz et al. 1990).

The growth of *H. butylicus* is strongly stimulated by the addition of sulfur (10 g/L) and H_2 (200 kPa in closed vessels or 20% [v/v] in continuously gassed culture) with the production of H_2S (Zillig, Holz et al. 1990). This study also confirmed that the cell density was decreased by five times in the absence of H_2 or sulfur. In addition, the growth of *H. butylicus* was directly correlated with the H_2 pressure, and the higher the H_2 pressure, the higher the final cell density. It is speculated H_2 and sulfur act as additional means for energy conservation, which is also observed in hyperthermophilic archaea *Pyrodictium abyssum* and *Pryococcus woesei* (Zillig, Holz et al. 1987).

4.2 Metabolic end-products and possible pathways

H. butylicus is named *butylicus* because of the similarity in fermentation products as *Clostridium butylicum*, also known as *C. beijerinckii* (Zillig, Holz et al. 1990). Unlike other *Clostridium* species, where n-butanol is produced at pH values below 5.0, *C. beijerinckii* produces over 60 mM of n-butanol in fermentation when pH was maintained constant at 6.8 (George, Johnson et al. 1983). However, other than 1-butanol and acetate, the other fermentation products in the butanol production pathway including 2-propanol, acetone, butyrate and ethanol are not reported. This study showed in addition to 1-butanol and acetate; acetone, 2-propanol, and butyrate were also produced by *H. butylicus*. The production of 1-butanol and acetone were not pH dependent but depended on the cell density. Moreover, the concentration of 1-butanol and acetate detected were lower than reported probably due to the lower cell density obtained in cultures. 2-propanol was produced after the production of acetone, which suggests it is the product of acetone reduction possibly catalyzed by an ADH from *H. butylicus*. This catalytic conversion is only reported in some of the *C. beijerinckii* strains such as *C. beijerinckii* DSM 6423 and *C. beijerinckii* NRRL B593 (Ismaiel, Zhu et al. 1993, Survase, Jurgens et al. 2011). Ethanol was not detected in the cultures of all the growth conditions; this might be because ethanol was produced in very low concentration that was below the detection limit of HPLC. The pathway of butanol production is not known and the possibility that ethanol was not produced can not be ruled out. The common fermentation end-products from carbohydrates metabolism including succinic acid and lactic acid were not detected. Isovaleric acid, the metabolic product from leucine, was detected. Formic acid was also likely produced from *H. butylicus* as the area of the peak corresponding to formic acid increased along with growth. Enzymes catalyzing the production of formic acid are pyruvate-formate lyase and formate dehydrogenase (Sawers et al. 1998, Schutte et al. 1976). In the genome of *H. butylicus,* Hbut_0136 and Hbut_1247 are genes annotated as pyruvate-formate lyase and

Hbut_1052 is the gene annotated as formate dehydrogenase. The annotation of these enzymes further suggests the production of formic acid from *H. butylicus*.

Due to the similarity in metabolic end products with *Clostridium* species, homologs of key enzymes in the *Clostridium's* butanol pathway were searched in the *H. butylicus* genome. However, those key enzymes including butyryl-CoA dehydrogenase, β-hydroxybutyryl-CoA dehydrogenase, acetoacetyl-CoA: acetate: CoA-transferase, acetoacetyl-CoA: butyrate: CoA transferase and butyraldehyde dehydrogenase have no significant homolog in the genome **(Table 16)**. Similarly, gene homologs for enzymes catalyzing acetate and butyrate productions in *Clostridium* species were searched in the *H. butylicus* genome. In *Clostridium* species, phosphotransacetylase and acetate kinase are enzymes catalyzing acetate production, whereas phosphotransbutyrylase and butyrate kinase are enzymes catalyzing butyrate production (Louis, Duncan et al. 2004). In the *H. butylicus* genome, out of the four enzymes, the only enzyme annotated is butyrate kinase, which is encoded by the gene Hbut_0767. Another group of enzyme called ADP/AMP-dependent acetyl-CoA synthetase can catalyze the production of acetate from acetyl-CoA, which is found in anaerobic microorganisms such as *Entamoeba histolytica* and *Giardia Lamblia* (Field, Rosenthal et al. 2000; Sanchez, Galperin et al. 2000). There are two genes from the *H. butylicus* genome annotated as acetyl-CoA synthetase, which are Hbut_0152 and Hbut_1337. If these enzymes were responsible for acetate production in *H. butylicus*, the similar catalytic reaction can be used for butyrate production from butyrate-CoA and phosphotransbutyrylase will not be needed. Acetoacetate decarboxylase, the enzyme catalyzing acetone production in *Clostridium* species, is not annotated in *H. butylicus* genome. However, the detection of acetone further suggests the metabolic end-products from *H. butylicus* resembles that of *Clostridium* species.

Table 16. Potential homologs of genes from *H. butylicus* encoding enzymes involved in the butanol metabolic pathway in *C. acetobutylicum* ATCC 824.

Enzymes from *C. acetobutylicum* ATCC 824	Homolog genes present in *H. butylicus*	E-value [a]	% identity [b]	Description
Pyruvate:ferredoxin oxidoreductase	Hbut_0730	$5.44e^{-134}$	28.23	Pyruvate ferredoxin oxidoreductase
	Hbut_0668	$1.45e^{-31}$	27.43	Pyruvate ferredoxin oxidoreductase
Thiolase	Hbut_1528	$9.53e^{-152}$	29.01	Acetyl-CoA acetyltransferase
β-hydroxybutyryl-CoA dehydrogenase	Hbut_0193	2.8	13.47	3-hydroxyisobutyate dehydrogenase
Crotonase	Hbut_1155	$8.62e^{-28}$	28.00	Methylmalonyl-CoA carboxyltransferase
Butyryl-CoA dehydrogenase	Hbut_0229	1.1	4.48	AbrB family transcriptional regulator
Acetoacetyl-CoA: acetate: CoA-transferase	Hbut_1028	0.9	7.71	Predicted ABC transporter
Acetoacetyl-CoA: butyrate: CoA transferase	Hbut_0788	3.5	11.48	Hypothetical protein
Butyraldehyde dehydrogenase	Hbut_0044	3.6	2.09	Hypothetical protein
Butanol dehydrogenase	Hbut_0414	$6.24e^{-10}$	10.56	Zinc-dependent alcohol dehydrogenase

[a] Expected value of homolog genes from *H. butylicus* DSM 5456 (taxid:415426) with the conserved domains of corresponding enzymes from *C. acetobutylicum* ATCC 824 (taxid:272562) [b] Showing the percentage of identity between the protein sequences of corresponding enzymes from *C. acetobutylicum* ATCC 824 and *H. butylicus* DSM 5456 using Clustal W2 available from http://www.genome.jp/tools/clustalw/. The enzymes are compared with genes from *H. butylicus* with the highest bit scores showed from blastp program (protein to protein blast) from database non-redundant protein sequence (nr) available at http://www.ncbi.nlm.nih.gov/ blast/Blast.cgiQUERY

H. butylicus utilizes only peptides as growth substrates, so it is possible that it uses the 1-butanol production pathway in *S. cerevisiae*. However, most homologs of corresponding enzymes in the pathway were not found in the genome of *H. butylicus* except for glycine oxidase and threonine dehydratase, which are also used for amino acid metabolism (Massey, Sokatch et al. 1976, Pederson, Steele et al. 1999). For malate synthase, α/β-isopropylmalate dehydrogenase, α-isopropylmalate synthase, α-isopropylmalate isomerase, pyruvate decarboxylase and 2-ketoacid decarboxylase, no significant homolog was found using blastp (protein to protein blast) or megablast (highly similar sequence) from NCBI. Moreover, blastn (somewhat similar sequences) showed no significant similarity with an e-value lower than 0.01. There is a total of 870 hypothetical proteins out of 1602 proteins in the genome of *H. butylicus*, and conserved domains in all of the proteins were searched with a batch web C-D (conserved-domains) tool available from http://www.ncbi.nlm.nih.gov/ structure/bwrpsb/mbwrpsb.cgi with an e-value threshold of 0.01. There was no conserved domain in the hypothetical proteins that was similar to those enzymes in either pathway. Both *S. cerevisiae* and *C. acetobutylicum* are divergent in evolution from *H. butylicus* and could be the reason for the lack of sequence homologs in the genome.

There is no complete alcohol production pathway identified in hyperthermophiles but ethanol had been reported as one of the metabolic end-products in several hyperthermophiles. An interesting group of enzymes, tungstoenzymes, which include carboxylic acid reductase (CAR) and aldehyde ferredoxin oxidoreductase (AOR) are ubiquitously found in thermophiles or hyperthermophiles (Mukund and Adams 1993). The amino acid sequences of purified CAR and AOR showed high sequence identities and suggest they are closely related to each other and have similar catalytic functions (Heider, Ma et al. 1995). Although the primary role of CARs and AORs is to catalyze the oxidation of aldehydes, they were also proposed to have the physiological role in the conversion of

carboxylic acids into aldehydes (Mukund and Adams 1991, Heider, Ma et al. 1995). Purified CARs from *Clostridium formicoaceticum* and *Clostridium thermoaceticum* are discovered to have the ability to reduce carboxylic acids into corresponding aldehydes (White, Stroel et al. 1989, White, Feicht et al. 1991). Substrates for reduction including both aliphatic and aromatic acids with apparent K_m values from 1 to 50 mM. The rates of reduction of aliphatic carboxylic acids are 5 to 10% compared to the rates of oxidization of corresponding aldehydes (White, Strobl et al. 1989, White, Feicht et al. 1991). In hyperthermophiles, AORs were purified and characterized from saccharolytic *P. furiosus* and proteolytic *Thermococcus* strain ES1 (Mukund and Adams 1991, Heider, Ma et al. 1995). The AOR purified from *Thermococcus* strain ES1 showed great similarity in catalytic properties with the CARs from the two *Clostridium* species and the AOR from *P. furiosus* (Heider, Ma et al. 1995). The physiological role of AOR in hyperthermophiles is unclear but based on the enzyme kinetics and substrate specificity of *Thermococcus* strain ES1 AOR, the role in the reduction of organic acid isovalerate, isobutyrate and phenylacetate from amino acid metabolism into corresponding aldehydes was proposed (Heider, Ma et al. 1995). Although the reaction is a very low potential reaction and the production of aldehyde is very unfavorable thermodynamically, the accumulation of organic acids and a high ratio of reduced ferredoxin to oxidized ferredoxin *in vivo* could drive the reaction.

There are four AOR genes annotated in the genome of *H.* butylicus, which are Hbut_1001, Hbut_0351, Hbut_1553, and Hbut_0737. Proteins from all the annotated AOR genes have over 33% identities with the characterized AOR from *P. furiosus*, and the protein encoded from Hbut_1001 has the highest protein identity (49.1%). It will be interesting to examine the enzyme activities of AORs from *H. butylicus* in the conversion of butyric acid into butyraldehyde, the precursor of 1-butanol. Butyrate was detected at a low concentration in the culture, there is a possibility that butyric acid is produced *in vivo* and converted into

butyraldehyde by AORs in *H. butylicus*. To test this hypothesis, the addition of high concentration of butyric acid in the culture of *H. butylicus* should increase 1-butanol production catalyzed by AORs.

The pathway for butanol production in *H. butylicus* is unknown but ADH is the only enzyme catalyzing the reduction of aldehyde into alcohol *in vivo* and it must be present in *H. butylicus* for 1-butanol production.

4.3 Physiological roles of ADHs

Two approaches were used to identify the ADH responsible for 1-butanol production in *H. butylicus*. The annotated zinc-containing ADH, Hbut_0414, in *H. butylicus* was cloned and overexpressed in *E. coli* Rosetta 2. The purified recombinant Hbut_0414 (ADH1) showed no enzymatic activity when NADP was used as a cofactor in the assay mixture. However, the ADH activity detected in the cell-free extract of *H. butylicus* showed a higher activity with NADP as the cofactor than NAD. The purification of this ADH2 from *H. butylicus* was also carried out to identify the ADH in the cell-free extract.

The biophysical properties and biochemical properties of purified ADH1 and ADH2 were significantly different. ADH1 was not oxygen sensitive but ADH2 was highly oxygen sensitive. The difference is most likely because ADH1 would be a zinc-containing ADH whereas ADH2 would be an iron-containing ADH. Moreover, ADH2 was remarkable more thermostable than ADH1. The time required for losing 50% of ADH2 activity was about 25 hours at 95 ºC, but for ADH1, the activity was reduced to only 15% of initial activity after incubation for 5 minutes at 95 ºC. 95 ºC is the optimal growth temperature for *H. butylicus*, the much lower thermostability of ADH1 brings to the question of whether Hbut_0414 was functionally expressed in *H. butylicus*. If *H. butylicus* do not use ADH1 encoded by Hbut_0414, the enzyme would not have the selection pressure to be

thermostable. The mechanisms for thermostability varied from enzyme to enzyme, which consisted of a combination of intrinsic stabilizing factors including the formation of salt bridges, hydrogen bonds or hydrophobic interactions, and enzymes could also be thermostable with extrinsic stabilizing factors (Matsumura, Yasumura et al. 1986, Gromiha, Oobatake et al. 1999). The analysis of primary structure, the amino acid sequences of ADH1 and its homologs showed a decreased in the percentage of charged amino acid and increased in percentages of hydrophobic amino acids compared to characterized thermostable ADHs. It is difficult to conclude whether the difference in amino acid composition led to low thermostability because decreased in the percentage of charged amino acid decreased the number of ion pairs and destabilize the enzyme but increased in small hydrophobic amino acids led to more hydrophobic interactions and stabilize the enzyme (Burg, Dijkstra et al. 1994, Kumar and Nussinov 2001). The elution profile of purification steps was also different for ADH1 and ADH2, and no ADH activity was detected in the fractions where ADH1 would be eluted out. This suggests that ADH2 has a much higher expression level than ADH1 *in vivo* if ADH1 would have any level of expression at all.

The optimal pH for catalyzing oxidation and reduction were also different for ADH1 and ADH2. The optimal pH for the reduction reaction in ADH1 was 5.0, which is lower than many hyperthermophilic ADHs (Radianingtyas and Wright 2003). The physiological roles of ADHs can be suggested by the enzyme kinetics and substrate specificity. Both ADH1 and ADH2 were primary/secondary ADHs and with higher relative activities toward primary alcohols than secondary alcohols. The apparent K_m values for both ADHs were lower with aldehydes than alcohols. It is interesting to note that for ADH1, the highest specificity constant k_{cat}/K_m was with propanal, which is converted into 1-propanol, and it is unknown for the physiological function of 1-propanol. ADH2 had the highest specificity constant k_{cat}/K_m with butyraldehyde, which is likely to be the ADH in *H. butylicus*

responsible for 1-butanol production. Acetone and isopropanol were both detected in culture, so the role of ADH2 for the conversion of acetone into isopropanol is also possible as the specificity constant k_{cat}/K_m for acetone is comparable to that of butyraldehyde.

The sequence analysis showed that ADH1 is a zinc-containing ADH and ADH2 is an iron-containing ADH with metal binding motifs and cofactor binding motifs identified. The presence of different types of ADHs in hyperthermophiles have been reported in *S. solfataricus* and *P. furiosus* (Ammendola, Raia et al. 1992, Ma and Adams 1999, van der Oost, Voorhorst et al. 2001, Contursi, Cannio et al. 2003). The sequence homology and identity between ADHs from *H. butylicus* with the same class of ADH is relative low compared to other hyperthermophilic ADHs. The low percentage in sequence identity and the diverse in protein sequences of iron-containing ADHs are the possible explanations for ADH2 not being annotated in the genome. ADH2 is encoded by Hbut_0924 and it is highly likely to be the ADH responsible for 1-butanol production in *H. butylicus* based on the enzyme kinetics, biophysical properties, and sequence alignment. Cloning of this gene and overexpression of its protein can overcome the limitation in the difficulty of collecting biomass for the enzyme structure study. The six Fe-ADHs used in sequence comparison with *H. butylicus* have not been characterized and 1-butanol is not reported to be produced. It is unclear why 1-butanol is produced in *H. butylicus*. 1-butanol is produced in *Clostridium* species as a solvent to maintain constant a intracellular pH (Isar and Rangaswamy 2012), but 1-butanol produced in *H. butylicus* is in a low concentration that is unlikely to be a way to maintain a constant pH. The butanol production pathway needs to be first identified to address this question and warrant further investigation.

4.4 Conclusions

The goal of this research was to identify the ADH that catalyzes the production of 1-butanol in *H. butylicus* and gain a better understanding of the metabolic profile of *H. butylicus*. The following conclusions can be made based on experimental results obtained:

1. Growth conditions were successfully optimized for studies on *H. butylicus*

2. Acetate and 1-butanol were confirmed to be produced by *H. butylicus*. It was found that *H. butylicus* also produced other metabolic end products including acetone, butyrate, formic acid, isovaleric acid and 2-propanol.

3. Hbut_0414 was cloned and overexpressed in *E. coli*. This study demonstrated the purified ADH1 encoded by Hbut_0414 is a functional ADH that is NAD-specific, but with a very low thermostability at 95 ºC. The biophysical and biochemical characteristics suggest it is unlikely the ADH catalyzing the production 1-butanol in *H. butylicus*.

4. ADH in cell free extract of *H. butylicus* was found to be NAD(P) dependent. The ADH2 was purified and its gene was identified. The gene encoding the ADH2 was identified to be Hbut_0924 and the sequence analysis suggests it is an iron-containing ADH. Its substrate specificity, enzyme kinetics and thermostability also suggest it is the ADH responsible for catalyzing the production of 1-butanol in *H. butylicus*.

4.5 Future study

The ADH in this study is the only ADH in hyperthermophiles that are able to produce 1-butanol *in vivo*. The production of 1-butanol might have important physiology function and there is a possibility of a novel butanol-pathway in *H. butylicus*. To understand the production of butanol, two studies are proposed to carry out.

Due to the low thermostability of ADH1, the purified enzyme should send out for mass spectrometry analysis to confirm it is the protein of interest. The first study proposed after the confirmation is to examine the expression level of ADH1 (Hbut_0414) and ADH2 (Hbut_0924) by real-time PCR. This can verify that Hbut_0924 is expressed and Hbut_0414 might not be expressed as proposed by this study. It is also interesting to examine the effect of pH and hydrogen pressure on the expression level of the ADH2 gene (Hbut_0924). A gene knock-out of Hbut_0924 in *H. butylicus* would likely crease 1-butanol production and further suggest ADH2 encoded by Hbut_0924 is responsible for 1-butanol production.

The second study proposed is to determine the butanol production pathway in *H. butylicus* by identifying and characterizing essential enzyme(s) from possible butanol pathways in *H. butylicus*. In the *clostridia* pathway, acetoacetyl-CoA: acetate-CoA transferase and acetoacetyl-CoA: butyrate-CoA transferase are essential enzymes. Although there is no gene annonation of those two enzymes in the *H. butylicus* genome, these enzymes could be identified by tracing their enzyme activities if present in the cell-free extract of *H. butylicus*. Pyruvate decarboxylase is also a candidate for identification in *H. butylicus* as there is no gene annotation in the genome but an essential enzyme for the production of butanol from 2-ketovalerate.

Understanding the butanol production pathway in *H. butylicus* can help to optimize the yield of butanol production and this highly thermostable ADH can be potentially used for biobutanol production.

References

Ammendola, S., et al. (1992). Thermostable NAD^+-dependent alcohol dehydrogenase from *Sulfolobus solfataricus*: gene and protein sequence determination and relationship to other alcohol dehydrogenases. Biochemistry **31**(49): 12514-12523.

Antoine, E., et al. (1999). Cloning and over-expression in *Escherichia coli* of the gene encoding NADPH group III alcohol dehydrogenase from *Thermococcus hydrothermalis*. European Journal of Biochemistry **264**(3): 880-889.

Antoni, D., et al. (2007). Biofuels from microbes. Applied microbiology and biotechnology **77**(1): 23-35.

Aristidou, A. and M. Penttilä (2000). Metabolic engineering applications to renewable resource utilization. Current Opinion in Biotechnology **11**(2): 187-198.

Aristidou, A. A., et al. (2011). Conversion of Renewable Resources to Biofuels and Fine Chemicals: Current Trends and Future Prospects. Fermentation Microbiology and Biotechnology: 225.

Atomi, H. (2005). Recent progress towards the application of hyperthermophiles and their enzymes. Current opinion in chemical biology **9**(2): 166-173.

Atomi, H., et al. (2011). Application of hyperthermophiles and their enzymes. Current opinion in biotechnology **22**(5): 618-626.

Atsumi, S., et al. (2008). Metabolic engineering of *Escherichia coli* for 1-butanol production. Metabolic engineering **10**(6): 305-311.

Atsumi, S., et al. (2008). Non-fermentative pathways for synthesis of branched-chain higher alcohols as biofuels. Nature **451**(7174): 86-89.

Balat, M., et al. (2008). Progress in bioethanol processing. Progress in energy and combustion science **34**(5): 551-573.

Balch, W. E., et al. (1979). *Methanogens*: reevaluation of a unique biological group. Microbiological reviews **43**(2): 260.

Ballesteros, M., et al. (2004). Ethanol from lignocellulosic materials by a simultaneous saccharification and fermentation process (SFS) with *Kluyveromyces marxianus* CECT 10875. Process Biochemistry **39**(12): 1843-1848.

Bell, S. D. and S. P. Jackson (1998). Transcription and translation in Archaea: a mosaic of eukaryal and bacterial features. Trends in microbiology **6**(6): 222-228.

Berezina, O. V., et al. (2010). Reconstructing the *clostridial* n-butanol metabolic pathway in *Lactobacillus brevis*. Applied microbiology and biotechnology **87**(2): 635-646.

Bhandiwad, A., et al. (2013). Metabolic Engineering of *Thermoanaerobacterium thermosaccharolyticum* for increased n-Butanol production.

Bhandiwad, A., et al. (2014). Metabolic engineering of *Thermoanaerobacterium saccharolyticum* for n-butanol production. Metabolic engineering **21**: 17-25.

Boynton, Z. L., et al. (1996). Cloning, sequencing, and expression of clustered genes encoding beta-hydroxybutyryl-coenzyme A (CoA) dehydrogenase, crotonase, and butyryl-CoA dehydrogenase from *Clostridium acetobutylicum* ATCC 824. Journal of bacteriology **178**(11): 3015-3024.

Bradford, M. M. (1976). A rapid and sensitive method for the quantitation of microgram quantities of protein utilizing the principle of protein-dye binding. Analytical biochemistry **72**(1): 248-254.

Branden, C., et al. (1975). Alcohol dehydrogenase. The enzymes **2**(part A).

Branduardi, P., et al. (2013). A novel pathway to produce butanol and isobutanol in *Saccharomyces cerevisiae*. Biotechnology Biofuels **6**(1): 68.

Brown, S. D., et al. (2011). Mutant alcohol dehydrogenase leads to improved ethanol tolerance in *Clostridium thermocellum*. Proceedings of the National Academy of Sciences **108**(33): 13752-13757.

Bruant, G., et al. (2010). Genomic analysis of carbon monoxide utilization and butanol production by *Clostridium carboxidivorans* strain P7T." PloS one **5**(9 (e13033)): 1-12.

Brugger, K., et al. (2007). The genome of *Hyperthermus butylicus*: a sulfur-reducing, peptide. Archaea **2**(2): 127-135.

Burg, B., et al. (1994). Protein stabilization by hydrophobic interactions at the surface. European Journal of Biochemistry **220**(3): 981-985.

Canganella, F., et al. (1998). *Thermococcus guaymasensis* sp. nov. and *Thermococcus aggregans* sp. nov., two novel thermophilic archaea isolated from the Guaymas Basin hydrothermal vent site. International journal of systematic bacteriology **48**(4): 1181-1185.

Cannio, R., et al. (1996). Cloning and overexpression in *Escherichia coli* of the genes encoding NAD-dependent alcohol dehydrogenase from two *Sulfolobus* species. Journal of bacteriology **178**(1): 301-305.

Cardona, C. A. and Ó. J. Sánchez (2007). Fuel ethanol production: process design trends and integration opportunities. Bioresource technology **98**(12): 2415-2457.

Cascone, R. (2008). Biobutanol: A Replacement for Bioethanol? Chemical Engineering Progress **104**(8).

Christensen, H. N. (1990). Role of amino acid transport and countertransport in nutrition and metabolism. Physiology Revolution **70**(1): 43-77.

Ciriacy, M. (1975). Genetics of alcohol dehydrogenase in *Saccharomyces cerevisiae*: I. Isolation and genetic analysis of adh mutants. Mutation Research/Fundamental and Molecular Mechanisms of Mutagenesis **29**(3): 315-325.

Contursi, P., et al. (2003). Development of a genetic system for hyperthermophilic Archaea: expression of a moderate thermophilic bacterial alcohol dehydrogenase gene in *Sulfolobus solfataricus*. FEMS microbiology letters **218**(1): 115-120.

Conway, T. (1992). The Entner-Doudoroff pathway: history, physiology and molecular biology. FEMS microbiology reviews **103**(1): 1-28.

Danson, M. J. and D. W. Hough (1998). Structure, function and stability of enzymes from the Archaea. Trends in microbiology **6**(8): 307-314.

Danson, M. J., et al. (1996). Enzyme thermostability and thermoactivity. Protein engineering **9**(8): 629-630.

Demirjian, D. C., et al. (2001). Enzymes from extremophiles. Current opinion in chemical

biology **5**(2): 144-151.

Dombek, K. and L. Ingram (1987). Ethanol production during batch fermentation with Saccharomyces cerevisiae: changes in glycolytic enzymes and internal pH." Applied and environmental microbiology **53**(6): 1286-1291.

Doran-Peterson, J., et al. (2008). Microbial conversion of sugars from plant biomass to lactic acid or ethanol. The Plant Journal **54**(4): 582-592.

Ermolaeva, M. D. (2001). Synonymous codon usage in bacteria. Current issues in molecular biology **3**(4): 91-97.

Ezeji, T., et al. (2007). Butanol production from agricultural residues: impact of degradation products on *Clostridium beijerinckii* growth and butanol fermentation. Biotechnology and Bioengineering **97**(6): 1460-1469.

Fiala, G. and K. O. Stetter (1986). *Pyrococcus furiosus* sp. nov. represents a novel genus of marine heterotrophic archaebacteria growing optimally at 100^{o}C. Archives of Microbiology **145**(1): 56-61.

Gao, S., et al. (1997). Aromatic amino acid catabolism by *lactococci*. Le Lait **77**(3): 371-381.

George, H., et al. (1983). Acetone, isopropanol, and butanol production by *Clostridium beijerinckii* (syn. *Clostridium butylicum*) and *Clostridium aurantibutyricum*. Applied and environmental microbiology **45**(3): 1160-1163.

George, H. A. and J.-S. Chen (1983). Acidic conditions are not obligatory for onset of butanol formation by *Clostridium beijerinckii* (synonym, *C. butylicum*)." Applied and environmental microbiology **46**(2): 321-327.

Gheshlaghi, R., et al. (2009). Metabolic pathways of clostridia for producing butanol. Biotechnology advances **27**(6): 764-781.

Girbal, L., et al. (1995). Regulation of metabolic shifts in *Clostridium acetobutylicum* ATCC 824." FEMS microbiology reviews **17**(3): 287-297.

Godfroy, A., et al. (1997). *Thermococcus hydrothermalis* sp. nov., a new hyperthermophilic archaeon isolated from a deep-sea hydrothermal vent. International journal of systematic

bacteriology **47**(3): 622-626.

Gottwald, M., et al. (1984). Formation of n-butanol from D-glucose by strains of the *Clostridium tetanomorphum* group. Applied and environmental microbiology **48**(3): 573-576.

Green, E. M. (2011). Fermentative production of butanol—the industrial perspective. Current opinion in biotechnology **22**(3): 337-343.

Grethlein, A. J., et al. (1991). Evidence for production of n-butanol from carbon monoxide by *Butyribacterium methylotrophicum*. Journal of fermentation and bioengineering **72**(1): 58-60.

Gromiha, M. M., et al. (1999). Important amino acid properties for enhanced thermostability from mesophilic to thermophilic proteins. Biophysical chemistry **82**(1): 51-67.

Guy, J. E., et al. (2003). The Structure of an Alcohol Dehydrogenase from the Hyperthermophilic Archaeon *Aeropyrum pernix*. Journal of molecular biology **331**(5): 1041-1051.

Heider, J., et al. (1995). Purification, characterization, and metabolic function of tungsten-containing aldehyde ferredoxin oxidoreductase from the hyperthermophilic and proteolytic archaeon *Thermococcus* strain ES-1. Journal of Bacteriology **177**(16): 4757-4764.

Hirakawa, H., et al. (2004). Properties of an alcohol dehydrogenase from the hyperthermophilic archaeon *Aeropyrum pernix* K1." Journal of bioscience and bioengineering **97**(3): 202-206.

Huber, R., et al. (2000). Towards the ecology of hyperthermophiles: biotopes, new isolation strategies and novel metabolic properties. FEMS microbiology reviews **24**(5): 615-623.

Ingram, L., et al. (1999). Enteric bacterial catalysts for fuel ethanol production. Biotechnology progress **15**(5): 855-866.

Inui, M., et al. (2008). Expression of *Clostridium acetobutylicum* butanol synthetic genes in *Escherichia coli*. Applied microbiology and biotechnology **77**(6): 1305-1316.

Isar, J. and V. Rangaswamy (2012). Improved n-butanol production by solvent tolerant

Clostridium beijerinckii. Biomass and Bioenergy **37**: 9-15.

Ismaiel, A. A., et al. (1993). Purification and characterization of a primary-secondary alcohol dehydrogenase from two strains of *Clostridium beijerinckii*. Journal of Bacteriology **175**(16): 5097-5105.

Jang, Y.-S., et al. (2012). Enhanced butanol production obtained by reinforcing the direct butanol-forming route in *Clostridium acetobutylicum*. Journal of Molecular Biology **3**(5): e00314-00312.

Jang, Y.S., et al. (2012). Butanol production from renewable biomass by *clostridia*. Bioresource technology **123**: 653-663.

Jeffries, T. W. (1981). Conversion of xylose to ethanol under aerobic conditions by *Candida tropicalis*. Biotechnology letters **3**(5): 213-218.

Johnson, M., et al. (1931). Oxidation and reduction relations between substrate and products in the acetonebutyl alcohol fermentation. Journal of Biological Chemistry **91**(2): 569-591.

Jones, D. T. and D. R. Woods (1986). Acetone-butanol fermentation revisited. Microbiological reviews **50**(4): 484.

Jornvall, H., et al. (1987). Characteristics of alcohol/polyol dehydrogenases. European Journal of Biochemistry **167**(2): 195-201.

Kelly, R. M. and M. W. Adams (1994). Metabolism in hyperthermophilic microorganisms. Antonie Van Leeuwenhoek **66**(1-3): 247-270.

Kinoshita, S., et al. (1957). Studies on the amino acid fermentation. The Journal of general and applied microbiology **3**(3): 193-205.

Kondo, T., et al. (2012). Genetic engineering to enhance the Ehrlich pathway and alter carbon flux for increased isobutanol production from glucose by *Saccharomyces cerevisiae*. Journal of biotechnology **159**(1): 32-37.

Kube, J., et al. (2006). Influence of temperature on the production of an archaeal thermoactive alcohol dehydrogenase from *Pyrococcus furiosus* with recombinant *Escherichia coli*. Extremophiles **10**(3): 221-227.

Kumar, S. and R. Nussinov (2001). How do thermophilic proteins deal with heat? Cellular and Molecular Life Sciences **58**(9): 1216-1233.

Laemmli, U. K. (1970). Cleavage of structural proteins during the assembly of the head of bacteriophage T4. Nature **227**(5259): 680-685.

Lamed, R. and J. Zeikus (1980). Ethanol production by thermophilic bacteria: relationship between fermentation product yields of and catabolic enzyme activities in *Clostridium thermocellum* and *Thermoanaerobium brockii*. Journal of Bacteriology **144**(2): 569-578.

Lamed, R. J. and J. Zeikus (1981). Novel NADP-linked alcohol-aldehyde/ketone oxidoreductase in thermophilic ethanologenic bacteria. Journal of Biochemistry **195**: 183-190.

Larkin, M. A., et al. (2007). Clustal W and Clustal X version 2.0. Bioinformatics **23**(21): 2947-2948.

Lee, S. Y., et al. (2008). Fermentative butanol production by *Clostridia*. Biotechnology and Bioengineering **101**(2): 209-228.

Li, F., et al. (2008). Coupled ferredoxin and crotonyl coenzyme A (CoA) reduction with NADH catalyzed by the butyryl-CoA dehydrogenase/Etf complex from *Clostridium kluyveri*. Journal of Bacteriology **190**(3): 843-850.

Lovitt, R., et al. (1984). Ethanol production by thermophilic bacteria: physiological comparison of solvent effects on parent and alcohol-tolerant strains of *Clostridium thermohydrosulfuricum*. Applied and environmental microbiology **48**(1): 171-177.

Ma, K. and M. W. Adams (1999). An unusual oxygen-sensitive, iron-and zinc-containing alcohol dehydrogenase from the hyperthermophilic archaeon *Pyrococcus furiosus*. Journal of Bacteriology **181**(4): 1163-1170.

Ma, K., et al. (1995). Effects of elemental sulfur on the metabolism of the deep-sea hyperthermophilic archaeon *Thermococcus* strain ES-1: characterization of a sulfur-regulated, non-heme iron alcohol dehydrogenase. Journal of bacteriology **177**(16): 4748-4756.

Machielsen, R., et al. (2006). Production and characterization of a thermostable alcohol

dehydrogenase that belongs to the aldo-keto reductase superfamily. Applied and environmental microbiology **72**(1): 233-238.

Margaritis, A. and P. Bajpai (1982). Direct fermentation of D-xylose to ethanol by *Kluyveromyces marxianus* strains. Applied and environmental microbiology **44**(5): 1039-1041.

Massey, L. K., et al. (1976). Branched-chain amino acid catabolism in bacteria. Bacteriological reviews **40**(1): 42.

Matsumura, M., et al. (1986). Cumulative effect of intragenic amino-acid replacements on the thermostability of a protein.Nature **323**(6086):356-8

Menon, S. and S. W. Ragsdale (1997). Mechanism of the *Clostridium thermoaceticum* pyruvate: ferredoxin oxidoreductase: evidence for the common catalytic intermediacy of the hydroxyethylthiamine pyropyrosphate radical. Biochemistry **36**(28): 8484-8494.

Mitchell, W. J. (1997). Physiology of carbohydrate to solvent conversion by *clostridia*. Advances in microbial physiology **39**: 31-130.

Mukund, S. and M. Adams (1991). The novel tungsten-iron-sulfur protein of the hyperthermophilic archaebacterium, *Pyrococcus furiosus*, is an aldehyde ferredoxin oxidoreductase. Evidence for its participation in a unique glycolytic pathway. Journal of Biological Chemistry **266**(22): 14208-14216.

Mukund, S. and M. Adams (1993). Characterization of a novel tungsten-containing formaldehyde ferredoxin oxidoreductase from the hyperthermophilic archaeon, *Thermococcus litoralis*. A role for tungsten in peptide catabolism. Journal of Biological Chemistry **268**(18): 13592-13600.

Nakamura, Y., et al. (2000). Codon usage tabulated from international DNA sequence databases: status for the year 2000. Nucleic acids research **28**(1): 292-292.

Ng, T. K., et al. (1981). Ethanol production by thermophilic bacteria: fermentation of cellulosic substrates by cocultures of *Clostridium thermocellum* and *Clostridium thermohydrosulfuricum*. Applied and environmental microbiology **41**(6): 1337-1343.

Nielsen, D. R., et al. (2009). Engineering alternative butanol production platforms in heterologous bacteria. Metabolic engineering **11**(4): 262-273.

Noll, K. M. and S. E. Childers (2000). Sulfur metabolism among hyperthermophiles. Journey to Diverse Microbial Worlds, Springer**:** 93-105.

Papoutsakis, E. T. (2008). Engineering solventogenic *clostridia*. Current Opinion in Biotechnology **19**(5): 420-429.

Park, C.-H., et al. (1993). Characteristics of butanol fermentation by a low-acid-producing *Clostridium acetobutylicum* B18. Applied microbiology and biotechnology **39**(2): 148-154.

Pederson, J. A., et al. (1999). Peptidases and amino acid catabolism in lactic acid bacteria. Lactic acid bacteria: Genetics, metabolism and applications, Springer**:** 217-246.

Peng, H., et al. (2008). The aldehyde/alcohol dehydrogenase (AdhE) in relation to the ethanol formation in *Thermoanaerobacter ethanolicus* JW200. Anaerobe **14**(2): 125-127.

Pennacchio, A., et al. (2010). Biochemical characterization of a recombinant short-chain NAD(H)-dependent dehydrogenase/reductase from *Sulfolobus acidocaldariu*s. Extremophiles **14**(2): 193-204.

Pfromm, P. H., et al. (2010). Bio-butanol vs. bio-ethanol: a technical and economic assessment for corn and switchgrass fermented by yeast or *Clostridium acetobutylicum*. Biomass and Bioenergy **34**(4): 515-524.

Pledger, R. J. and J. A. Baross (1989)."Characterization of an Extremely Thermophilic Archaebacterium Isolated from a Black Smoker Polychaete (*Paralvinella* sp.) at the Juan de Fuca Ridge. Systematic and applied microbiology **12**(3): 249-256.

Qureshi, N. and I. S. Maddox (1995). Continuous production of acetone-butanol-ethanol using immobilized cells of *Clostridium acetobutylicum* and integration with product removal by liquid-liquid extraction. Journal of fermentation and bioengineering **80**(2): 185-189.

Radianingtyas, H. and P. C. Wright (2003). Alcohol dehydrogenases from thermophilic and hyperthermophilic archaea and bacteria. FEMS microbiology reviews **27**(5): 593-616.

Ragauskas, A. J., et al. (2006). "The path forward for biofuels and biomaterials. Science **311**(5760): 484-489.

Raia, C. A., et al. (2001). Alcohol dehydrogenase from *Sulfolobus solfataricus*. Methods in enzymology **331**: 176.

Rogers, P., et al. (2007). *Zymomonas mobilis* for fuel ethanol and higher value products. Biofuels, Springer**:** 263-288.

Rogers, P., et al. (1982). Ethanol production by *Zymomonas mobilis*. Microbial reactions, Springer**:** 37-84.

Schneider, H., et al. (1981). Conversion of D-xylose into ethanol by the yeast *Pachysolen tannophilus*. Biotechnology letters **3**(2): 89-92.

Shaw, A. J., et al. (2008). End-product pathways in the xylose fermenting bacterium, *Thermoanaerobacterium saccharolyticum*. Enzyme and microbial technology **42**(6): 453-458.

Shaw, A. J., et al. (2008). Metabolic engineering of a thermophilic bacterium to produce ethanol at high yield. Proceedings of the National Academy of Sciences **105**(37): 13769-13774.

Shen, C. R. and J. C. Liao (2008). Metabolic engineering of *Escherichia coli* for 1-butanol and 1-propanol production via the keto-acid pathways. Metabolic engineering **10**(6): 312-320.

Simon, H., et al. (1985). Chiral compounds synthesized by biocatalytic reductions. New Synthetic Methods **24**(7): 539-553.

Steen, E. J., et al. (2008). Metabolic engineering of *Saccharomyces cerevisiae* for the production of n-butanol. Microbiology Cell Fact **7**(1): 36.

Stetter, K. O. (1996). Hyperthermophilic procaryotes. FEMS microbiology reviews **18**(2-3): 149-158.

Stetter, K. O. (1998). Hyperthermophiles: isolation, classification, and properties. Extremophiles: microbial life in extreme environments: 1-24.

Stetter, K. O. (2005). Volcanoes, hydrothermal venting, and the origin of life. Volcanoes and the Environment: 175-206.

Survase, S. A., et al. (2011). Continuous production of isopropanol and butanol using *Clostridium beijerinckii* DSM 6423. Applied microbiology and biotechnology **91**(5): 1305-1313.

Taylor, M. P., et al. (2009). *Thermophilic ethanologenesis*: future prospects for second-generation bioethanol production. Trends in biotechnology **27**(7): 398-405.

Tolan, J. S. and R. Finn (1987). Fermentation of D-xylose to ethanol by genetically modified *Klebsiella planticola*. Applied and environmental microbiology **53**(9): 2039-2044.

Uria, A. R., et al. (2006). Alcohol Dehydrogenases from Marine Hyperthermophilic Microorganisms and Their Importance to the Pharmaceutical Industry. International Seminar and Workshop on Marine in Indinesia

van der Oost, J., et al. (2001). Genetic and biochemical characterization of a short-chain alcohol dehydrogenase from the hyperthermophilic archaeon *Pyrococcus furiosus*. European Journal of Biochemistry **268**(10): 3062-3068.

Vitale, A., et al. (2010). Properties and evolution of an alcohol dehydrogenase from the Crenarchaeota *Pyrobaculum aerophilum*. Gene **461**(1): 26-31.

Walter, K. A., et al. (1992). Molecular characterization of two *Clostridium acetobutylicum* ATCC 824 butanol dehydrogenase isozyme genes. Journal of bacteriology **174**(22): 7149-7158.

Wang, S., et al. (2010). $NADP^+$ reduction with reduced ferredoxin and $NADP^+$ reduction with NADH are coupled via an electron-bifurcating enzyme complex in *Clostridium kluyveri*. Journal of Bacteriology **192**(19): 5115-5123.

Weber, C., et al. (2010). Trends and challenges in the microbial production of lignocellulosic bioalcohol fuels. Applied microbiology and biotechnology **87**(4): 1303-1315.

White, H., et al. (1991). Purification and some properties of the tungsten-containing carboxylic acid reductase from *Clostridium formicoaceticum*. Biological chemistry Hoppe-Seyler **372**(2): 999-1006.

White, H., et al. (1989). Carboxylic acid reductase: a new tungsten enzyme catalyses the

reduction of non-activated carboxylic acids to aldehydes. European Journal of Biochemistry **184**(1): 89-96.

Wiegel, J., et al. (1983). Production of ethanol from biopolymers by anaerobic, thermophilic, and extreme thermophilic bacteria. III. *Thermoanaerobacter ethanolicus* JW200 and its mutants in batch cultures and resting cell experiments. Biotechnol. Bioeng. Symp.;(United States), Univ. of Georgia, Athens.

Wu, X., et al. (2013). Thermostable alcohol dehydrogenase from *Thermococcus kodakarensis* KOD1 for enantioselective bioconversion of aromatic secondary alcohols. Applied and environmental microbiology **79**(7): 2209-2217.

Ying, X., et al. (2009). Molecular characterization of the recombinant iron-containing alcohol dehydrogenase from the hyperthermophilic Archaeon, *Thermococcus* strain ES1." Extremophiles **13**(2): 299-311.

Ying, X. and K. Ma (2011). Characterization of a zinc-containing alcohol dehydrogenase with stereoselectivity from the hyperthermophilic archaeon *Thermococcus guaymasensis*. Journal of bacteriology **193**(12): 3009-3019.

Zaldivar, J., et al. (1999). Effect of selected aldehydes on the growth and fermentation of ethanologenic *Escherichia coli*. Biotechnology and Bioengineering **65**(1): 24-33.

Zamora, F. (2009). Biochemistry of alcoholic fermentation. Wine Chemistry and Biochemistry, Springer**:** 3-26.

Zeikus, J. (1980). Chemical and fuel production by anaerobic bacteria. Annual Reviews in Microbiology **34**(1): 423-464.

Zhang, F., et al. (2011). Metabolic engineering of microbial pathways for advanced biofuels production. Current Opinion in Biotechnology **22**(6): 775-783.

Zheng, Y.-N., et al. (2009). Problems with the microbial production of butanol. Journal of industrial microbiology & biotechnology **36**(9): 1127-1138.

Zillig, W., et al. (1990). *Hyperthermus butylicus*, a hyperthermophilic sulfur-reducing archaebacterium that ferments peptides. Journal of bacteriology **172**(7): 3959-3965.

Zillig, W., et al. (1987). *Pyrococcus woesei*, sp. nov., an ultra-thermophilic marine

archaebacterium, representing a novel order, *Thermococcales*. Systematic and applied microbiology **9**(1): 62-70.

Appendix

Major Chemicals used in this study

Chemicals*	Corporation
Acetone	Fisher scientific company (ON, Canada)
Agarose	Fermentas Canada Inc. (ON, Canada)
40% Acrylamide/Bisacrylamide	MP Biomedicals (OH, USA)
Bio-Rad protein assay	Bio-Rad Laboratories, Inc. (ON, Canada)
1-butanol	Sigma-Aldrich Canada Ltd (ON, Canada)
Dithiothreitol	Sigma-Aldrich Canada Ltd (ON, Canada)
EZ-10 Spin column PCR products purification kit	Bio Basic Inc (ON, Canada)
FastDigest restriction enzymes	Thermo Scientific (ON, Canada)
GeneRuler 100bp	Fermentas (ON, Canada)
Isopropyl β-D-1-thiogalactopyranoside	Fermentas Canada Inc. (ON, Canada)
NAD(P)	Sigma-Aldrich Canada Ltd (ON, Canada)
NAD(P)H	Sigma-Aldrich Canada Ltd (ON, Canada)
Perfect DNA 1 kb DNA ladder	Novagen (WI, USA)
Sodium Dithionite	Sigma-Aldrich Canada Ltd (ON, Canada)
Taq DNA polymerase	Sigma-Aldrich Canada Ltd (ON, Canada)
T4 polymerase	Sigma-Aldrich Canada Ltd (ON, Canada)

*all other chemicals not mentioned were also of high technical grade and obtained from Sigma-Aldrich Canada Ltd (ON, Canada) or Fisher scientific company (ON, Canada).

Major Equipment used in this study

Instrument	Corporation
Agarose gel electrophoresis chamber	Bio-Rad Laboratories Inc (ON, Canada)
Centrifuge (Allegra 21R centrifuge)	Beckman Coulter (ON, Canada)
Centrifuge (Sorvall RC6-R-refrigerated super centrifuges)	Mandel Scientific Company Inc (ON, Canada)
Fast protein liquid chromatography (AKTA /Prime)	Amersham Biotech (Montreal, Quebec)
FluorChem 8000 Chemiluminescence and Visible Imaging System	Alpha Innotech Corporation (CA, USA)
High performance liquid chromatography (Shimadzu)	Mandel Scientific Company Inc (ON, Canada)
Incubation shaker	New Brunswick Science (NJ, USA)
Incubator	Fisher scientific company (ON, Canada)
Phase-contrast microscope (Eclipse E600)	Nikon (Japan)
Protein gel chamber	Bio-Rad Laboratories, Inc. (ON, Canada)
Spectrophotometer (Genesys 10Vis)	Thermospectronic Unicam (NY, USA)
Stirred cells (series 8200)	Ami (MA, USA)
Thermal-PCR-cycler TC-312	Techne incorporated (NJ, USA)
Ultrafiltration membranes	Millipore (MA, USA)
Vortex	Fisher scientific company (ON, Canada)
Waterbath	Fisher scientific company (ON, Canada)

Accessions numbers of ADHs used in protein sequences alignments

Protein	Accession number
A. profundus ADH	WP_012939782
D. fermentans ADH	WP_014767018
D. mucosus ADH	WP_013561843
Hbut_0414	WP_048061395
Hbut_0924	WP_011822090
P. islandicum ADH	WP_011763330
P. fumarii ADH	WP_014026672
S. sclerotialus ADH	WP_030623043
S. solfataricus ADH	WP_009988924
T. aggregans ADH	WP_013129339
T. cellulolyticus ADH	WP_014737928

HPLC chromatography

HPLC chromatography from culture medium grew at pH 7.0 with 3 atmosphere overpressure H_2 and 10 g/L of sulfur at different time intervals. Culture medium is 20 ml and 0.8ml of culture was withdrawn for HPLC measurement.

Initial time point after inoculation and before growth (t=0)

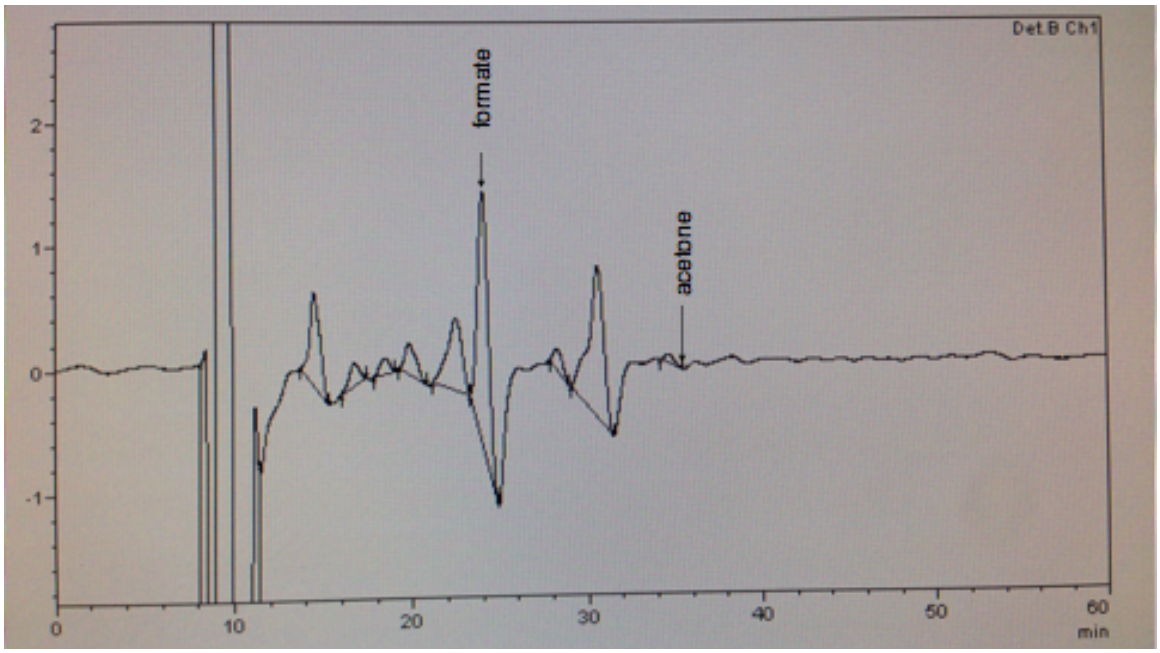

Cultivation after 16 hours (early log phase)

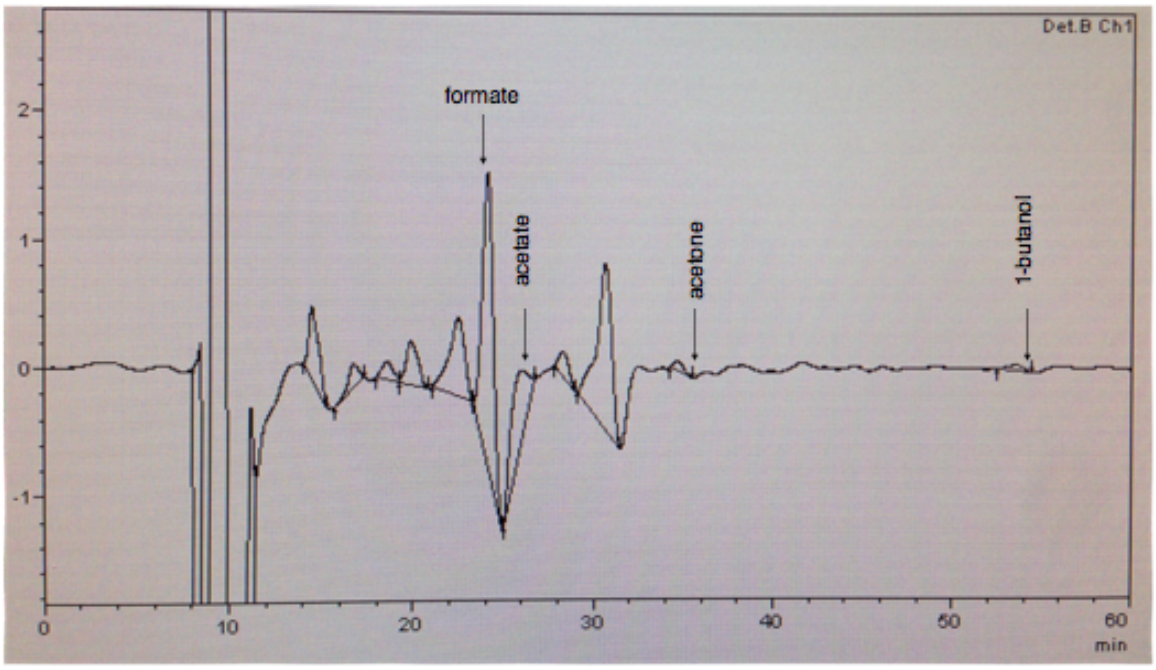

Cultivation after 25 hours (mid-log phase)

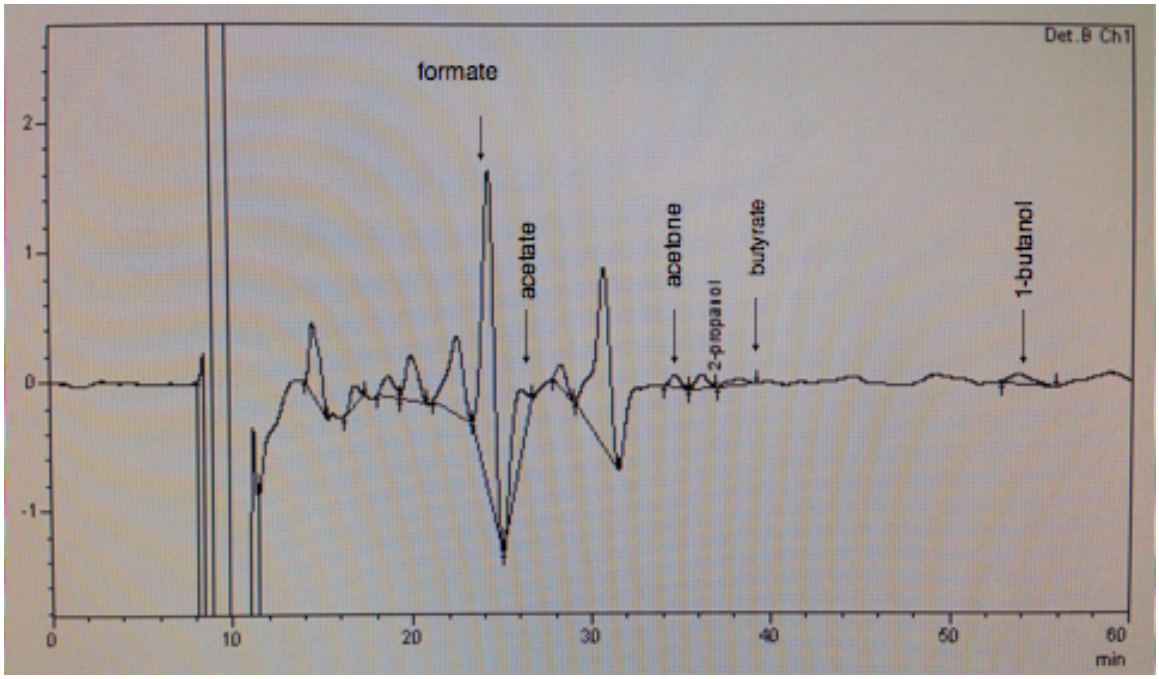

Cultivation after 39 hours (late log phase)

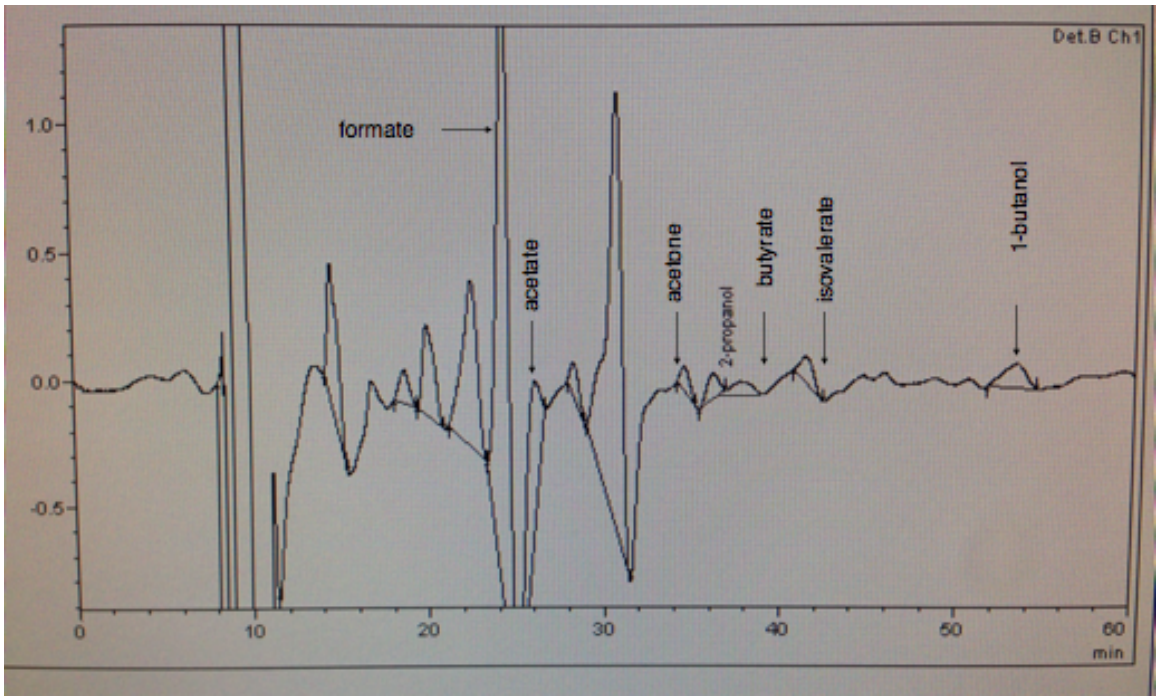

Cultivation after 50 hours (stationary phase)